EFFECT OF THE COMBINATION OF COPPER – NICKEL CATALYST SUPPORTED ON ACTIVATED CARBON (Cu - Ni/AC) AND ZEOLITE A IN THE DIRECT SYNTHESIS OF LINEAR CARBONATES

A Thesis Submitted in Partial Fulfillment of the Requirements for the Degree of Master in Chemical Engineering

Isis Elena Hernández Ramírez

Advisor

PhD. Lina María González Rodríguez

Environmental Catalysis Research Group

Universidad de Antioquia

Engineering Faculty

Medellín - Colombia

2016

"Sooner or later discipline will defeat intelligence"

Japanese proverb

ACKNOWLEDGEMENTS

At first, I am and I will be grateful with God every day of my live. He has given me everything; He has given me the capabilities and strength to complete this difficult but beautiful project. Thanks family for give me the God's and Mary´s love.

Infinite gratitude to my advisor, PhD. Lina María González, I feel admiration for her kindness and her honesty. Thank you for all the time and effort put into this project. Several years have passed, sometimes difficult, but you always gave me a lot of hope.

Thanks a lot PhD Aída Luz Villa, director of environmental catalysis research group, a great professor and an amazing woman. I do not tire to say her how important was her support in my life.

PhD. Felipe Bustamante, thanks for your key contributions. You were always willing to help me in the best way. Also, thanks PhD. Edwin Alarcón, PhD. Oscar Arbeláez and all members of the Environmental Catalysis group for their help and unconditional support all this time. During these years I met great people who I will never forget.

Química Básica Company for its interest in this Research Project. Thanks Dc. Adolfo Molina by his time and friendly advice. Special thanks for the inclusion of research work in the industrial field.

Off course, I would also like to recognize all comments and critical reviews that I received from my supervising committee members PhD Martha Cobo and PhD Jhon Jairo Fernández. Yours valuable observations have significantly improved my thesis work.

Finally, Thanks to University of Antioquia by the project PRG13-2-05 for its financial support, without which it would not have been possible to develop this work.

ABSTRACT

Direct synthesis of dimethyl carbonate (DMC) and diethyl carbonate (DEC) from CO_2 and alcohol is a strongly equilibrium limited reaction that tries to find cleaner production route. Since the thermodynamic limitation the DMC and DEC yield achieved (using Cu-Ni/AC catalyst) is around 1-2% when the produced water is not removed from the system. In order to get eliminated water, dehydrating agents were used in order to shift the reaction towards a higher DMC and DEC yield.

Therefore, test a novel combination of a fixed bed reactor combined with zeolite 4A is the main objective in this work. It will be analyzing the combination of the use of a dehydrative agent, such as zeolite 4A and butylene oxide with the Cu-Ni/AC catalyst at gas phase (92°C until 14 Bar) and liquid phase (92°C and 4 Bar). This unexplored option must be understood the effect of the presence of multicomponent mixtures on the adsorption capacity and kinetics of water behavior and presents the first results for the assembly zeolite 4A / Cu – Ni /AC in gas and liquid phase at same conditions. This study lets it contribute with the multicomponent adsorption determination because there are a few informations reported for this kind of systems and it proposes a simple experimental methodology that uses mass spectrometry as a new, practice and easy quantification technique in order to obtain the data.

The results showed that the equilibrium conversion is strongly influenced by the pressure and temperature of the system: Conversion increases when increasing the pressure and temperature, however the water adsorption capacity of zeolite always was worse when the temperature increases and it is not affected by pressure. About the multicomponent adsorption capacity, isothermal adsorption and kinetics of water, methanol and ethanol in 4A zeolite were studied at different temperatures and different number of compounds. It has been demonstrated that adsorption of water, methanol and ethanol follow Langmuir isotherms. The mixtures of compounds show a competitive adsorption (ethanol and methanol occupy the sites) and the presence of CO_2 block the access of the sites reduce the water adsorption capacity. Furthermore, the separation of water and methanol is in fact very difficult because polarities, chemical properties and even molecular sizes of water and methanol (2.6 Å and 3.6 Å) are similar. Finally, the kinetics follow by pure compounds were different when increase the number of compounds. Water, follow PFO kinetic but, in presence of methanol and CO_2 presence an Elovich or IPD tendency suggest a possible chemisorption. Any catalytic activity of the Cu-Ni/AC catalyst was obtained in the liquid phase reactions at 4 Bar and 92°C. Although, it presents loss of loading by a possible leaching, it is unable to increase the yield. Regardless what dehydrating agent was used (butylene oxide or zeolite 4A) the reaction tends to zero.

Keywords: *Dimethyl carbonate, diethyl carbonate, zeolite 4A, multicomponent adsorption, catalyst-adsorbent assembly.*

TABLE OF CONTENTS

ACKNOWLEDGEMENTS III

ABSTRACT IV

LIST OF FIGURES IX

LIST OF TABLES XII

GENERAL INTRODUCTION 1

SCOPE OF THIS WORK 4

OBJECTIVE 5

PUBLICATIONS 6

CHAPTER 1 7

MULTICOMPONENT ADSORPTION OF CARBON DIOXIDE (CO_2), ETHANOL, METHANOL, WATER, DIETHYL CARBONATE (DEC) AND DIMETHYL CARBONATE (DMC) MIXTURES ON ZEOLITE 4A. 7

1.1. INTRODUCTION 7

1.1.1. CHARACTERISTIC OF ZEOLITES A 8

1.1.2. METHODS TO CALCULATE ADSORPTION 10

1.1.3. ADSORPTION ISOTHERM 10

1.1.4. EQUILIBRIA ADSORPTION IN A MULTICOMPONENT SYSTEM 13

1.1.5. TYPE OF ADSORPTION 13

1.1.6. MULTICOMPONENT ADSORPTION ISOTHERMS 14

1.1.6.1. IAST THEORY 14

1.1.7. ADSORPTION KINETIC 15

1.2. EXPERIMENTAL PROCEDURE 17

1.2.1. MATERIALS 17

1.2.2. PROCEDURE 17

1.2.2.1. ADSORPTION AT AMBIENT PRESSURE 17

1.2.2.2. ADSORPTION AT MILD PRESSURE 18

1.2.3. CHARACTERIZATION 20

1.3. RESULTS AND DISCUSSION 21

1.3.1. EXPERIMENTAL METHOD VALIDATION 21

1.3.2. CHARACTERIZATION 21

1.3.2.1. MOISTURE DETERMINATION 21
1.3.3. ADSORPTION CAPACITY 22
1.3.3.1. ZEOLITE TYPE EFFECT 23
1.3.3.2. EFFECT OF THE WATER CONCENTRATION IN ADSORPTION 23
1.3.3.3. EFFECT OF THE TEMPERATURE IN THE ADSORPTION CAPACITY AT 0.83 ATM. 24
1.3.3.4. EFFECT OF THE NUMBER OF COMPONENTS 25
1.3.3.5. REGENERATION OF THE WATER CAPACITY ADSORPTION IN ZEOLITE 4A 27
1.3.4. ADSORPTION ISOTHERMS 28
1.3.4.1. ADSORPTION ISOTHERM FOR THE DIFFERENT ZEOLITES 28
1.3.4.2. EFFECT OF THE TEMPERATURE IN THE WATER ADSORPTION ISOTHERM 29
1.3.4.3. EFFECT OF THE PRESENCE OF CO_2, ETHANOL, METHANOL, DEC AND DMC IN THE ADSORPTION ISOTHERM 30
1.3.4.4. EFFECT OF THE PRESSURE IN THE WATER ADSORPTION CAPACITY ... 36
1.3.5. ADSORPTION KINETIC 36
1.3.5.1. KINETIC PARAMETERS OF DIFFERENT TYPE OF ZEOLITES 37
1.3.5.2. KINETIC PARAMETERS OF WATER, ETHANOL AND METHANOL IN ZEOLITE 4A AT DIFFERENT TEMPERATURE AND MIXTURES WITH ANOTHER COMPOUND. 39
1.3.5.3. MIXTURES WITH THREE AND FOUR COMPONENTS 40
1.3.5.4. IAST THEORY APPLICATION 41
1.3.5.5. EXPERIMENTAL ERROR 41
1.3.6. CHARACTERIZATION OF ZEOLITE 4A 47
1.3.6.1. ANALYSIS EDS 47
1.3.6.2. SEM 47
1.3.6.3. XRD ANALYSIS 47
1.4. PARTIAL CONCLUSIONS 50
CHAPTER 2 52
DIRECT SYNTHESIS OF DIETHYL CARBONATE (DEC) AND DIMETHYL CARBONATE (DMC) USING COPPER-NIQUEL CATALYST ON ACTIVETED CARBON (CU-NI/AC) IN THE PRESENCE OF ZEOLITE 4A 52
2.1. INTRODUCTION 52

2.1.1. MAIN APPLICATIONS LINEAR CARBONATES 52
2.1.1.1. SOLVENT 53
2.1.1.2. REACTANT 53
2.1.1.3. PHARMACEUTICAL PRODUCTS 53
2.1.1.4. OXYGENATE FUELS 54
2.1.1.5. RECHARGEABLE LITHIUM BATTERIES 54
2.1.2. METHODS TO PRODUCE DEC AND DMC IN GAS PHASE 54
2.1.2.1. PHOSGENATION 54
2.1.2.2. OXIDATIVE CARBONYLATION 55
2.1.2.3. METHYLNITRITE CARBONYLATION 56
2.1.2.4. UREA ALCOHOLYSIS 56
2.1.3. DIRECT SYNTHESIS FROM CO_2 AND ALCOHOL 57
2.1.4. POSSIBLE MECHANISMS FOR DMC AND DEC SYNTHESIS 64
2.1.5. USE OF CO_2 AS RAW MATERIAL 65
2.1.6. ALTERNATIVES TO SHIFT THE EQUILIBRIUM CONVERSION 66
2.1.7. COPPER – NICKEL CATALYST SUPPORT ON ACTIVATED CARBON 67
2.1.8. IMPORTANCE OF THE CATALYST PREPARATION 68
2.2. EXPERIMENTAL PROCEDURE 70
2.2.1. MATERIALS 70
2.2.1.1. CATALYST PREPARATION 70
2.2.1.2. ADSORBENTS 70
2.2.1.3. REACTION 71
2.2.2. CATALYST PREPARATION 71
2.2.2.1. PRETREATMENT OF ACTIVATED CARBON 71
2.2.2.2. INCREASE OF THE PARTICLE SIZE BY PELLETIZING 71
2.2.2.3. IMPREGNATION OF NI AND CU 72
2.2.2.4. CATALYTIC TEST IN GAS PHASE 73
2.2.3. CATALYTIC TEST IN LIQUID PHASE 75
2.2.4. CATALYST CHARACTERIZATION 76
2.3. RESULTS AND DISCUSSION 77
2.3.1. CATALYTIC ACTIVITY IN GAS PHASE 77
2.3.1.1. EFFECT OF THE REACTION TEMPERATURE IN THE CARBONATES YIELD 77
2.3.1.2. CATALYTIC ACTIVITY IN GAS PHASE FOR ASSEMBLY CATALYST – ADSORBENT 78
2.3.2. CATALYTIC ACTIVITY IN LIQUID PHASE FOR DEC AND DMC 79

2.3.2.1. RESULTS IN PRESENCE OF CATALYST (100 AND 200 G) 79
2.3.2.2. CATALYTIC ACTIVITY IN LIQUID PHASE FOR ASSEMBLY CATALYST – ADSORBENT 80
2.3.3. CATALYST REUSE TEST 81
2.4. CATALYST CHARACTERIZATION 81
2.4.1. PHYSICOCHEMICAL PROPERTIES OF CATALYST 81
2.4.1.1. XRD 82
2.4.2. TGA 86
2.4.3. SEM 86
2.4.4. EDS ANALYSIS 89
2.4.5. TEM 90
2.4.6. TPR ANALYSIS 91
2.5. PARTIAL CONCLUSIONS 91
GENERAL CONCLUSIONS 93
RECOMMENDATIONS 95
APPENDIXES 104

LIST OF FIGURES

Figure 1 LTA unit cell [26]....9
Figure 2 Adsorption isotherm of water vapor on different porous materials taken at 25 °C the saturation pressure being p_o=3.1kPa [27]....11
Figure 3 Types of physisorption isotherms [17]....12
Figure 4 Adsorption – desorption scheme with mass spectrometry detector (Based on Cortés et al.) [28]....18
Figure 5. Scheme high pressure....18
Figure 6 Experimental results with Mass Spectrometry (adsorption and desorption).....19
Figure 7 Scheme for the different mixtures tested.....20
Figure 8 Desorption profile of water at 12.28 mbar and 321 K on zeolite 13X (a) This work; (b) reported by Cortés et al [22]....21
Figure 9. Area under curve, Origin-Pro....22
Figure 10 Effect of the regeneration of the water capacity adsorption in zeolite 4A. Adsorption conditions water concentration: (2.3 % mol), zeolite A (80 mg), 92 °C, 0.84 atm.....28
Figure 11 Experimental adsorption process....28
Figure 12 Adsorption isotherm....28
Figure 13 Water isotherms in LTA zeolites. Adsorption conditions: water concentration (2.3 % mol), zeolite A (80 mg), 92° C, and 0.83 atm.....29
Figure 14 Effect of temperature in the water isotherm in zeolite 4A. Adsorption conditions: water concentration (2.3 % mol), zeolite A (80 mg), 92° C, and 0.83 atm....30
Figure 15 Water adsorption isotherm in water – ethanol mixture....31
Figure 16 Water adsorption isotherm in water – methanol mixture....31
Figure 17 Water adsorption isotherm in water – DEC mixture....32
Figure 18 Water adsorption isotherm in water – DMC mixture....32
Figure 19 Water adsorption isotherm in water – CO_2 mixture....32
Figure 20 Water adsorption isotherm at 92°C....33
Figure 21 Water adsorption isotherm in water – ethanol mixture at 92 °C....33
Figure 22 Water and ethanol adsorption isotherms in water, ethanol, DEC and CO_2 mixture at 92 °C.33
Figure 23 Effect of temperature in the ethanol isotherm in zeolite 4A. Adsorption conditions: ethanol concentration (1.4 % mol), zeolite A (80 mg), 92° C, and 0.83 atm....35
Figure 24 Ethanol adsorption isotherm in water – ethanol mixture....35
Figure 25 Effect of temperature in the methanol isotherm in zeolite 4A. Adsorption conditions: methanol concentration (12.9 % mol), zeolite A (80 mg), 92° C, and 0.83 atm....35
Figure 26 Methanol adsorption isotherm in water – methanol....35
Figure 27 Water adsorption capacity of zeolite 4A. Adsorption conditions: water concentration (XX % mol) and zeolite A (80mg)....36
Figure 28 Intra particle diffusion model adjust for water.....37
Figure 29 Comparison of the experimental and predicted water adsorption capacity of zeolite 4A for determining the values error.....46
Figure 30 Comparison of the experimental and predicted ethanol adsorption capacity of zeolite 4A for determining the values error.....46

Figure 31 Comparison of the experimental and predicted methanol adsorption capacity of zeolite 4A for determining the values error. 46
Figure 32 SEM analysis of Zeolite 4A 47
Figure 33 XRD zeolite 4A used in mixture of four components at 200°C. (a) Mixture: *water, ethanol, DEC and CO_2*; (b) Mixture: *water, methanol, DMC and CO_2* (c) Pattern of zeolite 4A [54]....48
Figure 34 XRD zeolite 4A used in mixture of two components at 200°C. (a) Mixture: *CO_2 - ethanol* (b) Mixture: *CO_2 - methanol.* (c) Pattern of zeolite 4A 48
Figure 35 XRD zeolite 4A used in a mixture two components at 200°C. (a) Mixture: *water - ethanol* (b) Mixture: *water - methanol* (c) Pattern of Zeolite 4A....49
Figure 36 Comparison between zeolite 4A used at 14 Bar and fresh at 1 Bar. (a) Used. (b) Fresh....49
Figure 37 Change of color in zeolites 4A used. (a) fresh zeolite 4A; (b) After methanol adsorption; (b) After CO_2 adsorption 50
Figure 38 Global DMC consumption by end use....53
Figure 39 Phosgenation....54
Figure 40 Phosgenation reaction....55
Figure 41 Oxycarbonylation of DEC....55
Figure 42 Oxycarbonylation of DMC....55
Figure 43 Methylnitrite Carbonylation of DEC 56
Figure 44 Methylnitrite Carbonylation of DMC 56
Figure 45 Urea alcoholysis of DEC....56
Figure 46 Urea alcoholysis of DMC....57
Figure 47 Direct synthesis from alcohol and CO_2 without dehydration systems [84]. 60
Figure 48 Non-reactive dehydration systems for organic carbonate synthesis from CO_2 and alcohol [84]. 61
Figure 49 Non-catalytically reactive dehydration systems for organic carbonate synthesis from CO_2 and alcohol [84]. 62
Figure 50 Catalytically reactive dehydration systems for organic carbonate synthesis from CO2 and alcohol [84]. 63
Figure 51 Catalytic mechanism for direct synthesis DMC from CH_3OH and CO_2 over Cu–Ni/graphite nanocomposite catalyst (M: Cu, Ni or Cu–Ni alloy) [86]....64
Figure 52 Possible mechanism for direct synthesis of DEC from ethanol and CO_2 ove r Cu–Ni/AC (M: Cu, Ni or Cu–Ni alloy) [12] 65
Figure 53 Alternatives to increase equilibrium conversion in direct synthesis linear carbonates from alcohols and CO_2 [8]. 66
Figure 54 Reaction system setup for gas phase synthesis of DMC from methanol and CO_2. (1) CO_2/He gas mixture, (2) pressure reducer, (3) mass flow control (MFC), (4) bubbler containing methanol, (5) valve, (6) pressure gauge, (7) Oven (Temperature Control), (8) tubular fixed-bed reactor (7 mm I.D), (9) check valve, (10) Control Valve, (11) MS Spectrometer (ThermoStar QMS 200, Pfeiffer), (12) Data Processor [81]....74
Figure 55 Catalyst – zeolite 4A assemblies evaluated (a) fixed bed: catalyst/adsorbent; (b) fixed bed: catalyst/adsorbent/catalyst/adsorbent; (c) Single bed; (d) Fluidized bed....74
Figure 56 Parr reactor (1) Stirring system, (2) Pressure Gauge, (3) Temperature Gauge, (4) gas inlet, (5) reactor, (6) jacket heating, (7) Temperature controller, and (8) CO_2 Cylinder....75
Figure 57 Effect of the temperature and pressure variation in the DMC yield using Cu-Ni/AC 78

Figure 58 Effect of the temperature in the DEC yield using Cu-Ni/AC 78
Figure 59 Reuse of Cu-Ni (2.1)/AC catalyst in DMC gas phase reaction. Conditions: 150°C, 14 Bar. ..81
Figure 60 XRD patterns of (a) CA; (b) Cu:Ni (2:1); (c) Cu:Ni (3:1); (d) Cu:Ni (2:1) used in gas phase; (e) Cu:Ni (3:1) used in gas phase; (f) Cu:Ni (2:1) used in liquid phase; (g) Patter cu/AC Ni/AC.....84
Figure 61 XRD patterns of (a) fresh catalyst; (b) Used gas phase; (c) Used mixture catalyst/zeolite gas phase; (d) Used liquid phase; (e) Used mixture catalyst/zeolite liquid phase; (f) Patter cu/AC Ni/AC .85
Figure 62 TGA profiles of Cu-Ni/AC catalysts.....86
Figure 63 SEM images of (a) AC; (b) Fresh Cu-Ni/AC; (c) Used Cu-Ni/AC gas phase;(d) Cu-Ni/AC (2:1) used in liquid; (e) Cu-Ni/AC (2:1) used in liquid phase.....87
Figure 64 Particle size distribution for fresh Cu:Ni/AC catalyst.....88
Figure 65 Cu-Ni/AC catalyst /Zeolite 4A used mixture. (a) Gas phase: Cu-Ni (2:1)/AC – Zeolite 4A; (b) Liquid phase: Cu-Ni (2:1)/AC – Zeolite 4A; (c) Liquid phase: Cu-Ni (3:1)/AC – Zeolite 4A.....88
Figure 66 Particle size distribution mixture: Cu-Ni/AC catalyst – Zeolite 4A. Used. Liquid phase. Molar ratio: 3:1.....89
Figure 67 EDS pattern for Cu-Ni (2:1)/AC 89
Figure 68 EDS pattern for Cu-Ni (2:1)/AC 89
Figure 69 TEM images for (a) Cu-Ni/AC (2:1); (b) Cu-Ni/AC (3:1); (c) Cu-Ni/AC (2:1) used gas phase; (d) Cu-Ni/AC (2:1) used liquid phase; (e) Cu-Ni/AC (3:1) used liquid phase. 90
Figure 70 TPR analysis of Cu-Ni (2:1)/AC fresh and used.....91

LIST OF TABLES

Table 1 Types of zeolite A and properties [24], [18] 9
Table 2 Adsorption parameters by methanol, CO_2 and water over zeolite 4A [32] 12
Table 3 Multicomponent Isotherm models 14
Table 4 Equations and parameters for kinetic models 15
Table 5 Moisture for different type of zeolites 21
Table 6 Water adsorption capacity for different kind of zeolites A (LTA) at 92°C. 23
Table 7 Effect of the water percent variation in the drag water adsorb at 92°C using Zeolite 4A 23
Table 8 Effect of temperature variation in the adsorption capacity of zeolite 4A 24
Table 9 Adsorption capacity of zeolite 4A in multicomponent mixtures (92°C) 26
Table 10. Adsorption capacity of zeolite 4A in multicomponent mixtures (150°C) 26
Table 11 Adsorption capacity of zeolite 4A in multicomponent mixtures (200°C) 27
Table 12 Kinetic Parameters by different type of zeolites. 38
Table 13 Kinetic parameters for mixtures between water and other compound 42
Table 14 Kinetic parameters for mixtures between ethanol and other compound 43
Table 15 Kinetic parameters for mixtures between methanol and other compound 44
Table 16 Kinetic parameters for water in the mixture: water, ethanol and CO_2 45
Table 17 Kinetic parameters for water in the mixture: water, methanol and CO_2 45
Table 18 Kinetic parameters for water in the mixture water- ethanol - DEC - CO_2 45
Table 19 Kinetic parameters for water in the mixture water- methanol - DMC - CO_2 46
Table 20 EDS analysis of zeolite 4A 47
Table 21 Direct synthesis of linear carbonates (previous work) 67
Table 22 Yield to DMC with the assembly system catalyst – zeolite 4A 78
Table 23 Conversion, Selectivity and yield in DEC synthesis 79
Table 24 Conversion, Selectivity and yield in DMC synthesis 80
Table 25 Conversion, selectivity and yield results in liquid phase DMC 80
Table 26 Conversion, selectivity and yield results in liquid phase DEC 80
Table 27 ASS for Cu-Ni/AC catalysts 82
Table 28 BET surface area of Cu-Ni/AC catalysts before and after use 82

APPENDIXES

Appendix 1 Zeolites references [96] [97] 104
Appendix 2 Conversion of concentration units (% Vol.) at μmol/gs 104
Appendix 3 Conversion % to μmol/gs 105
Appendix 4. Antoine Constants [98] 105
Appendix 5 Mass characteristics pattern used in mass spectrometer 106
Appendix 6 Calibration factor (the compounds percent). 106
Appendix 7 Isotherms two compounds 107
Appendix 8 Three components adsorption isotherms 109
Appendix 9 Four components adsorption isotherms 110
Appendix 10 Kinetics 111
Appendix 11 Chemical and physical properties of DEC and DMC 113
Appendix 12 Data of import and export market 115
Appendix 13 Description catalyst preparation of Cu-Ni/AC (3:1) catalyst (20% total load) 116
Appendix 14 Solutions preparations 117
Appendix 15 Preparation by incipient wet impregnation method for Cu-Ni catalyst support on active carbon. 118
Appendix 16. Calibration curves liquid phase (concentration vs. area under the curve) 119
Appendix 17 Chromatograph injection method 119

GENERAL INTRODUCTION

Dimethyl carbonate and diethyl carbonate (DMC and DEC, respectively) are nontoxic and biodegradable compounds with a wide industrial application [1]; DMC is used in the production of polycarbonate covers, in the synthesis of polyurethanes, fuel additives, carbonating and alkylating reagents, and as a green polar solvent [2]. DEC is used in the synthesis of biologically active molecules, farm products and polycarbonates, electrolyte in lithium batteries, raw material for manufacturing polycarbonates, green solvent and as an intermediate for various pharmaceutical products [3]. Both compounds, DMC and DEC, could be able to reduce emissions from gasoline and diesel engines. Due to the DEC high oxygen content (40.6 wt.%), it is considered a better candidate than ethanol for replacing methyl tertbutylether (MTBE) as additive in gasoline [4]. Compared with DMC, DEC has a higher energy content, a lower vapor pressure, a better distribution into gasoline versus water, and a safer hydrolysis products [5]. In addition, the interest towards the production of DEC is increased in the last years as it can be consider as bio-sourced compound derived from bioethanol with high environmental value [6]. In general, the use of carbonates as solvents due to their low toxicity and monomers to form polymers supposes a great increase of their demand on the world; the open market of DMC is around 110 Kt/year [6]. The multiple applications of these lineal carbonates show their importance at current time and the potential in future with higher economic benefits.

Current industrial methods for the production of DMC and DEC require the use of toxic, corrosive, flammable and explosive reactants. There are several methods for the production of lineal carbonates such as phosgenation, oxidative carbonylation, decarbonylation, transesterification of cyclic carbonates or acyclic carbonates, alkylation of carbonate salts, and transesterification of urea [7]. All these methods offer high yields to DMC and DEC but the operational costs and the use of very toxic raw materials make them unattractive.

Direct synthesis using carbon dioxide (CO_2) and methanol or ethanol, also known as dehydrated condensation with CO_2 (Reaction 1 and 2, respectively) is an interesting way since those are safe and clean compounds [1], [8]. The use of CO_2, main responsible of greenhouse effect, allows also reducing its emissions.

$$\mathbf{2CH_3OH + CO_2 \rightleftharpoons (CH_3O)_2CO + H_2O} \qquad \textbf{Reaction 1}$$

$$\mathbf{2C_2H_5OH + CO_2 \rightleftharpoons (C_2H_5O)_2CO + H_2O} \qquad \textbf{Reaction 2}$$

The current compounds used in the direct synthesis are: phosgene, isocyanates, hydrogen and CO [9]. However, the yield achieves in the direct synthesis are quite low due to the limited equilibrium conversion (around 2%) [6] and CO_2 is highly thermodynamically stable and kinetically inert [10].

For improving the yield in direct synthesis it has been proposed the use of high pressures (from 30 to 300 Bar) but this procedure is impractical at industrial level and expensive. Other option is the use of catalysts such as organometallic compounds, metal tetra-alkoxides, alkali metals, ZrO_2, BF_4/CH_3ONa, (Cu-KF)/MgSiO, $H_3PW_{12}O_4$-ZrO_2, Mg/smectite, (Cu-Ni)/VSO and Cu-(Ni, Mo, O)/SiO_2, however all those have been deactivated by the water produced during the reaction [11]. The most recent research suggests the use of copper – nickel supported on activated carbon (Cu-Ni /AC) at moderate pressures (P < 1.2 MPa) as good system for obtaining these DMC and DEC carbonates with yields near to 5 % and selectivities higher than 90% at moderate temperature and pressure (T<150 °C and P<10 bar) [12].

In the other hand, with the use of dehydrating agents such as molecular sieves, magnesium oxide and organic agents like acetals is possible to shift the equilibrium conversion towards the products. Sakakura et al. had reported the use of acetals as dehydrating agents in the direct synthesis of DMC with butyltin dimethoxide ($Bu_2Sn(OMe)_2$) as catalyst obtaining yields to DMC around 40 % (180°C, 300 bar) [8]. Also, the use of high pressure (30 MPa) showed an increase in the DMC yield until 55% using acetal as dehydrating agent and $TiO(Me)_4$ + polyether as catalyst [13]. Using the system dibutyltin dimethoxide as catalyst in the presence of a zeolite 3A (dehydrating agent) at 30 MPa and 180 °C the yield to DMC was around of 46 % [13]. However, those options are expensive and difficult to control at industrial level. Lower pressures are desired for this system, in that sense an increment to 17 % to DMC was obtained using a ZrO_2 catalyst with zeolite 3A (dehydrating agent) in a autoclave reactor at 248 K and 4.2 MPa [14]. Similarly, in the synthesis of DEC from ethanol and CO_2 over CeO_2 and butylene oxide (as dehydrating agent) an improvement of the yield of 9-fold to DEC (from 0.28 to 2.5 mmol to DEC) at 180 °C and 9 MPa was reported [9]. Currently, some technologies use zeolites as dehydrating agents or integrated with membrane reactors. The zeolite adsorption is a widely employed in industrial processes in which water must be removed; zeolites that has been used for obtaining anhydrous alcohol and gas drying [15].

Until moment, there are not registers about the addition effect of the zeolite A as dehydrative agent in the direct synthesis of DEC and DMC using Cu-Ni/AC at mild conditions. For the direct synthesis, almost all experiments have been reported in catalytic liquid phase and/or under high pressure (supercritical conditions), with the aforementioned disadvantages [16].

In this work it was analyzed the effect of the combination of a catalytic system with an adsorbent (zeolite 4A) in the direct synthesis of DEC and DMC. This report is divided in two parts: (1) the mono-component and multi-component adsorption analysis and (2) the direct

synthesis of DMC and DEC using Cu-Ni/AC catalyst in the presence of the drying agent (zeolite A and organic agent).

First chapter shows the effect in the adsorption capacity when water, CO_2, ethanol, methanol, DEC, DMC pass through a bed of zeolite A in order to analyze if these compounds are adsorbed on the zeolite at different conditions of temperature and pressure. Mixtures of these compounds (two, three and four components), adsorption capacity, isothermal adsorption and kinetic of adsorption of water, ethanol and methanol in zeolite 4A will be also studied, since they could change the water adsorption capacity of zeolite.

In the second chapter will be presented the results of the direct synthesis in liquid and gas phase without dehydrated. They represent the best operation conditions: phase, pressure, temperature, feed and composition that produce the best carbonate yield. This chapter presents the assembly between Cu-Ni/AC catalyst and zeolite A as dehydrated agent too. The reactions will be made in gas phase with different configurations (separate fixed bed, single fixed bed and fluidized beds) as strategy to improve the carbonate yield. Reactions in liquid phase will be performed with organic and inorganic agents. These changes will be evaluated for determining their effect in the direct synthesis of DMC and DEC under mild conditions (1 - 14 Bar and 90°C – 200°C).

SCOPE OF THIS WORK

To develop a novel, safe and environmentally acceptable catalytic systems is the main objective in many research works for DMC and DEC production since the common methods are highly toxic and pollutants, highlighting the phosgene use as a major drawback. The high production of CO_2 with known environmental consequences (global warming, ozone layer reduction, and greenhouse effect), implies necessity to decrease its emissions. For this reason, the use CO_2 as a raw material in the synthesis of these carbonates could help. However, the necessary change in the pathway production forces the scientific community to improve a better option.

Direct synthesis is an option that satisfies environmental standards but, it does not have the yield required until moment, however the yields are still low. The most recent research suggests the use of Cu-Ni/AC catalyst at moderate pressures ($P < 1.2$ MPa) as good system for obtaining these carbonates. Many studies also show the advantages of zeolite A as dehydrating agents but its behavior into the direct synthesis reaction at the same conditions, in presence of the CO_2 excess, another compounds and the Cu-Ni/AC catalyst it is unknown.

The question of this research work will be: How could the presence of a zeolite 4A modify the yield to DMC or DEC produced by direct synthesis used Cu-Ni/AC catalyst under mild conditions?. This work provides valuable experimental data about the effect of integration of molecular sieve such as zeolite A with Cu-Ni/AC catalyst. As well as the adsorption and desorption multicomponent curves will give a novel data since the information available is poor.

OBJECTIVE

General Objective:

Evaluate the effect of the use of dehydrating agents in the yield to DMC or DEC produce by direct synthesis over Cu-Ni/AC catalyst.

Specific Objectives:

- ✓ Identified the effect of ethanol, methanol, CO_2, DMC, and DEC in the water adsorption capacity of zeolites A.
- ✓ Determine the zeolite A regeneration capacity for the water adsorption during the direct synthesis under mild conditions.
- ✓ Determine the effect in DMC and DEC yield in the presence of a zeolite A.
- ✓ Determine the best conditions of assembly catalyst/adsorbent to produce DMC or DEC by direct synthesis under mild conditions.

PUBLICATIONS

Papers:

- ✓ Hernández E., González L.M.,Villa A.L., "Multicomponent Adsorption Kinetics of compounds involved in the Direct Synthesis of Diethyl carbonate (DEC) and dimethyl carbonate (DMC)", *Article in preparation*

National and international scientific events:

- ✓ Hernández E., González L.M., Villa A. L., "*Actividad del sistema catalizador Cu-Ni/CA – Zeolita 4A en la síntesis directa de carbonato de dimetilo*". XXVIII Congreso Colombiano de Ingeniería Química (CCIQ), 28-30 de octubre de 2015, Bogotá D.C., Colombia. (Poster).
- ✓ Hernández E., Alcántara V., González L.M., Villa A. L., "*Adsorption of water in the multi-component system used in the synthesis of linear carbonates*". 2do Simposio Iberoamericano de Adsorción (IBA), 27-30 de abril de 2015, Cartagena, Colombia. ISBN 978-958-8530-84-0. (Oral).
- ✓ Hernández E., Alcántara V., González L.M., Villa A. L., "*Determinación de la capacidad de adsorción de agua de la zeolita 4A mediante espectrometría de masas*". Optimización de procesos y recursos para un desarrollo sostenible (parte 1). XXVII Congreso Interamericano y Colombiano de Ingeniería Química (CIIQ), 06-08 de octubre de 2014, Cartagena, Colombia. ISBN 978-958-58438-0-6. (Oral).

CHAPTER 1

MULTICOMPONENT ADSORPTION OF CARBON DIOXIDE (CO_2), ETHANOL, METHANOL, WATER, DIETHYL CARBONATE (DEC) AND DIMETHYL CARBONATE (DMC) MIXTURES ON ZEOLITE 4A.

1.1. INTRODUCTION

The zeolites are molecular sieves able to adsorb water. The adsorption characteristics of zeolites are largely based on their aluminosilicate framework based structure, where $[SiO_4]^{4-}$ and $[AlO_4]^{5-}$ tetrahedra are linked to each other by sharing the oxygen atoms at the corners. The framework has a negative charge when aluminum is incorporated in the zeolite structure, which is compensated by cations, such as Na^+, K^+, Ca^{2+} or H^+. So, the crystalline aluminosilicates have a three-dimensional interconnecting network of silica and alumina tetrahedrons. Aluminum in the structure makes zeolites hydrophilic: the lower the Si/Al ratio of the zeolite, the higher its hydrophibicity [17]. Zeolites can be classified by number of oxygen in the ring (8, 10 or 12), dual pore and mesoporous systems [14]. The size of the channels and cages in different zeolites covers a wide range, and accordingly, the type of molecules that can penetrate and get absorbed varies widely [14].

Zeolites have excellent adsorption and molecular sieving properties, making them good candidates for catalysis and adsorption [18]. Small pore zeolites have gained especially increasing interest in application fields such as selective gas adsorption selective membrane separation and ion-exchange agents because of their high selectivity of adsorption and transportation for small size molecules [14]. The adsorption of gases and vapors by zeolites is important in the field of gas separation, purification and the removal of environmentally harmful components form waste streams. In industrial applications, zeolites have attracted a lot of attention because of possessing the superior separation performance and low cost [19].

Zeolites retain their adsorption capacity at higher temperatures and show higher selectivity to water. Zeolites 3A, 4A and 5A showed the highest adsorption capacity for water. These zeolites have Linde

Type A (LTA, zeolite A) structure and they are synthesized with low Si/Al ratios to favor its hydrophilic character [20], thus the zeolites allow to adsorb large quantities of steam at low partial pressures [21].

The zeolite A is common used in order to adsorb water, but, it could able to adsorb another compound present in the reaction mixture to produce linear carbonates. In this chapter it must be answered: Is zeolite A able to adsorb methanol, ethanol, DMC, DEC or CO_2? and Could the presence of those compounds modify the water adsorption capacity of zeolite A?. To know the adsorption behavior of all components that will be present in the direct synthesis reaction allows understanding the actual adsorption capacity of zeolite A, and, validated if the other compounds could be adsorbed and reduce the water adsorption capacity of zeolite A.

For other side, it is important to highlight that this chapter present an interest methodology, the use of mass spectrometry in order to calculate the adsorption behavior. This is a novel, exact and simple way to obtain the adsorption capacities and isotherms for one or several compounds [22]. Also, this chapter presents information about the effect temperature and pressure change in the water adsorption as well as regeneration, type of zeolite A and vapor of water effect.

1.1.1. Characteristic of zeolites A

Zeolite A is a typical small-pore zeolite which was widely used (dehydration agents for separation processes, additives for detergents, adsorptions and membranes). Currently, it has the biggest production scale among all small-pore zeolites [14]. Zeolite type A is widely use because is cheap, ready available, easy to handle, and recyclable [9]. The use of zeolite A is recommended when there must be a control of the final moisture in the medium [15]. In this work, the use of zeolite A as water trap for shifting chemical equilibriums is really important.

All zeolites A have the same structure but they have a different compensation cations such as Na^+, K^+, Ca^{2+} or H^+ and they showed a bigger difference in their use as adsorption agents, especially for water in low alcohols (see Table 1). The change in the compensation cation influences the way that zeolites can only absorb molecules whose kinetic diameter or minimum cross sectional diameter is smaller than the pore openings of zeolites [18] [23]. However, studies have indicated that 3A zeolites absorb large amounts of methanol at certain conditions, whose kinetic diameter is 3.6 Ångstroms, being already larger than the acknowledged pore opening dimension of 3A zeolite [14]. This exception generates the necessity to verify the study conditions (adsorption and temperature and pressure dependences). Other properties for zeolites used in this study are shown in Appendix 1.

Table 1 Types of zeolite A and properties [18][24]

Zeolite	3A	4A	5A
Pore diameter (Å)	3	4	5
Moisture (%)	< 2	< 2	< 2
Compensation cation	K^+	Na^+	Ca^{2+}
Water capacity (%)	20.0	28.5	28.0
Bulk density (lb/ft^3)	40	50	45

Type 3A is the potassium form of the compound; it adsorbs molecules that have a critical diameter of less than three Ångstroms. For example: water (2 Å), helium, hydrogen, and carbon monoxide (CO). Type 4A has sodium as compensation cation; it absorbs molecules having a critical diameter of less than four Ångstroms, such as ammonia. Type 5A is the calcium form of molecular sieves. This zeolite adsorbs molecules such as methanol, ethane, and propane, as well as species with less a 5 Å of diameter. All three zeolites (3A, 4A and 5A) have the same Si/Al ratio = 1 [25].

Adsorption capacity of the zeolites is also showed in Table 1, according with those data the theoretical adsorption capacity (q_{max}) should be roughly 20 - 28% by weight. Analyzing, the water adsorption capacity increasing in the sequence 3A < 5A < 4A, indicating that $K^+/Na^+/Ca^{2+}$molar ratio affect the water adsorption capacity.

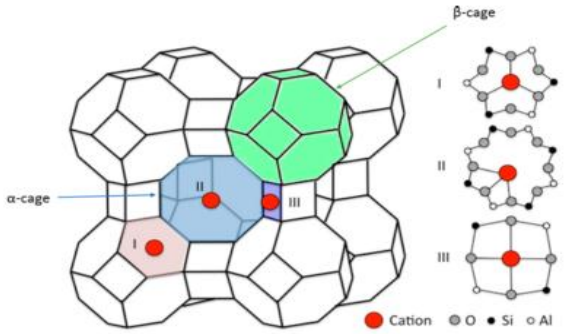

Figure 1 LTA unit cell [26]

Figure 1 shows a graphical representation of the Zeolite A (LTA unit cell). For hydrated sodium type or fully K^+ exchanged zeolite A, the statistical location sites of cations are almost identical. Among these 12 sodium cations in the unit cell eight are displaced by 0.2 Å into the α-cage from the center of six-membered rings (site I). Three Na^+ are locate in the plane of 8-membered rings 1.2 Å of the center (site II). The twelfth Na^+ is located in the center of the α-cage and is coordinated with water molecules (site III). For fully K^+ exchanged A, the statistical location sites are almost the same and the differences are related to minor variations of the distances from sites I to the center of six-membered rings, and from sites II, which are occupied by K^+ cations near the center of the eight-membered rings [26].

1.1.2. Methods to calculate adsorption

There are different methods to measure the adsorption isotherms: Volumetric, gravimetric, oscillometric and electroscopy impedance [27]. The latter two are not suitable for zeolite adsorption. Oscillometric method is recommended for polymeric substance which finds substantial changes in mass and allows the analysis of the mass inertia to detect changes due to the adsorption of gas. Electroscopy impedance is useful for analyzing the adsorption in heterogeneous energy materials that present high values of impedance or resonance phenomena in the molecules. The water adsorption in zeolite has frequencies in the range of GHz and THz, which are low for the method. Furthermore, the spectrum of the pore of adsorbent material cannot be easily detected by dielectric permittivity measurements as need electrical fields that with high frequency (near infrared) which are strongly absorbed by radiation or material [27].

The volumetric or manifold method is widely used for the measurement of pure gas adsorption. To analyze multicomponent mixtures the assembly must be complemented with a gas analyzer (chromatograph or mass spectrometer) to find the balance of adsorption. The assembly is simple and allows variety in the measure unit (pressure, temperature) but, it is not good for measure of little ranges (milligrams is able to use gravimetric method) and require long times, possible wall adsorption and it do not present kinetic information [27]. The gravimetric method must be the most appropriate option. Through highly sensitive microbalances can be measure with greater accuracy. The method is used to characterize porous media, measurement of adsorption equilibrium for gases and adsorption kinetics. The main problem is the high cost and complex procedure [27].

So, this work presents an interesting option in order to obtain the adsorption information: the use of mass spectrometry based on previous reports [28]. This is a simple and economic way to obtain the data. The equipment allows to know the quantities adsorbed and desorbed for mono or multicomponent systems each second. The units shown by mass spectrometry could be recalculated in order to evaluate adsorption capacities and isotherms for water and other compounds and their mixtures (see Appendix 2 Conversion of concentration units (% Vol.) at μmol/gs and Appendix 3 Conversion % to μmol/gs)

1.1.3. Adsorption isotherm

Figure 2 shows a set of adsorption isotherms describing the amount of water vapor adsorbed per unit mass of sorbent at given pressure and temperature of the vapor at T = 298.15 K and relative pressure in the range $0<p/p_0<0.8$ [27]. These curves are characteristic for the hydrophilic behavior of the zeolites. Analyzing, NaX or 13X zeolite and KA or 3A zeolite are the most adsorbents. Both zeolites exhibit type I isotherm shapes with very large Henry's law constants (13X = 20 g/g and 3A > 58g/g). The very strong adsorption of water on these zeolites is caused by interaction of the permanent and large dipole moment of water with a zeolite cation. The Henry's law constant for adsorption of water on KA zeolite is much larger than that for the NaX zeolite due to the smaller cavity of the A zeolite and the higher charge density of the K ion. At higher pressure, the slope of

the isotherm decreases progressively with increasing gas pressure and finally approaches asymptotically the saturation adsorption capacity of the zeolite. The Henry's law constant K decreases with increasing temperature because adsorption is an exothermic process [29]. When increase the partial pressure increase the adsorption capacity of zeolite until it saturation[18].

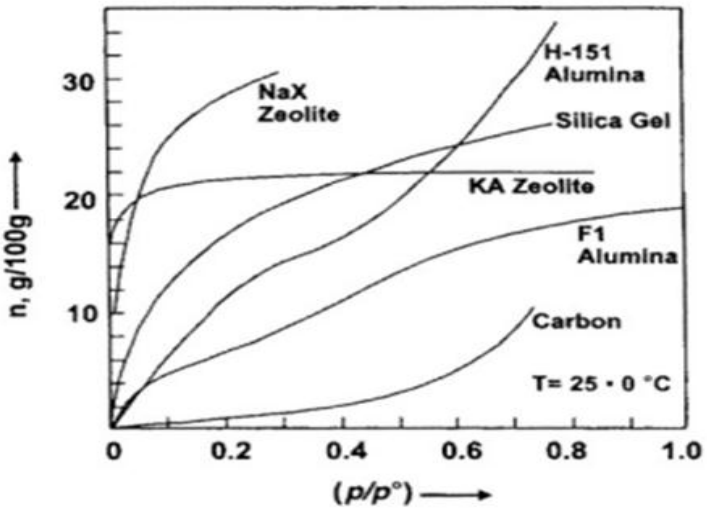

Figure 2 Adsorption isotherm of water vapor on different porous materials taken at 25 °C the saturation pressure being p_o=3.1kPa [27]

According to the IUPAC (International Union of Pure and Applied Chemistry) the classification of physisorption isotherm types for gaseous component adsorption on porous adsorbents are six (Figure 3) [17]. Type I is typical for adsorbents with relatively small external surface, such as zeolites, where the limiting uptake is governed by the accessible micropore volume. Due to the wide spectrum of adsorption characteristics that are aimed to be modeled, a number of isotherm formulations have been proposed in the literature for gaseous component adsorption on porous adsorbents [17].

Among the adsorption models, the single-site Langmuir or simply Langmuir adsorption isotherm predicts more accurately the behavior of pure water and ethanol adsorption on zeolite A [30]. Some experimental studies have been carried out on adsorption of water and alcohols in 4A zeolite, and most of them revealed that Langmuir isotherm model fit their data adequately [31]. However, due to the complexity of such experiments, only limited data are available, and research effort on A zeolites is still lacking.

Adsorption data concerning the water and alcohols on various zeolites is presented as a function of P/P_i^{sat} and summarized and results demonstrate that the maximum adsorption loading $q_{i,sat}$ of components on zeolite is practically independent of temperature [17]. The adjustable parameters in the adsorption isotherms are usually determined on the basis of experimental adsorption data, however, they are not many information about pressure effect in the isotherm.

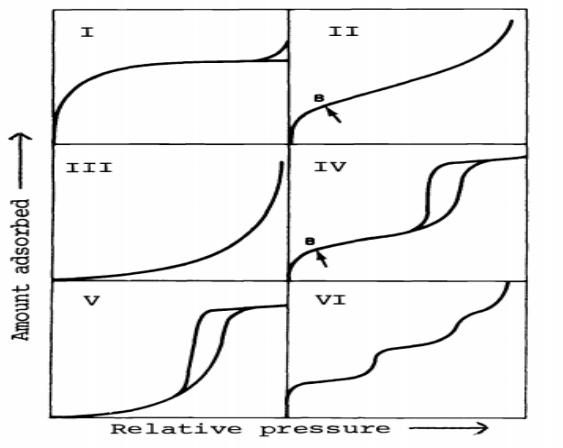

Figure 3 Types of physisorption isotherms [17]

Table 2 shows some parameters and their respective equations. As a result, not only the equilibrium parameter b_i and the dimensionless parameter n, but also the maximum adsorption loading (or saturation loading) q_i^{sat} (mol/kg), it may vary significantly with temperature. However, a significant variation of the q_i^{sat} value on zeolites is confusing, since the saturation loading should be constant and independent of the operating temperature [17]. The dependency of q_i^{sat} is due to adsorbate compound, because the differences in the size, geometry, and affinity [32].

Table 2 Adsorption parameters by methanol, CO_2 and water over zeolite 4A [32]

Specie	Model	Parameter		
Water	**Langmuir**	Preexponential factor	K_0 (KPa-1)	1.5
	$\mathbf{q_i = q_i^{sat}\frac{K_i p_i}{1+K_i p_i}}$ **(Equation 1)**	Adsorption Enthalpy	ΔH_{ads} (KJ/mol)	45
	$\mathbf{K_i = K_0 exp\left[\frac{\Delta H_{ads}}{R}\left(\frac{1}{T}-\frac{1}{T_o}\right)\right]}$ **(Equation 2)**	Saturation charge	q_{sat} (mol/kg)	11.4
		Reference temperature	T_o (K)	363.4
CO_2	**Langmuir – Freundlich**	Preexponential factor	K_0 (atm-1)	0.323
	$\mathbf{q_i = q_i^{sat}\frac{K_i p_i^n}{1+K_i p_i^n}}$ **(Equation 3)**	Adsorption Enthalpy	ΔH_{ads} (KJ/mol)	4.18
		Saturation charge	q_{sat} (mol/kg)	5.043
	$\mathbf{n = a + bT}$ **(Equation 4)**	Parameter a	A	$4.53x10^{-3}$

		Parameter b	B	-1.07
Methanol	**Langmuir** Equations 1 and 2	Preexponential factor	K_0 (Pa-1)	$2.07x10^{-8}$
		Adsorption Enthalpy	ΔH_{ads} (KJ/mol)	52.4
		Saturation charge	q_{sat} (mol/kg)	6.75
Ethanol	**Langmuir** Equations 1 and 2	Preexponential factor	K_0 (Pa-1)	$2.07x10^{-8}$
		Adsorption Enthalpy	ΔH_{ads} (KJ/mol)	50.208
		Saturation charge	q_{sat} (mol/kg)	6.35

**qi*, adsorption charge; *pi*, pressure; *R*, ideal gas constant; *Ki*, adsorption constant

1.1.4. Equilibria adsorption in a multicomponent system

Adsorption is a surface phenomenon where a compound dissolved in one phase is retained on the surface of a solid phase. The substance retained on the surface or adsorbed is called "adsorbate" and the phase where it is retained is called "adsorbent". In this process, a series of parameters such as thermodynamics equilibrium and physicochemical kinetics are important to describe the capacity of adsorption of a component. There are many factors influencing the adsorption process: particle size, contact time, pH, temperature and type of adsorption [33]

1.1.5. Type of adsorption

Adsorption from a solution to a solid occurs as a result of one of the two characteristic properties of a solute – solvent system (or their combination): (1) the solute lyophobic character respects the solvent or a high solute affinity for solid and (2) solute affinity for the solid. Between the adsorbent and the solute the can exist electrical attraction, physisorption, or chemisorption.

The electrical attraction is a process by which ions are concentrated on a surface as a result of electrostatic attraction. When the adsorption takes place with the Van der Waals forces is generally called physical adsorption or physisorption (commonly referred to as "ideal" adsorption), in this case the adsorbed molecule is not fixed in a specific site and the molecule moves free within the surface. Finally, the chemisorption considers that adsorbate suffers chemical interaction or covalent binding with the adsorbent [34].

1.1.6. Multicomponent adsorption isotherms

The adsorption isotherm is a function of the variation of the adsorbate concentration in the bulk solution at constant temperature. When the mixture has two or more adsorbates, the compounds can experience three situations: (1) increase the adsorption, (2) act independently or (3) presents interferences. For multicomponent systems, the models that describe the equilibria process are: (1) Extended Langmuir, (2) Extended and modified Langmuir and (3) Multicomponent Freundlich, Table 3 [34].

Table 3 Multicomponent Isotherm models

Multicomponent Isotherm model	Description	Equation	
Extended Langmuir	Competitive interaction depends of the ratio among the adsorbate concentrations	$q_{e,i} = \frac{q_{máx,i} K_i C_{eq,i}}{1+ \sum_{j=1}^{n} K_j C_{eq,j}}$	**Equation 5**
Extended and modified Langmuir	Add parameters in order to describe the interactions among the adsorbates	$q_{e,i} = \frac{q_{máx,i} K_{a,i} (C_{eq,i}/\eta_i)}{1+ \sum_{j=1}^{n} K_{a,j} (C_{eq,j}/\eta_j)}$	**Equation 6**
Multicomponent Freundlich	Interaction among the compounds	$q_{i} = K_i C_i \left(\sum_{j=1}^{k} a_{ij} C_j\right)^{m_i - 1}$	**Equation 7**

1.1.6.1. IAST theory

Estimation of the multicomponent adsorption isotherm of the gas mixture to describe the behavior of the adsorption loadings of the mixture in the zeolite is very important. Mayers and Prausnitz [35] proposed the theory of Ideal Adsorbed Solution Theory (IAST), which is thermodynamically consistent and allows multicomponent isotherms calculated from the isotherms of individual of each species present in the mixture adsorption. IAST has been successful for multicomponent adsorption equilibria in a wide variety of gas systems [29]. These authors assert that the application of the definition of the change in Gibbs free energy and internal energy in the adsorption corresponds to the same theoretical basis of the volumetric technique used to obtain experimental adsorption isotherms.

The IAST model treats each adsorbed mixture as ideal. This is an interesting theory widely accepted. Using individual isotherm and IAST model supposes the possibility to find an expression to relate the composition of each species in the adsorbed phase with pressure dispersion that is unique and constant [32]. However this model is not accurate in all situations. It has been pointed out that IAST frequently becomes less accurate at high densities of the adsorbed species, even for mixtures that are relatively ideal [35]. For the IAST application it is necessary to make sure about the quality of the single component adsorption data and an excellent curve fitting model [19], [35].

The theory was developed using three major assumptions: (1) adsorbate molecules in the mixture have equal access to the entire surface area of the adsorbent, (2) the adsorbent is homogeneous, and (3) the adsorbed phase is an ideal solution in which interactions between molecules are equivalent in strength [36]

This method has gained industrial relevance because it is used for predicting mixture adsorption as of Langmuir isotherms of pure components without the necessity to include additional parameters in the thermodynamic treatment [17], [30]. Further modifications of the original IAST model, such as the Real Adsorbed Solution Theory (RAST) and the Predictive Adsorbed Solution Theory (PRAST) to account for no ideality of the adsorbate mixture has been proposed as well [30].

The IAST was applied as simulation to describe the multicomponent adsorption isotherm of mixture CO_2 - methanol - water or and CO_2 – methanol – water – DMC from individual adsorption isotherms of the species CO_2, Methanol, water, and DMC in zeolite A [37]. However, other author reports that IAST theory could underestimate the amount of adsorbed water, making very large mistakes for low alcohol solution concentrations. The simulations indicate that, at lower loadings, the adsorbed alcohol molecules can serve as seeds for water adsorption but, at higher loadings, alcohols displace water molecules of their preferred region [38]. The presence of alcohol molecules allows formation of favorable hydrogen bonds with water molecules, leading to water adsorption.

1.1.7. Adsorption kinetic

Adsorption kinetic shows the adsorption adjusting based on experimental data multicomponent systems. The models of kinetics adsorption provide practical information in order to define the behavior of those systems. Adsorption kinetics is one of the most important parameters for determining the adsorption mechanism and also to evaluate the adsorbent efficacy [39].

Four models to predict the adsorption behavior of experimental data are Pseudo First Order (PFO), Pseudo Second Order (PSO), Intra Particle Diffusion (IPD) and Elovich model, and their parameters could be obtained from the slope and intercept as show in Table 4.

Table 4 Equations and parameters for kinetic models

Kinetic Model	Linear form	Equation	Data	Fit type	a	b
PFO	$\ln(q_e - q_t) = \ln q_t - k_1 t$	**Equation 8**	t vs. $\ln(q_e - q_t)$	$a - b * x$	$\ln q_e$	k_1
PSO	$\frac{t}{q_t} = \frac{1}{k_2 {q_e}^2} + \frac{1}{q_e} t$	**Equation 9**	t vs. $\frac{t}{q_t}$	$a + b * x$	$\frac{1}{k_2 {q_e}^2}$	$\frac{1}{q_e}$
IPD	$q_t = k_{dif} t^{\frac{1}{2}} + C$	**Equation 10**	$t^{\frac{1}{2}}$ vs. q_t	$a * x + c$	k_{dif}	
Elovich	$q_t = \frac{1}{\beta} \ln(\alpha\beta) + \frac{1}{\beta} \ln t$	**Equation 11**	$\ln t$ vs. q_t	$a * b + a * x$	$\frac{1}{\beta}$	$\ln(\alpha\beta)$

The mathematical expression for the PFO model is defined as show in Equation 8 where $q_t\ (mg/g)$ is the amount of adsorbed compound at time $t\,(min)$ and $q_e\ (mg/g)$ is the amount adsorbed at equilibrium (adsorption capacity), $k_1(min^{-1})$ is the rate constant of PFO model [40]. This model suggests that the driving force $(q_e - q_t)$ is proportional to the fraction of sites available. The PFO model supposes that each molecule of adsorbent has a unique adsorption site [41].

The PSO model is defined as show in Equation 9. Where $q_t\ (mg/g)$ and $q_e\ (mg/g)$ are the same parameters as the PFO mode and $k_2\ (g/mg \cdot min)$ is the rate constant of PSO model [40]. It assumes that the adsorbate adsorbed on two different sites [41].

The IPD model (Equation 10) allows to know the $k_{dif}\ (mg/g \cdot min^{-0.5})$, the intra particle diffusion constant. This model uses an empiric ratio of time adsorption ($t^{1/2}$) [40]. The hypotheses on the mechanism of diffusion intraparticle inside the pores of the adsorbent particle is based on solute transport through the internal pore structure of the adsorbent and the diffusion itself in solid, leading to that the adsorbent possesses a homogeneous porous structure. When an adsorption process is controlled in the pores, the initial velocity is directly proportional to the solute concentration [41].

Finally, the Elovich model is another useful model applied to the study of kinetics of sorption and its linear form is presented by Equation 11, where α is is the initial adsorption rate $(mg/g \cdot min)$ and β is the desorption constant (g/mg) [42]. This model is generally applicable in chemisorption processes, where the active sites are in the heterogeneous adsorbent and therefore exhibit different activation energies based on a reaction mechanism of the second order for a heterogeneous reaction process [41].

The experimental isotherms obtained by mass balance were fitting with different kinetic models using CFTOOL- MATLAB program. This tool allows obtaining the best fit for each kind of system (mono or multicomponent).

The experimental results obtained by adsorption kinetic are related with the information of the kinetic for water, ethanol, and methanol, respectively. Using the experimental data, the math analysis was to do with the aim to identify the best model to describe the adsorption process. Data were selected for a time equal or larger than 1 minute to reach equilibrium. The best fit was obtained using the experimental isotherm data in order to find the parameters a, b or c for every one with different meaning (see Table 4) and the x in order to express the time. For all data, the temperature of water, ethanol, methanol, DEC, DMC or mixtures among those are 20°C. The temperature of bed of zeolite 4A changes around 36°C, 92°C, 150°C and 200°C.

1.2. EXPERIMENTAL PROCEDURE

1.2.1. Materials

Adsorbents

- ✓ Zeolites 3A, 4A and 5A, Sigma-Aldrich, United States.
- ✓ Zeolite 13X, Micromeritics, United States. This molecular sieve was used to validate the experimental methodology.

All materials were sieved to obtain a particle size of about 512.5 μm.

Adsorbates

- ✓ Carbon dioxide (CO_2) from Praxair 2.8 degree, United States.
- ✓ Helium UAP (99.9995 % purity) from Linde, Colombia.
- ✓ Deionized water Millipore type II, Colombia.
- ✓ Anhydrous DEC (≥ 99% purity) from Sigma-Aldrich, United States.
- ✓ Anhydrous ethanol (purity 99.5%) from JT Baker, United States.
- ✓ Anhydrous DMC (≥ 99% purity) from Sigma-Aldrich, United States.
- ✓ Anhydrous methanol (purity 99.5%) from JT Baker, United States.
- ✓ Argon (99.995 % purity) from Linde, Colombia. It was used as calibration gas.

1.2.2. Procedure

1.2.2.1. Adsorption at ambient pressure

Adsorption capacity evaluation of water, ethanol, methanol, DEC, DMC and CO_2 was performed in chemisorption Autochem II 2920 (Micromeritics, made in United States) couple with Thermostar QMS 200 (Pfeiffer, made in Germany) mass spectrometer, equipped with SEM (Secondary Electron Multiplier) and Faraday detectors (Figure 4). 80 mg of zeolite was placed in a quartz U-tube. Before starting adsorption, zeolites were pretreated at 450 ° C for 4 hours with helium (60 mL/min). A continuous mixture flow of 60 mL/min (Helium-water; Helium-Ethanol; Helium-Methanol; Helium-CO_2; Helium-DMC; Helium-DEC) passed through the zeolite bed. The mixture flow temperature was controlled to ensure a uniform flow (21 °C and 40°C with water and 21°C for others compounds) and the adsorption temperature was maintained constant (36, 92, 150 and 200 ° C) for 2 hours. Subsequently, desorption of the compound was performed. The mixture flow was changed to pure helium flow (60 mL/min) and the zeolite was heated to 450 ° C at a rate of 5 ° C/min. The tests were conducted at ambient pressure (0.85 bar). With the isolation of the lines after the saturator and their temperature 20 ° C above the vapor temperature was prevented the heat loss to the environment and the possible vapor condensation. [22]. The description of the adsorption experimental set-up for multicompound adsorption was similar. Adsorption capacity evaluations of

mixtures with two, three or four components were performed in the same assembly used for mono-compound systems.

Appendix **4.** Antoine Constants [104]and Appendix 5 Mass characteristics pattern used in mass spectrometer present the Antoine constants and mass characteristics patter used in mass spectrometer in order to define differences among each compound. The percentage by volume of steam water and other gases was determined by masses calibration (see Appendix 6 Calibration factor (the compounds percent).).

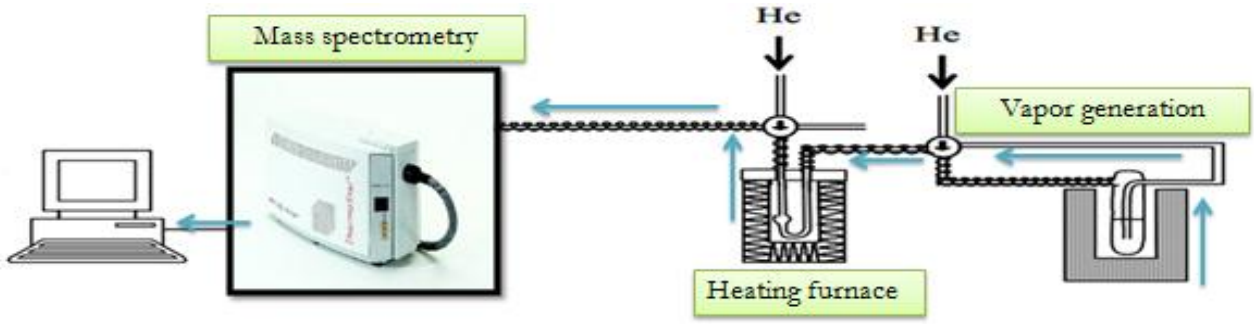

Figure 4 Adsorption – desorption scheme with mass spectrometry detector (Based on Cortés et al.) [28]**.**

1.2.2.2. Adsorption at mild pressure

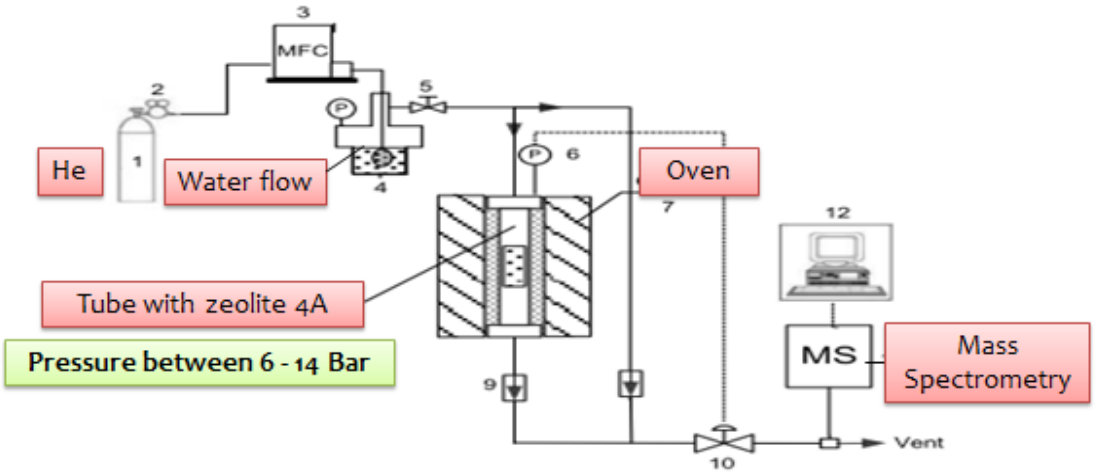

Figure 5. Scheme high pressure

Figure 5 The test at high pressure were performed in a continuous stainless steel (SS) tubular bed (ID 7 mm) packed with 0.5 g of zeolite 4A (512 μm), previously purged with argon during 12 hours. The water flow was introduced into the tubular bed by a stream of water / Helium through a SS bubbler (temperature for water was always 21°C) containing the liquid water. All adsorptions were carried out at 6-14 bar, 92-150°C and total gas flow was about 50 mL/min until adsorption

equilibria. The adsorption system was installed inside an oven that preventing possible condensation. The outline was monitored online by the mass spectrometer.

According to Figure 6 it is possible to analyzed two zones: adsorption and desorption part at continuous time using mass spectrometry. The adsorption tests were carried out at atmospheric pressure (0.83 atm) and at 92 °C, 150°C and 200 °C until saturation. The desorption test, occurs at the same pressure, with an increment of the temperature until constant temperature (450°C in order to desorb any compound). When the concentration value is constant, the system achieves the equilibrium and this value is considering the adsorption capacity $\mathbf{q_e}$.

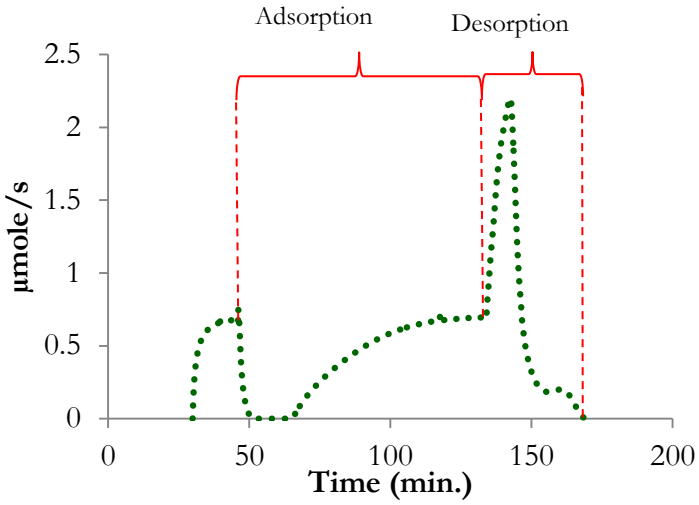

Figure 6 Experimental results with Mass Spectrometry (adsorption and desorption).

In order to know the adsorption isotherm, the mass balance was used in the adsorption zone with Equation 12. The mass spectrometry data express the mass outlet, and, consider a constant flow (mass inlet) it is possible to calculate all time the mass accumulated. Using EXCEL software was possible to express like mass accumulation the behavior of any adsorption profile, and this data was easily transform in an isotherm.

$$\textbf{Mass inlet} - \textbf{Mass outlet} = \textbf{Mass accumulated} \qquad \textbf{Equation 12}$$

The water adsorption capacity (g_{H2O} / $g_{zeolita}$) was calculated analyzing the desorption data. Assume the absence of chemisorption in the zeolite A (subsequently checked in Adsorption Kinetic experimental results) was possible to calculate (by area under curve the adsorption capacity. Using the software ORIGIN-PRO (Type analysis>Fit-Mult-ipeaks>Type of peak: Guassian), and define the initial and end point for the area, the integrating (between adsorption temperature and 450 °C) express the adsorption capacity. The experimental error was calculated using Equation 13

$$\%\mathbf{Error} = \left|\frac{\mathbf{Experimental\ value - Theoretical\ value}}{\mathbf{Theoretical\ value}}\right| \times \mathbf{100} \quad \textbf{Equation 13}$$

Figure 7 shows the different mixtures tested in order to know their effect in the water adsorption capacity of zeolite 4A (inhibitory effect), and, some mixtures without water were evaluate too, in order to analyze if it was possible a competitive adsorption.

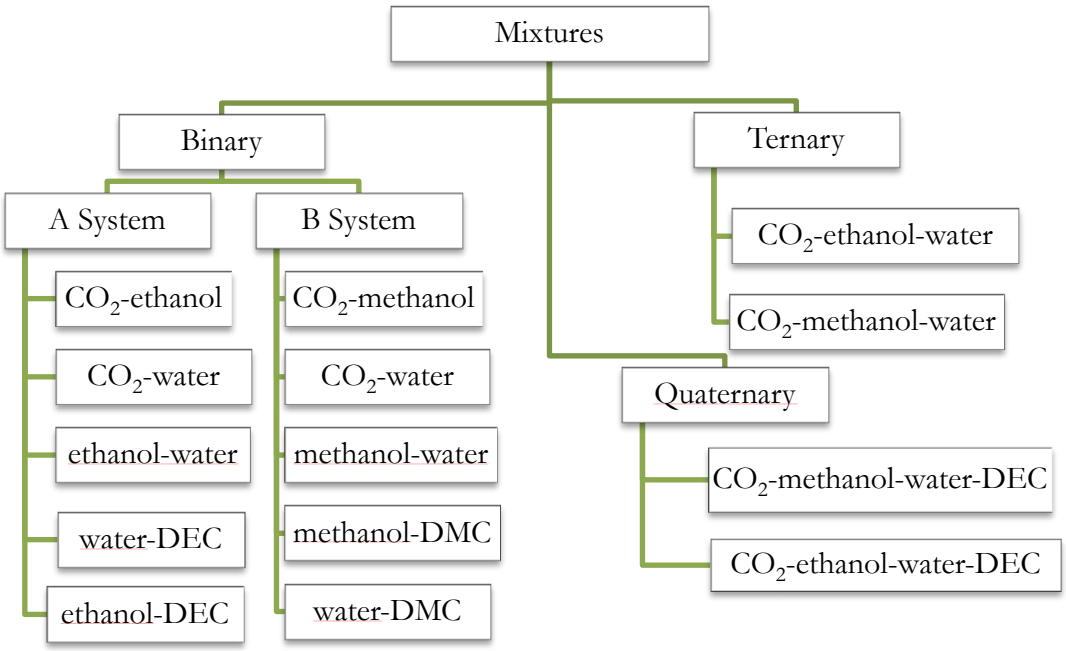

Figure 7 Scheme for the different mixtures tested.

1.2.3. Characterization

The morphology of the zeolite 4A used as adsorbent was determined by a Scanning Electron Microscope (SEM) with a JEOL JSM-6490 microscope using an accelerating voltage of 20kV. Elemental analysis was performed by Energy Dispersive X-ray Spectroscopy (EDS) instrument coupled to the SEM equipment. The crystallinity was determined by X-ray diffraction (XRD) at room temperature on a Phillips PW 1740 using Ni-filtered and Cu Kα radiation. The scanning range was $5° \leq 2\theta \leq 50°$ at 2°/min. The diffractograms were compared to JCPDS (Joint Committee of Powder Diffraction Standards) data.

The moisture content in zeolites was specified by thermogravimetric analysis (TGA) on a Q500 TGA V20.8 (TA Instruments), the sample was heated up to 600 ºC at 10 ºC/min in flowing air (100 mL/min. The moisture in the zeolite was also reported by calcination method on a Vulcano's muffle. The sample was heated up to 400 ºC at 10 ºC/min in flowing air (100 mL/min).

1.3. RESULTS AND DISCUSSION

1.3.1. Experimental method validation

Adsorption tests were performed according to the experimental methodology proposed using mass spectrometry [22], [28]. Figure 8 shows the similar profile for water adsorption using zeolite 13X, the graphical comparison let to affirm that the system used in this study is similar to reported in literature. It ensures that the method is suitable.

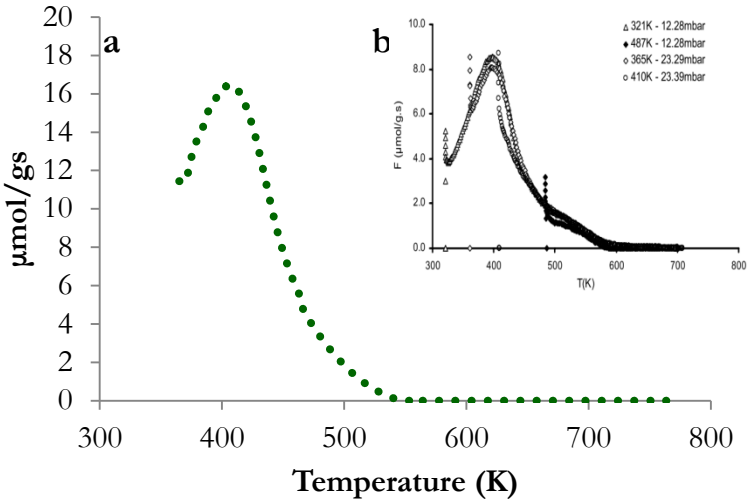

Figure 8 Desorption profile of water at 12.28 mbar and 321 K on zeolite 13X (a) This work; (b) reported by Cortés et al [22].

1.3.2. Characterization

1.3.2.1. Moisture determination

Table 5 shows the TGA and calcination results obtained in order to know the exact content of water. This data was important to determine the dry weight for next calculations. Equation 14 allows calculating the moisture by calcination.

$$\textbf{Moisture}\ (\%) = \frac{W_w - W_d}{W_d - W_c} \times\ 100 \qquad \textbf{Equation 14}$$

Where,

$$\textbf{Mw} = \textbf{weight}\ (\textbf{container} + \textbf{wet sample}) \qquad \textbf{Equation 15}$$
$$\textbf{Md} = \textbf{weight}\ (\textbf{container} + \textbf{wet dry}) \qquad \textbf{Equation 16}$$
$$\textbf{Mc} = \textbf{weight container} \qquad \textbf{Equation 17}$$

Table 5 Moisture for different type of zeolites

Type of zeolite	Moisture (%)	
	TGA	Calcination
3A	15.19	4.47
4A	20.11	5.94
5A	20.01	4.38
13X	20.52	13.25

It is possible to note lower values by calcination in comparison with TGA data, but according to the porous materials evaluated, it could be possible to find water inside the porous and it needs a temperature more than 400°C in order to be evaporated. For other side, the TGA method was more accurate than calcination, especially with very low weights.

1.3.3. Adsorption capacity

The adsorption capacity was calculated analyzing the desorption data in the experimental results using Origin – Pro software and calculating area under curve. Figure 9 shows the procces.

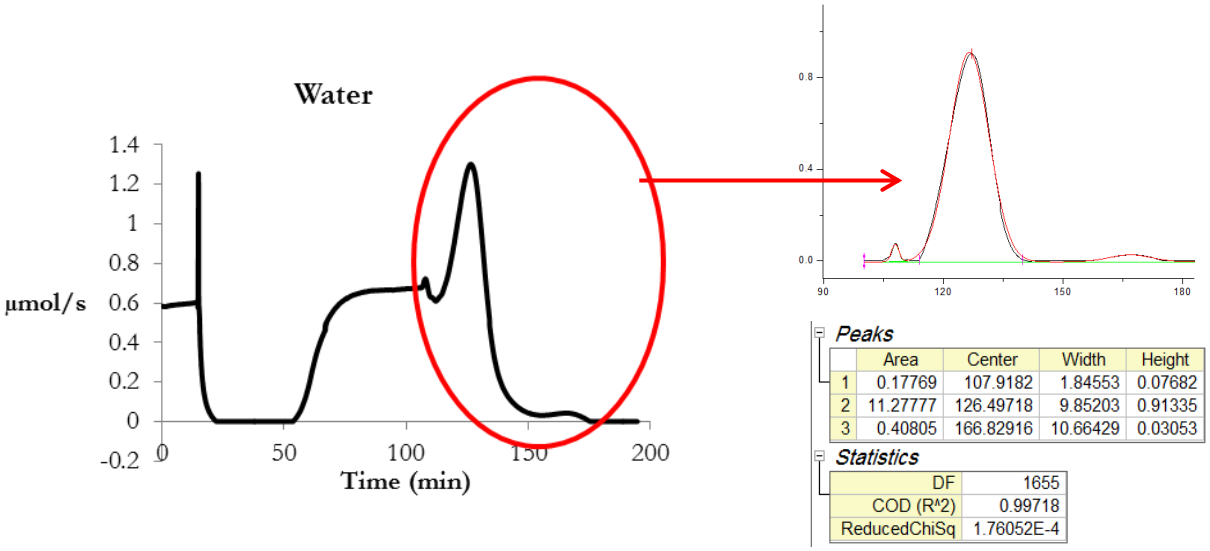

Figure 9. Area under curve, Origin-Pro

Several variations as type of zeolite, temperature, pressure of zeolite and compound percent were evaluated. There was also included the experimental method validation and regeneration test. In general terms, the adsorption analysis allows to select what is the best zeolite A in order to adsorb water and what are the best conditions of water percent and temperature for those the adsorbents.

The multicomponent adsorption capacity was also calculated analyzing the desorption part in the experimental results. The temperature and number of compounds in the mixture were evaluated taking as constant the type of zeolite (always zeolite 4A), the pressure and the percent of these compounds. The multicomponent adsorption analysis allows to define what is the effect of the

others compounds in the water adsorption capacity and define the best temperature in order to adsorb more water.

1.3.3.1. Zeolite type effect

Table 6 show the zeolite A adsorption capacity for four types: 3A, 4A, 5A and zeolite 13X (presented in order to validate the methodology). The result confirms that zeolite 4A has the best adsorption capacity [20].

Table 6 Water adsorption capacity for different kind of zeolites A (LTA) at 92°C.

Zeolite type	$H_2O_{(v)}$, % Vol.	µmol H_2O	Experimental $\left(\frac{g_{H_2O}}{g_{zeolite}}\right)$	Theoretical $\left(\frac{g_{H_2O}}{g_{zeolite}}\right)$	Experimental Error (%)
13X	3.08	657.78	0.1826	0.21	8.7
3A	3.23	883.32	0.2278	0.20	13.9
4A	3.31	1067.75	0.2916	0.285	2.3
5A	3.17	983.59	0.2797	0.28	0.1

After compare the adsorption capacity of water for the zeolites 3A, 4A and 5A, the zeolite 4A offers the highest adsorption capacity allowing to retain until 223 mg_{H20}/g_{4A}

1.3.3.2. Effect of the water concentration in adsorption

Table 7 shows the adsorption capacity for different concentration of water in the feed stream in the adsorption system. The variations of steam stripping were performed at atmospheric pressure and they did not correspond to the bubble point. Helium allowed drag water of the liquid phase through the pipe. The results report that the adsorption capacity is not mainly affected by the changes in the water concentration (2.87 to 4.35 % mol). The average water adsorption capacity was 0.2944 $g_{H_2O}/g_{zeolite\ 4A}$. The increment in the water concentration in the gas phase does not generate significant increments in the amount of water absorbed (average capacity 235.2 mg_{H20}/g_{4A} at 92°C). This is a logic result considering the main dependence of adsorption capacity with the available sites and the size of the column packing.

Table 7 Effect of the water percent variation in the drag water adsorb at 92°C using Zeolite 4A.

$H_2O_{(v)}$, % mol	µmol H_2O	$g_{H2O}/g_{zeolite\ 4A}$
2.87	993.12	0.2716
3.31	1067.75	0.2916
4.35	1164.44	0.3200

1.3.3.3. Effect of the temperature in the adsorption capacity at 0.83 atm.

Analysis of the adsorption temperature was held in zeolite 4A at 36, 92, 150 and 200 °C. The composition (mol, %) of any compound in the feed stream to the adsorption system is present in Table 7. Neither linear carbonates nor carbon dioxide were adsorbed on the zeolite 4A (Table 8). Ethanol and methanol were also adsorbed on zeolite 4A, possibly due to their nature and tendency to be adsorbed on hydrophilic sites of a zeolite [43]. Also, Table 8 shows that water, ethanol and methanol adsorption capacity of the zeolite 4A decreases with increasing adsorption temperature [44]. The adsorption temperature affected the adsorption capacity at 0.84 atm, when temperature was increased from 20 to 150 °C the water adsorption decreased from 233 until 10 $mg_{H20}/g_{4A}$for water. The desorption process is achieved by increasing the bed temperature up to 200 C which increases the internal energy of the gas and allowed the gas molecules to escape from the column packed of adsorbent [45].

Table 8 Effect of temperature variation in the adsorption capacity of zeolite 4A

Compound	Composition (mol, %)	Adsorption temperature (T_{ads})	Adsorption capacity ($mg/g_{zeolite\ 4A}$)
Water	2.3	36	208
		92	292
		150	245
		200	25
CO_2	7.9	36	N.D
		92	N.D
		150	N.D
		200	N.D
Ethanol	1.4	36	27
		92	29
		150	8
		200	4
DEC	1.9	36	N.D
		92	N.D
		150	N.D
		200	N.D
Methanol	12.9	36	65
		92	6
		150	3
		200	0
DMC	2.52	36	N.D
		92	N.D

	150	N.D
	200	N.D

N.D: not detected

1.3.3.4. Effect of the number of components

Table 9 presents the results for different mixtures (one, two, three and four components) at 92 ° C. In the presence of the complete reaction mixture, the adsorption capacity of water decreased in a 75 % in the components of DEC synthesis and near to 60 % in the DMC synthesis. The same phenomenon was observed for ethanol (58 %) and methanol (40 %) adsorption. In the multicomponent mixtures at 92°C ethanol and methanol were also adsorbed on zeolite 4A but in lower quantities, possibly because of their tendency to be adsorbed on hydrophilic sites of a zeolite 4A [46] and this result could represent an competitive effect [30]. In other words, the increment of number of compounds reduces the adsorption capacity of water at constant temperature (92°C). Neither linear carbonates (DEC and DMC) or carbon dioxide (CO_2) were adsorbed on the zeolite 4A, however, their presence affects the water adsorption capacity with an inhibitory effect. The reason could be associated with the formation of hydrogen bonds between CO_2 and alcohols. The water molecules form about twice as many hydrogen bonds to alcohol molecules than to other water molecules [38]. At these concentrations, adsorbed water molecules are "sandwiched" between two alcohol molecules. About The CO_2 may form a hydration shell from a symmetrical dodecahedral arrangement of 18 water molecules where each CO_2 oxygen atom is hydrogen bonded to three water molecules [47].

Table 10 and Table 11 present similar results at 150°C and 200°C. The temperature effect is discuses in the next section. In the mixtures at 150 °C, Table 10 show how the water adsorption capacity was reduce in a 92 % in the mixture of DEC synthesis and near to 90 % in the DMC synthesis, and it decreased also for ethanol (13 %) and methanol (67%) adsorption. Table 11 presents the results at 200 °C. At this temperature, the worst water adsorption was obtained in the monocomponent system (26 mg/g), and it was reduced in the presence of more compounds. Again, the adsorption capacity of water decreased until 66 % in the DEC synthesis and near to 41 % in the DMC synthesis in the complete reaction mixture. The information defines as unfavorable working conditions above 100 °C, in the presence of the complete reaction mixture.

Table 9 Adsorption capacity of zeolite 4A in multicomponent mixtures (92°C)

Mixture	Inlet mixture composition* (mol, %)						Adsorption capacity ($mg/g_{zeolite\ 4A}$)		
	Water (1.26)	CO_2 (3.85)	Ethanol (0.77)	DEC (0.16)	Methanol (3.61)	DMC (0.56)	Water	Ethanol	Methanol
	X						292	0	0
1			X				0	29	0
					X		0	0	6
	X	X					199	0	0
	X		X				79	19	0
	X			X			122	0	0
	X				X		49	0	13
2	X					X	218	0	0
		X	X				0	13	0
		X			X		0	0	0
			X	X			0	9	0
					X	X	0	0	6
3	X	X	X				61	11	0
	X	X			X		48	0	9
4	**X**	**X**	**X**	**X**			71	12	0
	X	**X**			**X**	**X**	116	0	3

*Helium balance

Table 10. Adsorption capacity of zeolite 4A in multicomponent mixtures (150°C)

Mixture	Inlet mixture composition* (mol, %)						Adsorption capacity ($mg/g_{zeolite\ 4A}$)		
	Water (1.31)	CO_2 (3.78)	Ethanol (0.66)	DEC (0.17)	Methanol (3.69)	DMC (0.52)	Water	Ethanol	Methanol
	X						245	0	0
1			X				0	8	0
					X		0	0	3
	X	X					83	0	0
	X		X				23	7	0
	X			X			21	0	0
	X				X		5	0	0
2	X					X	23	0	0
		X	X				0	16	0
		X			X		0	0	10
			X	X			0	8	0

					X	X	0	0	7
3	X	X	X				16	7	0
	X	X			X		8	0	1
4	X	X	X	X			19	7	0
	X	X			X	X	25	0	1

*Helium balance

Table 11 Adsorption capacity of zeolite 4A in multicomponent mixtures (200°C)

	Inlet mixture composition* (mol, %)						**Adsorption capacity ($mg/g_{zeolite\ 4A}$)**		
Mixture	**Water (1.31)**	**CO_2 (5.31)**	**Ethanol (0.65)**	**DEC (0.15)**	**Methanol (3.52)**	**DMC (0.49)**	**Water**	**Ethanol**	**Methanol**
	X						25	0	0
1			X				0	19	0
					X		0	0	0
	X	X					10	0	0
	X		X				17	2	0
	X			X			10	0	0
	X				X		8	0	0
2	X					X	3	0	0
		X	X				0	11	0
		X			X		0	0	0
			X	X			0	5	0
					X	X	0	0	2
3	X	X	X				5	3	0
	X	X			X		7	0	0
4	X	X	X	X			9	4	0
	X	X			X	X	15	0	0

1.3.3.5. Regeneration of the water capacity adsorption in zeolite 4A

The water adsorption in zeolite 4A was measure for five times under the same conditions (Figure 10). The process was carried out under the same conditions of adsorption and desorption tests for water at 92 °C. The zeolite 4A was always into the U tube (during five tests) and it was regenerated with an argon flow for 12 hours. According with the results, there are not changes in the water adsorption capacity of zeolite A and it can be used at least five times.

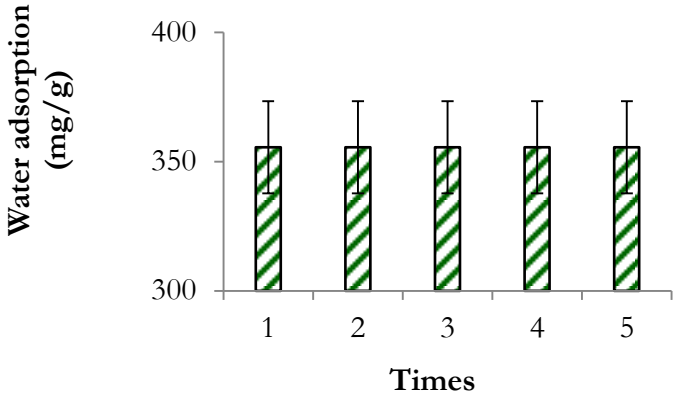

Figure 10 Effect of the regeneration of the water capacity adsorption in zeolite 4A. Adsorption conditions water concentration: (2.3 % mol), zeolite A (80 mg), 92 °C, 0.84 atm.

1.3.4. Adsorption Isotherms

As it stated in the experimental description, the experimental data (shown in Figure **11**) could be transformed in the adsorption isotherm (Figure 12) using the mass balance (Equation 12) in order to calculate the adsorption isotherm**.**

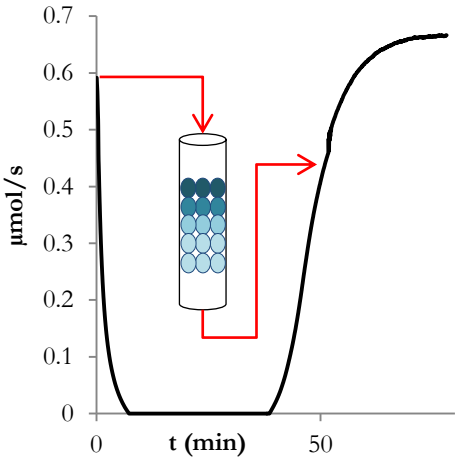

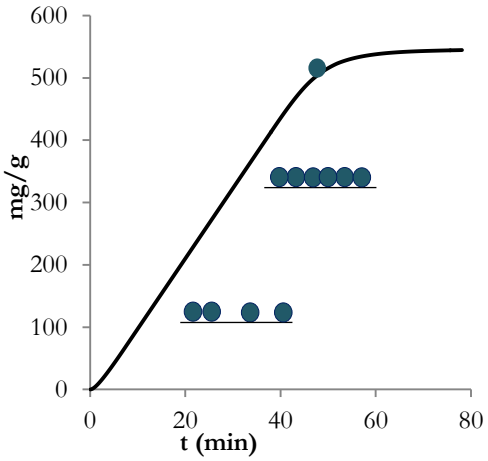

Figure 11 Experimental adsorption process

Figure 12 Adsorption isotherm

The next result presents the adsorption isotherms in zeolite 4A, under mild conditions, for ethanol, methanol and water in different mixtures of compounds.

1.3.4.1. Adsorption isotherm for the different zeolites

Figure 13 shows the adsorption capacity for the different zeolites (3A, 4A, 5A and 13X) at the same conditions of temperature, pressure and stream. When the adsorption capacity achieves a constant

value (q_e), the equilibrium is reached. The best adsorption capacity was obtained with zeolite 4A ($q_{e,4A} = 424\ mg/g$), as expected. Zeolite 3A presents the lowest adsorption ($q_{e,3A} = 316\ mg/g$). The values for Zeolite 5A and 13X were ($q_{e,5A} = 351\ mg/g$) and ($q_{e,13X} = 378\ mg/g$), respectively.

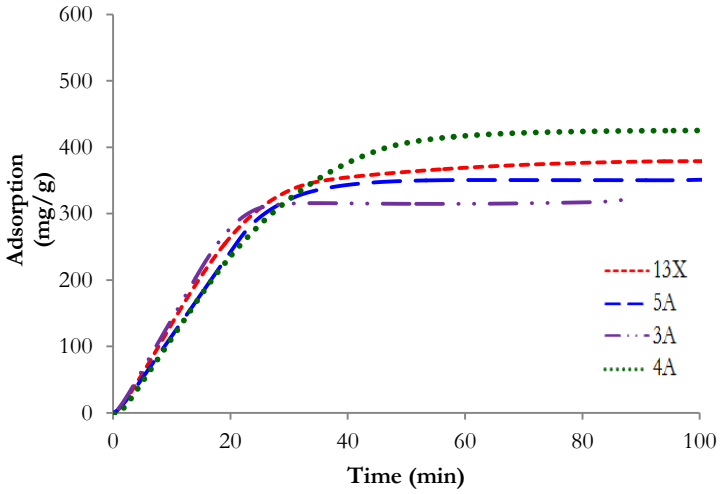

Figure 13 Water isotherms in LTA zeolites. Adsorption conditions: water concentration (2.3 % mol), zeolite A (80 mg), 92° C, and 0.83 atm.

1.3.4.2. Effect of the temperature in the water adsorption isotherm

Figure 14 shows the water isotherms at different temperatures in zeolite 4A. It is observed when the adsorption temperature increases the adsorption capacity decreases. Zeolite 4A is able to adsorb 537 mg/g at 36°C, but, when the temperature increased until 200°C, it is only possible to absorb 84 mg/g. The shape of the adsorption isotherms follows the Langmuir adsorption, at all temperatures. This means that the adsorbent has a homogeneous surface in what takes place the adsorption process forming a monolayer.

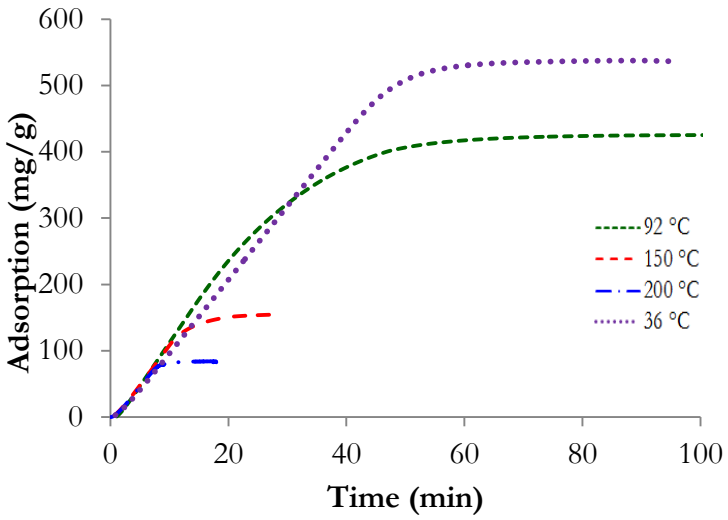

Figure 14 Effect of temperature in the water isotherm in zeolite 4A. Adsorption conditions: water concentration (2.3 % mol), zeolite A (80 mg), 92° C, and 0.83 atm

.

1.3.4.3. Effect of the presence of CO_2, ethanol, methanol, DEC and DMC in the adsorption isotherm.

Figure 15 until Figure 19 present the adsorption of water and another compound (ethanol, methanol, DEC, DMC and CO_2) in zeolite 4A. From these results are clearly seen, again, that the any adsorption isotherms obey Langmuir model: the adsorbate covering the adsorbent which has a smooth surface until a monolayer is formed and then the process stops. This model describes the adsorption for microporous materials, like zeolites and, the chemisorption phenomena [48] [49].

The zeolite is able to adsorb ethanol even though the molecular size of ethanol is 4.6 Å (bigger than the pore opening size of zeolite 4A). This result suggests that probably the ethanol polarity allows its absorption over the zeolite 4A [14]. The effect in this part is different because at higher temperature there are more ethanol adsorb ($q_{e,ethanol,200°C} = 231\ mg/g$) while at lowest temperature was adsorbed only 69 mg/g.

It is really important to remark that CO_2, DMC and DEC were not adsorbed under the test conditions. The kinetic diameter of the CO_2 molecule is 3.9 Å, what is only slightly lower than the pore diameter of molecular sieve 4A, so the mobility of the CO_2 molecule may be restricted inside the pores of molecular sieve 4A [50]. DMC and DEC molecules are bigger than the pore size of zeolite 4A (DMC and DEC are in the range of 4.7 Å to 6.3 Å, respectively), however, it is quite important to prove if the presence of those compounds could affect the water adsorption capacity.

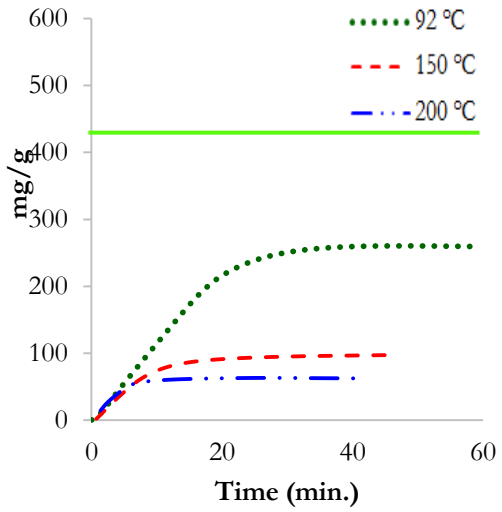

Figure 15 Water adsorption isotherm in water – ethanol mixture

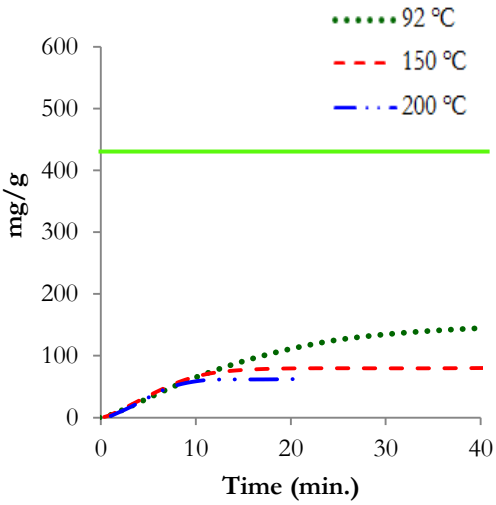

Figure 16 Water adsorption isotherm in water – methanol mixture

The mixtures water – DEC (Figure 17), water – DMC (Figure 18) and water – CO_2 (Figure 19); only present adsorption of water, but, the presence of these compounds reduce the adsorption capacity along with the temperature change. Comparing these graphics, it is possible to conclude that at 92°C the presence of CO_2 affects the water adsorption capacity higher than linear carbonates. The reduce of water adsorption at 150°C and 200°C is expected but, CO_2 at 150°C has the same behavior at 92°C.

The possible reason for all these changes in the adsorption capacity must be related with the hydrogen bonds between water and CO_2 that changes the available water and modify the size of water molecule increase it and reduce the quantity adsorbed. About the alcohols, it size allows the pass through pore of zeolite, mainly for methanol occupying the sizes and reduces the water adsorption. The increase of temperature and the subsequent reduction of adsorption in presence of both compounds depend mainly of properties of zeolite 4A but, the possible chemisorption could be related.

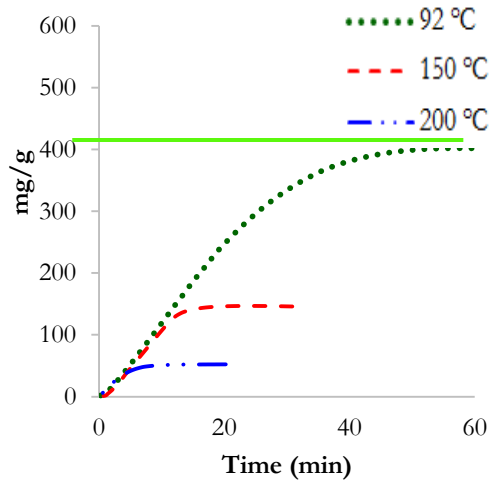

Figure 17 Water adsorption isotherm in water – DEC mixture

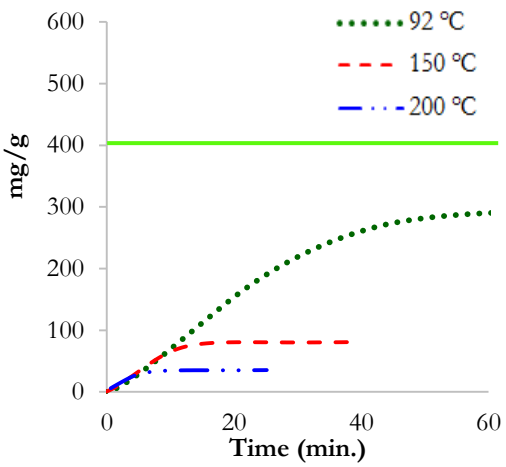

Figure 18 Water adsorption isotherm in water – DMC mixture

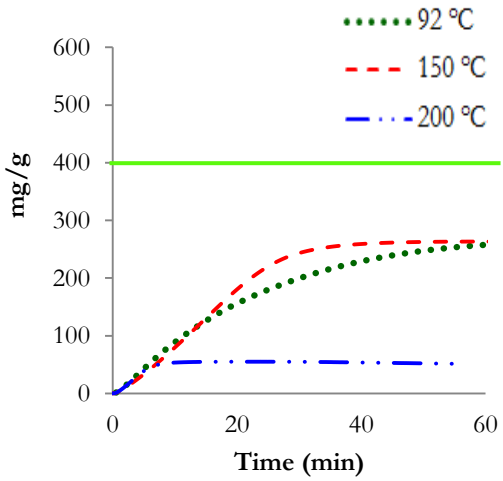

Figure 19 Water adsorption isotherm in water – CO_2 mixture

In comparison to the single isotherm for water (Figure 20) with two compound system: ethanol and water (Figure 21) at 92°C, it is possible to note that the addition of the adsorption capacity of water and ethanol is the same adsorption capacity for water alone. In these figures it is easy to see the competitive effect for the sites in a binary system [14]. This fact suggests that the available sites are the same, but, these are occupied for both compounds: water and ethanol what reduce the possibility to adsorb more quantities of water. The results allow affirming that the interactions between water and ethanol can be neglected to define the adsorption isotherm. Both compounds ethanol and water follows for two components system the Langmuir isotherm adsorption. At similar analysis can be performed in a binary system with four compounds system: water, ethanol, CO_2 and DEC (Figure 22) the results show although CO_2 and DEC are not adsorbed, the adsorption capacity at the same conditions is reduce again due to a possible blockade of the channels.

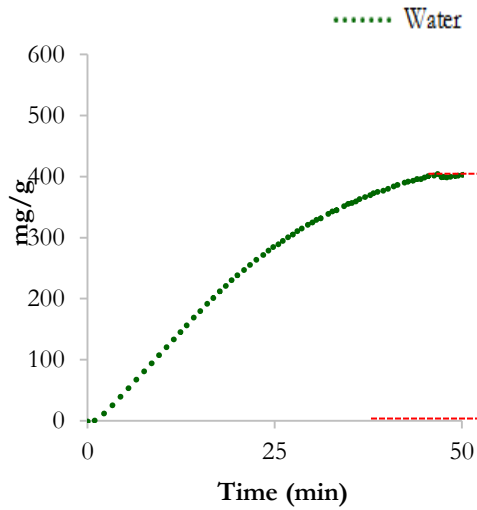

Figure 20 Water adsorption isotherm at 92°C

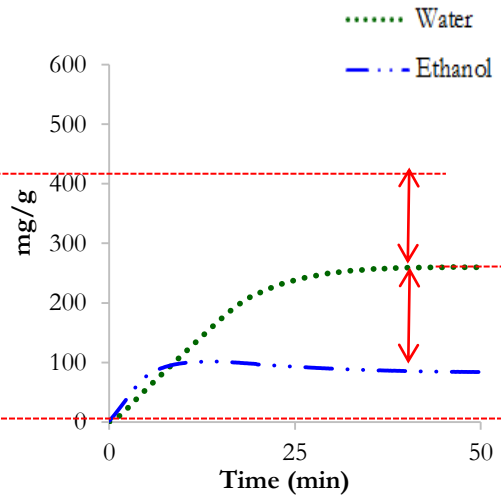

Figure 21 Water adsorption isotherm in water – ethanol mixture at 92 °C

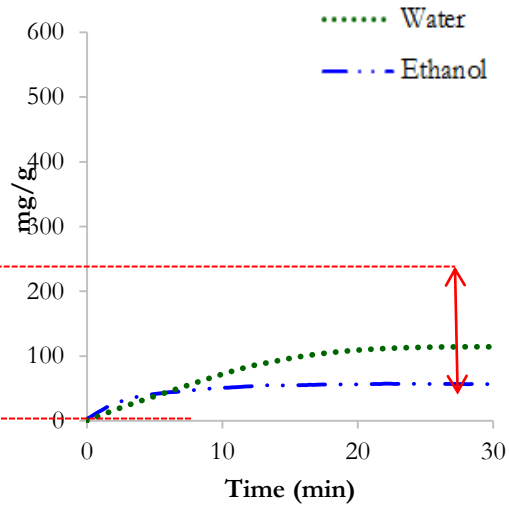

Figure 22 Water and ethanol adsorption isotherms in water, ethanol, DEC and CO_2 mixture at 92 °C

Appendix 7 **Isotherms two compounds** shows the isotherms with two compounds for ethanol and methanol with compounds different to water. The specific information is expressed in the appendix, but, in general terms, ethanol and methanol fallow a contrary tendency, to increase the adsorption with the temperature, mainly with CO_2.

The isotherms for three (Appendix 8) and four (Appendix 9) compouds shows the adsorption isotherms. The behavior is quite similar, in the case of water, ethanol, (adsorb in zeolite 4A) the presence of DEC and CO_2, affect the adsorption capacity (although they are not adsorb). This means that the system presents a competitive effect because ethanol and water tries to occupy the free sites generating an inhibitory effect, as more components present in the mixtures as lower the water adsorption. The adsorption isotherm for water and methanol in the mixture with DMC and CO_2 favors the methanol adsorption. This is an undesirable effect, since the idea is to absorb water in order to shift the equilibrium conversion in the direct synthesis of linear carbonates.

In general terms, all these results show how the water adsorption capacity is affected in a negative way for the presence of more components and for the increment of temperature. The increment in the number of compounds and temperature help to achieve the equilibrium faster, this is another undesirable effect because, the zeolite 4A will be saturated in a short time and the reaction could occur a longer time.

Figure 23 shows the adsorption isotherms for ethanol and the mixture water – methanol respectively. Again, the temperature and number of compounds reduces the adsorption capacity. Figure 24 show the behavior of the mixture water-ethanol at 92°C, 150°C and 200°C. Both compounds water and ethanol are adsorbing in zeolite 4A at the same time and present independent adsorption isotherm. The water is more adsorbed than ethanol, but all compounds reduce their adsorption capacity with the temperature increasing. Figure 25 shows the methanol isotherm adsorption. Since the diameter size of methanol is 3.6 Å, it is adsorb in the zeolite 4A. In very short time (30 min), the zeolite achieves the saturation and was able to adsorb 452 mg/g at 36°C and 403 mg/g at 92°C. The lowest adsorption was 291 mg/g at 200°C. The adsorption isotherms of methanol also follow the Langmuir adsorption model and reduce the adsorption capacity as it is shown in Figure 26.

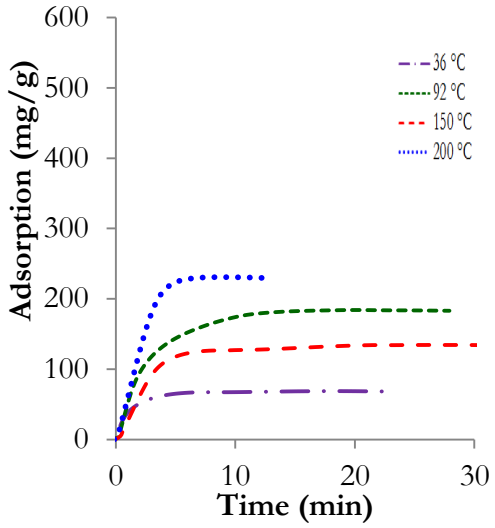

Figure 23 Effect of temperature in the ethanol isotherm in zeolite 4A. Adsorption conditions: ethanol concentration (1.4 % mol), zeolite A (80 mg), 92° C, and 0.83 atm

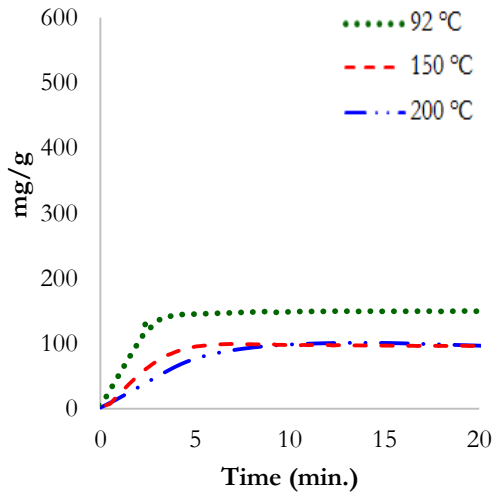

Figure 24 Ethanol adsorption isotherm in water – ethanol mixture

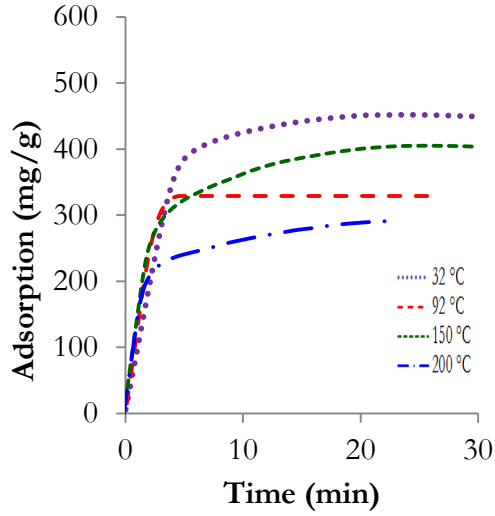

Figure 25 Effect of temperature in the methanol isotherm in zeolite 4A. Adsorption conditions: methanol concentration (12.9 % mol), zeolite A (80 mg), 92° C, and 0.83 atm

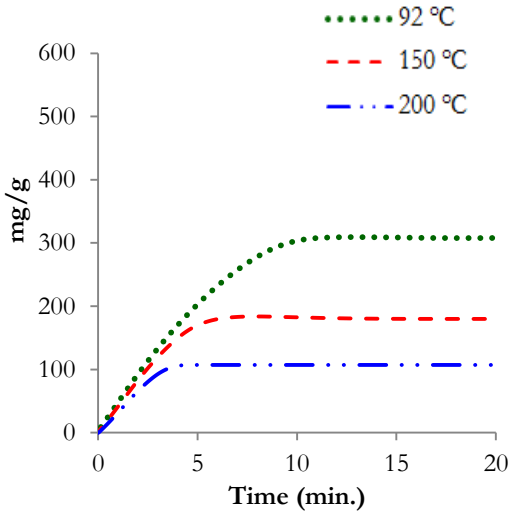

Figure 26 Methanol adsorption isotherm in water – methanol

1.3.4.4. Effect of the pressure in the water adsorption capacity

Figure 27 shows the effect in the water adsorption capacity. It is possible to see that the adsorption at temperatures like 120°C and 150°C the capacity is not affect by the pressure. This means that the temperature has a dominant effect in the reduction of the water adsorption capacity. At low temperatures (20°C and 92°C) the adsorption capacity is reduced from 368 mg/g until 159 mg/g at 20°C and 242 mg/g until 102 mg/g at 92 °C when the pressure was increased from 1 Bar (0.98 atm) to 6 Bar (5.92 atm). For pressure higher than 6 bar the effect in the adsorption capacity is not significant.

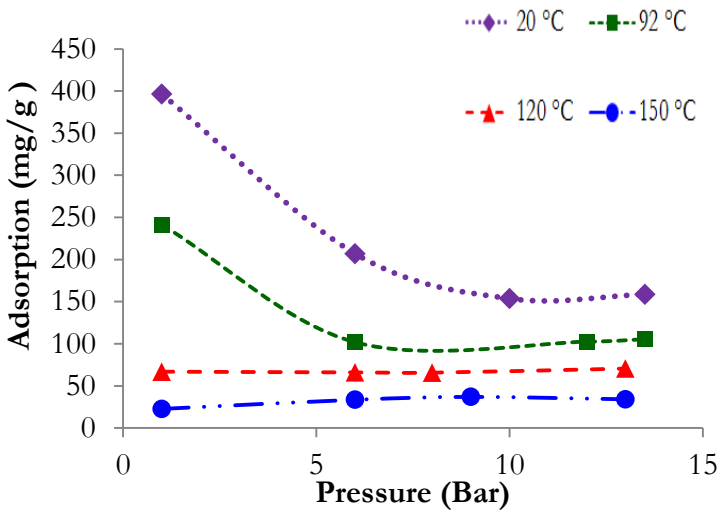

Figure 27 Water adsorption capacity of zeolite 4A. Adsorption conditions: water concentration (XX % mol) and zeolite A (80mg)

This behavior is opposite to the general profile: the increasing of pressure leads to increase of adsorption capacity and the decrease of pressure causes desorption. However, since the control of volume flow and temperature, the moles in gas phase needs to increase in order to alleviate the increase of pressure that means the water resistance to be adsorbed onto the zeolite 4A.

1.3.5. Adsorption Kinetic

A mathematical treatment for the experimental data (Adsorption isotherms) allows adjusting the adsorption kinetic for ethanol, methanol and ethanol. These isotherms were the experimental basis for determining the adsorption kinetics. Figure 28 shows the fit for experimental data probe the Intraparticle Diffusion model (Equation 18).

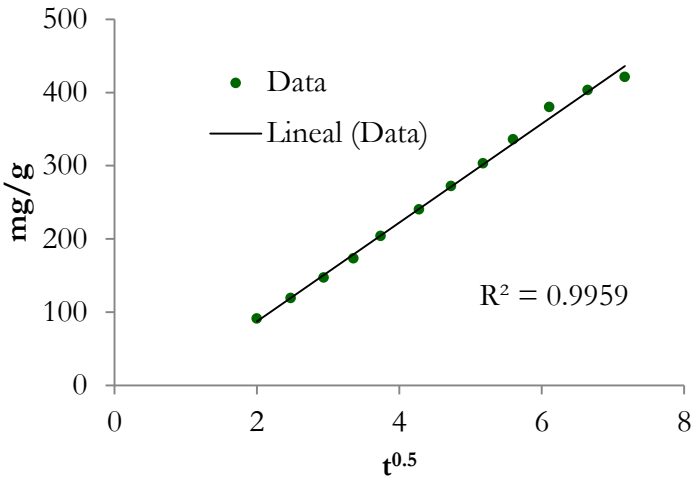

Figure 28 Intra particle diffusion model adjust for water.

1.3.5.1. Kinetic parameters of different type of zeolites

Table 12 shows the fit for different types of zeolites proving the four models for each type. The best results are present with bold font. According with the result was possible to observe that at same temperature and pressures conditions (92°C and 0.83 atm) the water kinetic adsorption mechanism is PFO for all zeolites. This means that each water molecule is adsorbed over unique adsorption site and the adsorption process is reversible [41]. The best water adsorption capacity was 726.33 mg/g by 4A zeolite. Zeolite 3A had k_1 higher than others zeolites, what it is associated with a short time to achieve the equilibrium.

Table 12 Kinetic Parameters by different type of zeolites.

Type of zeolite	PFO			PSO			IPD		Elovich		
	q_e $\left(\frac{mg}{g}\right)$	k_1 (min^{-1})	R^2	q_e $\left(\frac{mg}{g}\right)$	k_1 $\left(\frac{g}{mg \cdot min}\right)$	R^2	k_{dif} $\left(\frac{mg}{g \cdot min^{0.5}}\right)$	R^2	β $\left(\frac{g}{mg}\right)$	α $\left(\frac{mg}{g \cdot min}\right)$	R^2
3A	**508.26**	**0.0941**	**0.9932**	2884.34	1.77E-06	0.2602	93.12	0.9911	0.00595	41.91	0.9863
4A	**726.33**	**0.0795**	**0.9821**	1160.09	1.00E-05	0.7424	73.39	0.9798	0.04331	23.09	0.9223
5A	**649.37**	**0.0704**	**0.991**	1035.84	1.31E-05	0.6637	75.37	0.9573	0.00619	35.91	0.9788
13X	**384.14**	**0.065**	**0.9857**	501.25	9.94E-05	0.9551	42.85	0.8171	0.00826	48.17	0.91796

*Adsorption conditions: water concentration (2.3 % mol), zeolite, 20° C, and 0.83 atm.

Adsorption* capacity (q_e), Adsorption velocity (k) and correlation coefficient between zeolite 4A and type of zeolite (R^2).

1.3.5.2. Kinetic parameters of water, ethanol and methanol in zeolite 4A at different temperature and mixtures with another compound.

Table 13, Table 14 and Table 15 present the kinetic parameters of water, ethanol and methanol respectively for one and two compounds.

Considering that increment of temperature for the same material does not change the kinetic models, it is possible to use the average adjust in order to select the best fit. The boldface data represents the best results with the best average underlined. When the temperature was varied, the water kinetics follows the IPD model (R^2 =0.9844), ethanol follows the PFO model (R^2 =0.9943) and methanol the PSO model (R^2 = 0.9817).

Table 12 had shown PFO behavior for zeolite 4A but, the changes in temperature present a better fit with IPD model (Analyzing the average R^2). This result suggest a possible contradiction, but, it has not sense that zeolite 4A fallow PFO model at 92°C and IPD model at more temperature. So, the IPD is the best model to describe the water adsorption in zeolite because average R^2 its much better than PFO (0.9844 vs. 0.9366). The IPD model allows affirm that the chemisorption is not a determined step in the adsorption process and the zeolites have homogeneous porous structures.

Under the conditions used in this study, the adsorption of water in zeolite 4A is governed by the diffusion from the bulk phase to their inner pores. This model express that the diffusion in the pores is the step limit and it also suggest that the adsorbent has a homogenous porous structure [41]. Intra diffusion always plays the key step for the adsorption and offers the main resistance in total diffusion, as the adsorption of water in LTA zeolites whose adsorption vacancies mostly locate inside the crystals [14]. Analyzing the change in the adsorption velocity, it is possible to say that the increase of temperature decreases the k_{diff} value, because the process is faster at high temperatures than lower but, it reduces the adsorption capacity.

Ethanol follows the PFO model. This supposes that each molecule of adsorbent has a unique adsorption site; this could be means a possible physisorption, but it is not possible to depreciate the perhaps chemisorption. Methanol follows the PSO model and suggests that the adsorption of methanol occurs in two active sites or a possible chemisorption for this compound as limit of the adsorption. This is a very understand phenomena consider different studies that show the chemisorption at relative low temperatures (100 -300 °C) following two different ways. In the first of them there is an associative adsorption (molecular adsorption). In a second there is a dissociative mechanism and methanol adsorbed methoxy species [51], [52].

The XRD results for some zeolites used in methanol adsorption show some changes as physical evidence about the chemisorption in 4A zeolite. Finally, the adsorption velocity for both alcohols increase when temperature increases, reducing the adsorption capacity.

Now, consider the kinetic results for two compound systems with water (Table 13) and another compound (CO_2, ethanol, methanol, DEC or DMC), it is possible to affirm that the presence of CO_2 or methanol changes the kinetic for an Elovich model. In mixture ethanol – water, the last was adsorbed by PFO (single ethanol mechanism too). Only DEC and DMC did not change the kinetic but it decreases the quantity of water adsorbed. The kinetic absorption for ethanol is present in Appendix 10 showed that the presence of DEC or water do not affect the kinetic adsorption. Single ethanol was adsorbed follows a PFO mechanism, but, it is similar than water, CO_2 presence changed the kinetic adsorption of ethanol by Elovich model.

The behavior for methanol is really different (see Appendix 10), the mixture methanol – CO_2 follows PSO tendency, this means that the methanol adsorption does not change (single kinetic adsorption was PSO), but, DMC and water are more adequate PFO and IPD kinetics, respectively. It is possible to think that mixture methanol – water is strong and for this reason methanol follows the water kinetic. It is very interesting to note that the presence of CO_2 strongly affects the kinetics even if it does not adsorb. In presence of CO_2 the water adsorption mechanism changes to Elovich or PSO and both mechanisms suggest chemisorption. In the other side, Elovich is a model used to determine the kinetics of chemisorption of gases on solids [53] and PSO suggest heterogeneous active sites. The results have sense base on theoretical information about the model. The CO_2 presence affect the adsorption capacity maybe for a porous blocked and, maybe for the interaction between CO_2 and hydrogen form hydrogen bonds. The kinetic results, confirm this idea since the structure does not behaves as homogeneous (PSO). The other binary systems (with DEC or DMC) follow a methanol and ethanol kinetic type IPD or PFO model and they compounds do not affect the kinetic.

1.3.5.3. Mixtures with three and four components

Follow the same process, the kinetic parameters for two, three and four compounds mixtures that contain water was calculated using the same mathematical models, (see Appendix 10 in order to see the kinetic for ethanol or methanol). The kinetic for CO_2, DEC and DMC were not present because these compounds were not adsorbed, but, they affected the kinetic of adsorption of water. Again, the best kinetic are highlighted with the bold symbols and the best average of correlation coefficients was underlined. Ethanol was adsorbing according to PFO kinetic for all temperatures. That suggests again the influence of CO_2. The water follows PFO or IPD kinetics, what confirms the homogenous structure of zeolite 4A and, the unique type active site for the adsorption of water. Table 16 describes the kinetic parameters for water in mixture: water, ethanol and CO_2. For these mixture there are not changes in the models that describe single water adsorption (IPD model), but, the adsorption velocity value for single water, k_{diff} at 92°C was 75.37 mg/g*min$^{0.5}$; at 150°C was 54.65 mg/g*min$^{0.5}$, and at 200 °C was 45.09 mg/g*min$^{0.5}$ change in the mixture decreasing the water velocity (k_{diff} was at 92°C = 29.57 mg/g*min$^{0.5}$, at 150°C = 21.44 mg/g*min$^{0.5}$and at 200°C = 33.79 mg/g*min$^{0.5}$).

About the kinetic adsorption of ethanol k_1 (min^{-1}) was in single adsorption system at 92°C = 0.31 , at 150°C = 0.64, and at 200°C = 0.83, and for the mixture k_1 was at 92°C = 0.23 min^{-1}, at 150°C = 0.66 min^{-1}, and at 200°C = 1.46 min^{-1} (See Appendix 10). These results showed that the adsorption of ethanol in the mixture is faster than in mono-component system. A contrary effect for the water adsorption was observed in Table 17 that present the results for the mixture water, methanol, CO_2. Again, the kinetic for water was IPD (quite similar to ethanol system). About the methanol kinetic adsorption, it follows the Elovich model (The Appendix 10), so, it is possible to think that the presence of CO_2 and methanol produce an undesirable effect with probably chemisorption at the evaluated conditions.

The model to describe the water kinetic behavior in four compounds (Table 18 and Table 19) was exactly the same as the obtained in the three component mixtures: IPD for water, PFO for ethanol and Elovich for methanol (See Appendix 10 for the two last). The adsorption velocity is faster than three compounds and this system reduces the adsorption capacity of water, ethanol and methanol. Water and ethanol present a physisorption process and methanol presents a chemisorption behavior with zeolite 4A, possible for the presence of CO_2.

1.3.5.4. IAST theory application

After to see the adsorption isotherms obtained for multicomponent systems and the changes in the kinetic and adsorption capacities, it is possible to see that the multicomponent system water, ethanol, CO_2 and DEC and water, ethanol, CO_2 and DEC are not ideal mixtures. Some of the evidences are the no possibility to sure that water and alcohols are adsorbed at the same concentrations, the results show preferences for the water adsorption, the presence of alcohol molecules allows formation of favorable hydrogen bonds with water molecules leading the absorption of both alcohols (ethanol and methanol) even if the zeolite 4A presents a steric hindrance, and there are some interactions between the adsorbate molecules in the adsorbed phase mixture [36], without considering the system interactions with CO_2.

1.3.5.5. Experimental error

Figure 29, Figure 30 and Figure 31 show the determination of the experimental error for water, ethanol and methanol adsorption, respectively, at different temperatures. The adsorption capacities, q_e, calculated as max and very establish line in the adsorption isotherm (obtaining by mass accumulation in the experimental data) could to compare with the adsorption capacity obtained in the kinetics models (value of q_e fit). The fit for water is better than ethanol and methanol. The maximum error is around 20% and there are two strange tendencies: ethanol at 200°C and methanol at 92°C, however it is important to remark that the change of variable in the PFO and PSO models implies the use of neperiane logarithm and this setting is very sensible, mainly at very low values, change the q_e value with strength.

Table 13 Kinetic parameters for mixtures between water and other compound

Compound	°C	PFO			PSO			IPD		Elovich		
		$\mathbf{qe}$ $\left(\frac{\mathbf{mg}}{\mathbf{g}}\right)$	$\mathbf{k_1}$ $(\mathbf{min^{-1}})$	$\mathbf{R^2}$	$\mathbf{qe}$ $\left(\frac{\mathbf{mg}}{\mathbf{g}}\right)$	$\mathbf{k_1}$ $\left(\frac{\mathbf{g}}{\mathbf{mg \cdot min}}\right)$	$\mathbf{R^2}$	$\mathbf{k_{dif}}$ $\left(\frac{\mathbf{mg}}{\mathbf{g \cdot min^{0.5}}}\right)$	$\mathbf{R^2}$	$\boldsymbol{\beta}$ $\left(\frac{\mathbf{g}}{\mathbf{mg}}\right)$	$\boldsymbol{\alpha}$ $\left(\frac{\mathbf{mg}}{\mathbf{g \cdot min}}\right)$	$\mathbf{R^2}$
Water (single)	36	1446.64	0.0775	0.8789	-	-	0.0789	**105.60**	**0.9901**	0.0422	3.33	0.9197
	92	719.10	0.0704	0.9821	1160.09	1.00E-05	0.7424	**75.37**	**0.9798**	0.0433	3.31	0.9223
	150	530.07	0.0191	0.9568	796.18	1.83E-05	0.4044	**54.65**	**0.9743**	0.0115	29.34	0.9895
	200	302.17	0.4608	0.9284	-	-	0.4575	**45.09**	**0.9932**	0.0198	26.46	0.9822
				0.9366			0.4208		**0.9844**			0.9534
CO_2	92	391.51	0.0583	0.9906	498.26	5.31E-05	0.9833	45.32	0.9787	**0.0091**	**28.33**	**0.9965**
	150	1045.24	0.1419	0.9154	-	-	0.0028	79.11	0.9880	**0.0063**	**30.74**	**0.9807**
	200	179.47	0.4894	0.9880	260.82	1.39E-04	0.3875	29.02	0.9586	**0.0303**	**24.15**	**0.9850**
Average				0.9647			0.4579		0.9751			**0.9874**
Ethanol	92	**548.95**	**0.1479**	**0.9371**	1300.05	7.11E-06	0.4116	64.75	0.9876	0.0094	37.18	0.9673
	150	**118.75**	**0.1692**	**0.9978**	138.93	7.50E-04	0.9748	20.53	0.9299	0.0288	26.71	0.9691
	200	**60.52**	**0.2596**	**0.9758**	88.73	2.16E-03	0.9542	17.76	0.8865	0.0468	33.51	0.9589
Average				**0.9702**			0.7802		0.9347			0.9651
Methanol	92	198.54	0.0822	0.9979	252.27	1.36E-04	0.9260	25.13	0.9450	**0.0073**	**123.62**	**0.9836**
	150	521.65	0.0078	0.8807	184.37	2.58E-04	0.7599	24.10	0.9418	**0.0288**	**20.99**	**0.9792**
	200	166.67	0.3561	0.9704	-	-	0.5363	29.68	0.9842	**0.0283**	**22.20**	**0.9884**
Average				0.9497			0.7407		0.9570			**0.9837**
DEC	92	707.69	0.0824	0.9746	1830.16	3.95E-06	0.5691	**86.38**	**0.9930**	0.0054	36.30	0.9903
	150	275.89	0.1977	0.9474	-	-	0.6638	**62.39**	**0.9932**	0.0129	30.49	0.9643
	200	57.86	0.3097	0.9898	76.28	2.79E-03	0.9764	**16.51**	**0.9319**	0.0529	30.31	0.9751
Average				0.9706			0.7364		**0.9727**			0.9766
DMC	92	642.91	0.0919	0.9020	4266.21	3.99E-07	0.0599	**59.30**	**0.9951**	0.0078	23.01	0.9783
	150	169.02	0.2628	0.9611	434.97	3.70E-05	0.4089	**28.72**	**0.9874**	0.0274	20.52	0.9794
	200	41.43	0.3431	0.9958	54.53	3.59E-03	0.9738	**12.93**	**0.9641**	0.0897	26.17	0.9586
Average				0.9530			0.4809		**0.9822**			0.9721

Adsorption conditions: water concentration (2.3 % mol), zeolite A (80 g), 20° C, and 0.83 atm.

Table 14 Kinetic parameters for mixtures between ethanol and other compound

Compound	T (°C)	PFO			PSO			IPD		Elovich		
		$\mathbf{qe}\ \left(\frac{\mathbf{mg}}{\mathbf{g}}\right)$	$\mathbf{k_1}\ (\mathbf{min^{-1}})$	$\mathbf{R^2}$	$\mathbf{qe}\ \left(\frac{\mathbf{mg}}{\mathbf{g}}\right)$	$\mathbf{k_1}\ \left(\frac{\mathbf{g}}{\mathbf{mg \cdot min}}\right)$	$\mathbf{R^2}$	$\mathbf{k_{dif}}\ \left(\frac{\mathbf{mg}}{\mathbf{g \cdot min^{0.5}}}\right)$	$\mathbf{R^2}$	$\boldsymbol{\beta}\ \left(\frac{\mathbf{g}}{\mathbf{mg}}\right)$	$\boldsymbol{\alpha}\ \left(\frac{\mathbf{mg}}{\mathbf{g \cdot min}}\right)$	$\mathbf{R^2}$
Ethanol	36	**55.09**	**0.5816**	**0.9993**	7.80	1.24	0.9997	18.58	0.9222	0.0633	191.14	0.9824
	92	**173.82**	**0.3051**	**0.9895**	233.26	1.28E-03	0.9758	52.43	0.9277	0.0195	51.21	0.9945
	150	**218.98**	**0.6377**	**0.9963**	353.11	2.90E-04	0.6490	68.72	0.9593	0.0173	88.65	0.9876
	200	**550.04**	**0.8314**	**0.9921**	601.68	2.21E-04	0.8363	137.90	0.9690	0.0086	176.03	0.9891
				0.9943			0.8652		0.9446			0.9884
CO_2	92	550.04	0.8314	0.9921	130.14	1.77E-03	0.9932	137.90	0.9690	**0.0317**	**57.47**	**0.9921**
	150	550.04	0.8314	0.9921	601.68	2.21E-04	0.8363	43.14	0.9045	**0.0211**	**55.57**	**0.9676**
	200	488.33	0.6092	0.9569	925.93	3.45E-05	0.3613	88.16	0.9793	**0.0119**	**83.56**	**0.9835**
Average				0.9804			0.7303		0.9509			**0.9811**
DEC	92	**122.73**	**0.3888**	**0.9977**	163.85	1.69E-03	0.9797	41.08	0.9384	0.0253	87.99	0.9852
	150	**130.71**	**0.5904**	**0.9910**	104.90	2.90E-03	0.9744	25.03	0.9017	0.0389	60.26	0.9648
	200	**240.81**	**0.4967**	**0.9968**	239.06	7.21E-04	0.9356	54.16	0.9344	0.0178	82.69	0.9778
Average				**0.9952**			0.9632		0.9248			0.9759
Water	92	**149.46**	**0.3474**	**0.9989**	273.00	2.73E-04	0.8739	47.19	0.9855	0.0094	37.18	0.9964
	150	**242.50**	**0.6495**	**0.9868**	804.51	5.43E-05	0.1584	82.46	0.9797	0.0163	110.95	0.9845
	200	**129.93**	**0.7196**	**0.9653**	185.67	1.49E-03	0.9104	55.20	0.9334	0.0259	120.99	0.9638
Average				**0.9837**			0.6476		0.9662			0.9816

Adsorption conditions: ethanol concentration (1.4 % mol), zeolite A (80mg), 20° C, and 0.83 atm.

Table 15 Kinetic parameters for mixtures between methanol and other compound

Compound	T (°C)	PFO			PSO			IPD		Elovich		
		qe $\left(\frac{\mathbf{mg}}{\mathbf{g}}\right)$	**k_1** $(\mathbf{min^{-1}})$	**R^2**	**qe** $\left(\frac{\mathbf{mg}}{\mathbf{g}}\right)$	**k_1** $\left(\frac{\mathbf{g}}{\mathbf{mg \cdot min}}\right)$	**R^2**	**k_{dif}** $\left(\frac{\mathbf{mg}}{\mathbf{g \cdot min^{0.5}}}\right)$	**R^2**	**β** $\left(\frac{\mathbf{g}}{\mathbf{mg}}\right)$	**α** $\left(\frac{\mathbf{mg}}{\mathbf{g \cdot min}}\right)$	**R^2**
Methanol	36	241.77	0.2130	0.9782	**492.13**	**1.21E-03**	**0.9974**	51.60	0.7341	0.0125	1445.05	0.8370
	92	1072.77	0.2940	0.9774	**649.77**	**4.27E-04**	**0.9330**	199.20	0.9567	0.0066	359.28	0.9843
	150	261.39	0.2020	0.9526	**431.78**	**1.34E-03**	**0.9994**	48.10	0.8806	0.0148	1410.89	0.9657
	200	143.88	0.1965	0.8510	**283.69**	**3.92E-03**	**0.9971**	66.47	0.7902	0.0174	760.52	0.9283
				0.9398			**<u>0.9817</u>**		0.8404			0.9288
CO_2	92	287.44	0.8388	0.9898	**329.82**	**1.82E-03**	**0.9985**	118.10	0.9707	0.0130	400.19	0.9952
	150	247.89	0.8173	0.9994	**322.79**	**2.52E-03**	**0.9961**	114.70	0.9338	0.0132	520.60	0.9870
	200	33.52	0.6857	0.9159	**110.66**	**3.04E-02**	**0.9992**	15.60	0.8531	0.0806	13693.77	0.9074
Average				0.9684			**<u>0.9979</u>**		0.9192			0.9632
DMC	92	**1269.02**	**0.8624**	**0.9948**	-	-	0.1376	139.00	0.9031	0.0070	97.71	0.9459
	150	**305.21**	**0.4978**	**0.9681**	434.22	8.32E-04	0.9617	123.40	0.9148	0.0092	289.07	0.9594
	200	**241.05**	**1.2340**	**0.9965**	247.95	3.76E-03	0.9923	95.95	0.9292	0.0172	458.12	0.9785
Average				**<u>0.9865</u>**			0.6972		0.9157			0.9613
Water	92	1253.88	0.5214	0.9265	620.35	1.54E-04	0.9623	**113.90**	**0.9752**	0.0191	20.69	0.9919
	150	335.96	0.6753	0.9169	750.75	7.99E-05	0.8229	**100.80**	**0.9939**	141.19	0.0146	0.9454
	200	154.93	0.6904	0.9629	332.01	7.57E-05	0.0880	**76.70**	**0.9916**	0.0236	106.57	0.9413
Average				0.9354			0.6244		**<u>0.9869</u>**			0.9595

Adsorption conditions: methanol concentration (19.9 % mol), zeolite A (80mg), 20° C, and 0.83 atm.

Table 16 Kinetic parameters for <u>water</u> in the mixture: water, ethanol and CO_2

T (°C)	PFO			PSO			IPD		Elovich		
	$\mathbf{qe}\ \left(\frac{\mathbf{mg}}{\mathbf{g}}\right)$	$\mathbf{k_1}\ (\mathbf{min^{-1}})$	$\mathbf{R^2}$	$\mathbf{qe}\ \left(\frac{\mathbf{mg}}{\mathbf{g}}\right)$	$\mathbf{k_1}\ \left(\frac{\mathbf{g}}{\mathbf{mg \cdot min}}\right)$	$\mathbf{R^2}$	$\mathbf{k_{dif}}\ \left(\frac{\mathbf{mg}}{\mathbf{g \cdot min^{0.5}}}\right)$	$\mathbf{R^2}$	$\boldsymbol{\beta}\ \left(\frac{\mathbf{g}}{\mathbf{mg}}\right)$	$\boldsymbol{\alpha}\ \left(\frac{\mathbf{mg}}{\mathbf{g \cdot min}}\right)$	$\mathbf{R^2}$
92	145.18	0.1495	0.9678	245.22	1.55E-04	0.9848	**29.57**	**0.9961**	0.0264	24.69	0.9573
150	80.72	0.3710	0.9907	100.61	1.33E-03	0.9742	**21.44**	**0.9771**	0.0718	20.85	0.9886
200	51.42	0.4388	0.9808	137.93	3.74E-04	0.6456	**33.79**	**0.9929**	0.0659	98.69	0.9696
Average			0.9798			0.8682		**<u>0.9887</u>**			0.9718

Table 17 Kinetic parameters for <u>water</u> in the mixture: water, methanol and CO_2

T (°C)	PFO			PSO			IPD		Elovich		
	$\mathbf{qe}\ \left(\frac{\mathbf{mg}}{\mathbf{g}}\right)$	$\mathbf{k_1}\ (\mathbf{min^{-1}})$	$\mathbf{R^2}$	$\mathbf{qe}\ \left(\frac{\mathbf{mg}}{\mathbf{g}}\right)$	$\mathbf{k_1}\ \left(\frac{\mathbf{g}}{\mathbf{mg \cdot min}}\right)$	$\mathbf{R^2}$	$\mathbf{k_{dif}}\ \left(\frac{\mathbf{mg}}{\mathbf{g \cdot min^{0.5}}}\right)$	$\mathbf{R^2}$	$\boldsymbol{\beta}\ \left(\frac{\mathbf{g}}{\mathbf{mg}}\right)$	$\boldsymbol{\alpha}\ \left(\frac{\mathbf{mg}}{\mathbf{g \cdot min}}\right)$	$\mathbf{R^2}$
92	222.07	0.1696	0.9568	212.90	1.91E-04	0.9520	**25.67**	**0.9769**	0.0225	18.96	0.9941
150	40.21	0.5021	0.9344	-	-	0.5202	**15.74**	**0.9857**	0.0948	16.26	0.9292
200	80.88	0.4425	0.9692	358.17	4.83E-05	0.2263	**20.80**	**0.9926**	0.0506	18.22	0.9837
Average			0.9535			0.5662		**<u>0.9851</u>**			0.9690

Table 18 Kinetic parameters for <u>water</u> in the mixture water- ethanol - DEC - CO_2

T (°C)	PFO			PSO			IPD		Elovich		
	$\mathbf{qe}\ \left(\frac{\mathbf{mg}}{\mathbf{g}}\right)$	$\mathbf{k_1}\ (\mathbf{min^{-1}})$	$\mathbf{R^2}$	$\mathbf{qe}\ \left(\frac{\mathbf{mg}}{\mathbf{g}}\right)$	$\mathbf{k_1}\ \left(\frac{\mathbf{g}}{\mathbf{mg \cdot min}}\right)$	$\mathbf{R^2}$	$\mathbf{k_{dif}}\ \left(\frac{\mathbf{mg}}{\mathbf{g \cdot min^{0.5}}}\right)$	$\mathbf{R^2}$	$\boldsymbol{\beta}\ \left(\frac{\mathbf{g}}{\mathbf{mg}}\right)$	$\boldsymbol{\alpha}\ \left(\frac{\mathbf{mg}}{\mathbf{g \cdot min}}\right)$	$\mathbf{R^2}$
92	203.98	0.1699	0.9741	289.86	1.09E-04	0.9265	**31.98**	**0.9880**	0.0203	22.26	0.9861
150	118.39	0.4007	0.9934	110.46	8.17E-04	0.8798	**19.89**	**0.9446**	0.0405	20.52	0.9761
200	124.84	0.3488	0.8760	167.53	4.32E-03	0.9941	**28.82**	**0.9945**	0.0361	575.77	0.9745
Average			0.9478			0.9335		**<u>0.9757</u>**			0.9789

Table 19 Kinetic parameters for water in the mixture water- methanol - DMC - CO_2

T (°C)	PFO			PSO			IPD		Elovich		
	$\mathbf{qe}\ \left(\frac{\mathbf{mg}}{\mathbf{g}}\right)$	$\mathbf{k_1}\ (\mathbf{min^{-1}})$	R^2	$\mathbf{qe}\ \left(\frac{\mathbf{mg}}{\mathbf{g}}\right)$	$\mathbf{k_1}\ \left(\frac{\mathbf{g}}{\mathbf{mg \cdot min}}\right)$	R^2	$\mathbf{k_{dif}}\ \left(\frac{\mathbf{mg}}{\mathbf{g \cdot min^{0.5}}}\right)$	R^2	$\boldsymbol{\beta}\ \left(\frac{\mathbf{g}}{\mathbf{mg}}\right)$	$\boldsymbol{\alpha}\ \left(\frac{\mathbf{mg}}{\mathbf{g \cdot min}}\right)$	R^2
92	163.04	0.2078	0.9669	-	-	0.0152	**22.01**	**0.9841**	0.0295	11.40	0.9880
150	40.33	0.2817	0.9804	-	-	0.2575	**55.41**	**0.9871**	0.0921	8.37	0.9516
Average			0.9737			0.1364		**0.9856**			0.9698

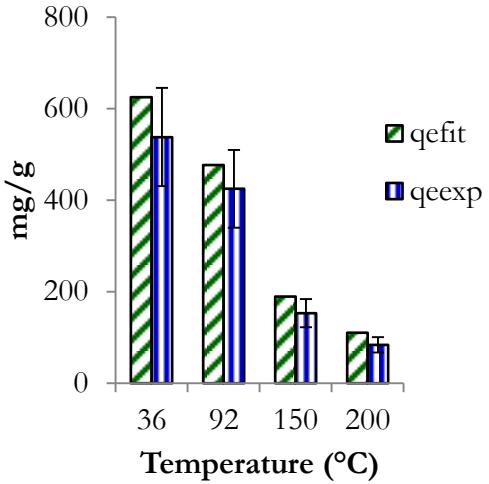

Figure 29 Comparison of the experimental and predicted water adsorption capacity of zeolite 4A for determining the values error.

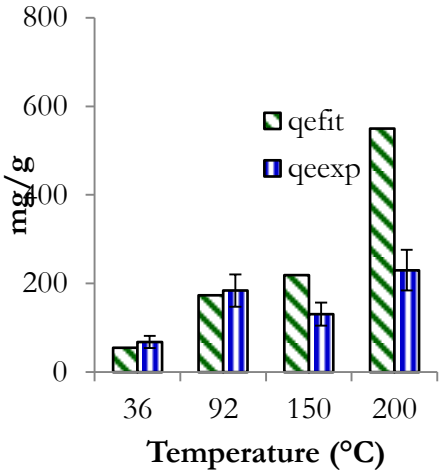

Figure 30 Comparison of the experimental and predicted ethanol adsorption capacity of zeolite 4A for determining the values error.

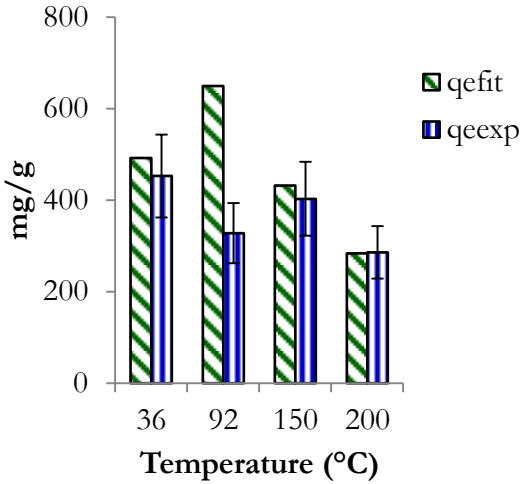

Figure 31 Comparison of the experimental and predicted methanol adsorption capacity of zeolite 4A for determining the values error.

1.3.6. Characterization of Zeolite 4A

1.3.6.1. Analysis EDS

Table 20 presents the EDS analysis of the fresh zeolite 4A. The Si/Al ratio (1.11) and Na/Al ratio (0.998) are close to 1, which is expected for the structural formula. These ratios guarantee the hydrophilic character of the material.

Table 20 EDS analysis of zeolite 4A

Element	Atomic%
O	61.49
Na	12.26
Al	12.29
Si	13.63
K	0.32

1.3.6.2. SEM

SEM micrographs for Zeolite 4A at 1000X and 5000X is shown in Figure 32. Zeolite 4A shows very well developed cubes, which can be associated with its geometric structure.

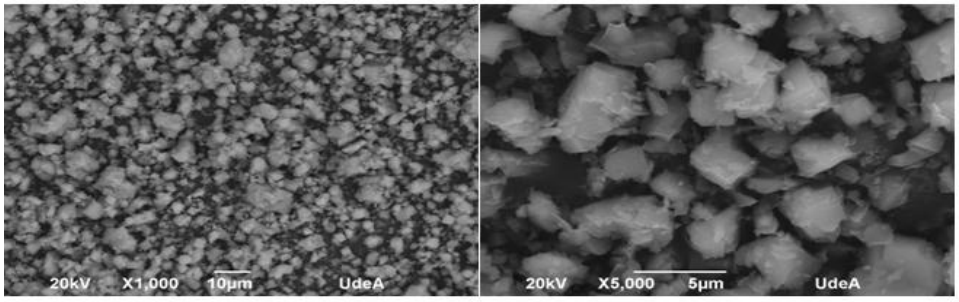

Figure 32 SEM analysis of Zeolite 4A

1.3.6.3. XRD Analysis

The standard patter of zeolite shows a good crystallinity. The characteristic peaks for zeolite 4A are correctly identified when this is compared to the pattern for Linde Type A (LTA) [54]. Analysis of the effect of the use of this zeolite in adsorption processes, the solid was analyzed after use by XRD. For understanding the changes in the kinetic when the mixtures contain CO_2 due to possible changes in the structure of the zeolite 4A, the XRD for mixtures of four compounds (Figure 33) and two compounds (Figure 34) used at 200°C were made.

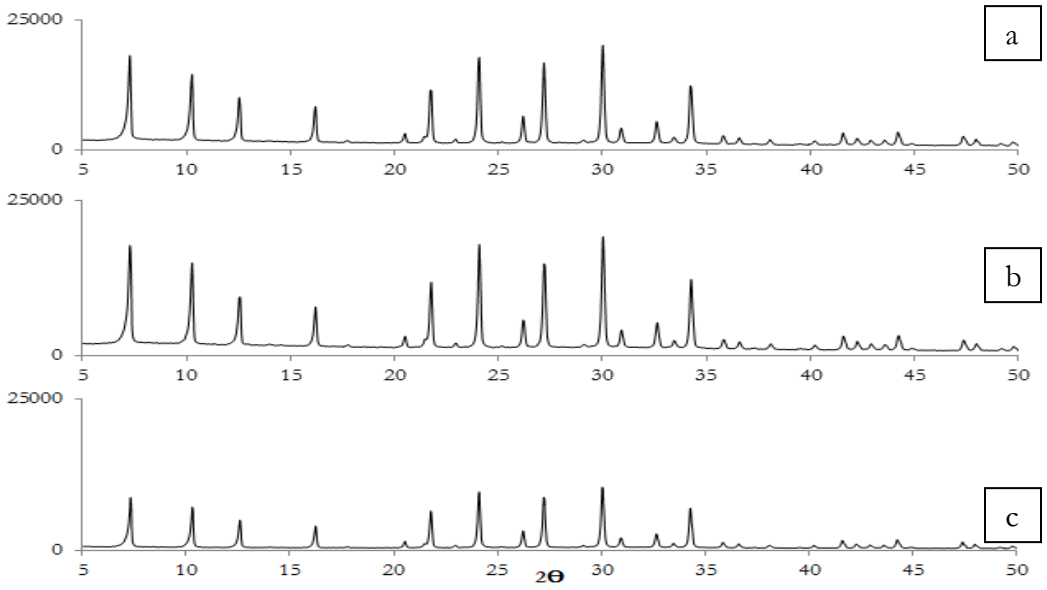

Figure 33 XRD zeolite 4A used in mixture of four components at 200°C. (a) Mixture: *water, ethanol, DEC and CO_2*; (b) Mixture: *water, methanol, DMC and CO_2* (c) Pattern of zeolite 4A [54].

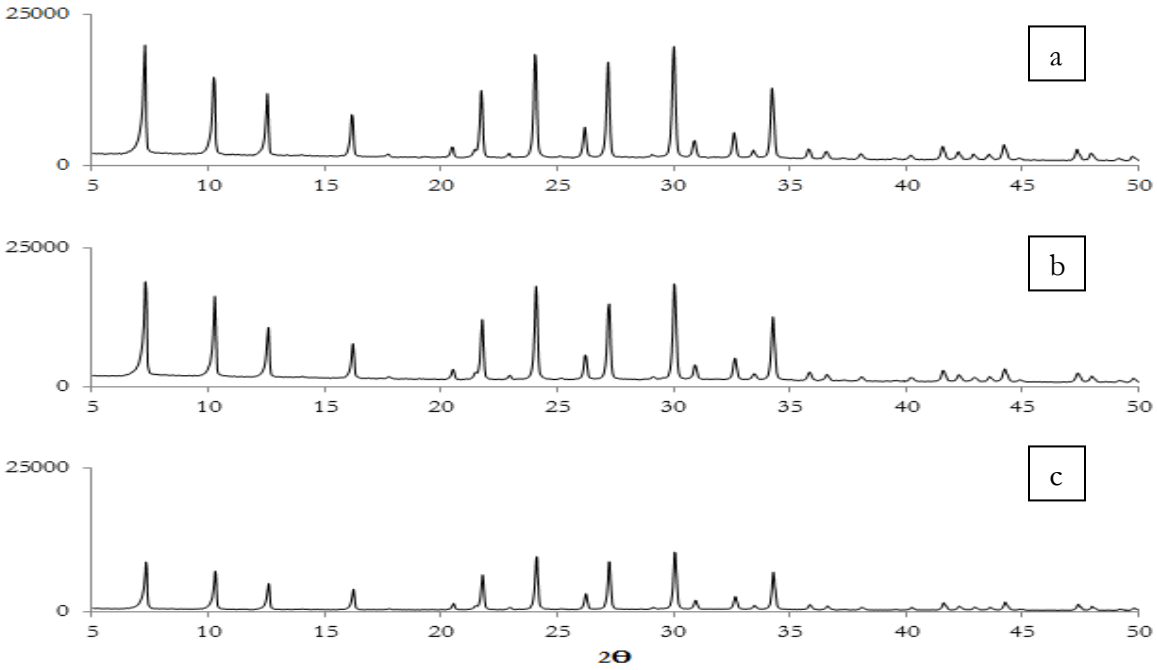

Figure 34 XRD zeolite 4A used in mixture of two components at 200°C. (a) Mixture: *CO_2 - ethanol* (b) Mixture: *CO_2 - methanol.* (c) Pattern of zeolite 4A .

The results of the zeolite used in the mixtures water-alcohol (Figure 35) were not significant changes in the structure, in all used samples is possible to see the characteristic peaks for zeolite 4A. A possible increment in the intensity and thickening of some characteristics peaks

express a growing in the crystal size [55], probably, due to the increment of the temperature that could help the crystal formation [56] About the signal intensity, the changes could mean a little change in the homogeneously of this material [57].

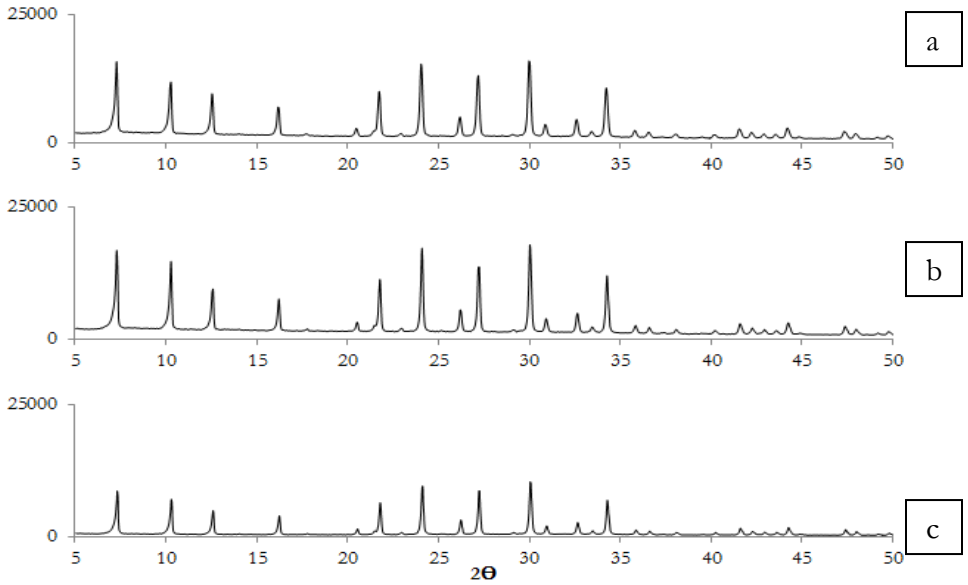

Figure 35 XRD zeolite 4A used in a mixture two components at 200°C. (a) Mixture: *water - ethanol* (b) Mixture: *water - methanol* (c) Pattern of Zeolite 4A.

In order to analyze the effect in the change of pressure for this system, Figure 36 shows the XRD patter. Similar to previous description, only small changes in the intensity and thickening are observed. That suggests that the pressure does not affect the structure.

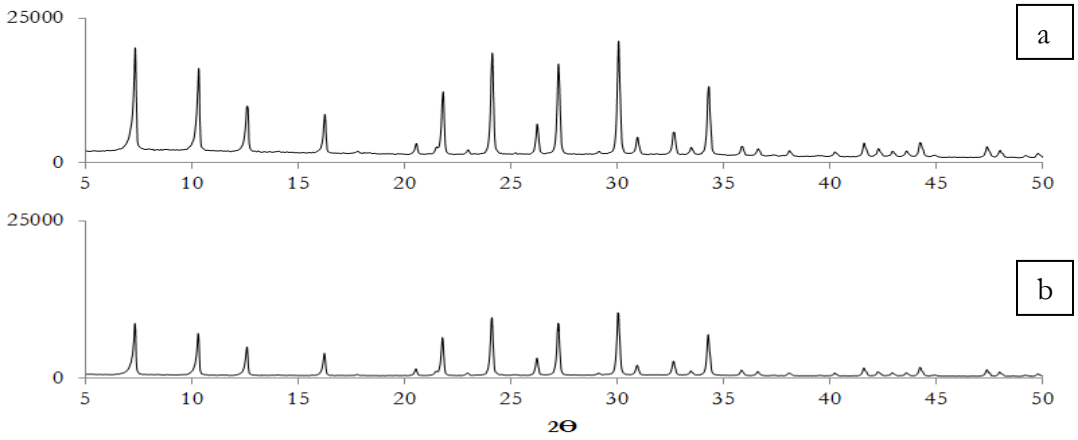

Figure 36 Comparison between zeolite 4A used at 14 Bar and fresh at 1 Bar. (a) Used. (b) Fresh

Figure 37 shows the color changes in some samples of zeolite 4A used, mainly, with methanol and CO_2. Fresh zeolite 4A presents a white color but, when it was used in mixtures with methanol (a) and CO_2 (b) the results show pale yellow color. Although the structure does not change strongly, the possible cluster, reduction and fully dehydration [58].

Figure 37 Change of color in zeolites 4A used. (a) fresh zeolite 4A; (b) After methanol adsorption; (b) After CO_2 adsorption .

1.4. PARTIAL CONCLUSIONS

The previous result allows to observe that the Langmuir adsorption model interprets all adsorption data; this means the adsorption of water, ethanol and methanol over zeolite 4A and their mixtures are all in one layer when inner pores of zeolites can be filled with a constant amount of molecules.

The adsorption of water, methanol and ethanol followed the Langmuir isotherm patterns. Relevant kinetic parameters were fitting using the equilibrium adsorbed amount of water, ethanol and methanol in zeolite 4A for determining the adsorption isotherm measurements at different temperatures. The kinetic of the adsorption of water was affected in the multicomponent system. In general terms, water, ethanol and methanol follow the Pseudo First Order (PFO), Pseudo Second Order (PSO), Intra Particle Diffusion (IPD) and Elovich models. For ethanol and methanol, the increment of adsorption temperature decreases the adsorption capacity since the adsorption velocity increase, The behavior of ethanol could be related with a possible chemisorption, common phenomena in methanol reaction, but, it is necessary a further study. The comparing the effect of the pressure and the temperature in the water adsorption capacity, it is possible to say that both ones affect the adsorption in negative way but the effect of temperature is predominant. Zeolite 4A presents an excellent regeneration capacity and it can be used at least 5 times without a significant reduction in the water adsorption capacity.

Since the pore diameter of 4A zeolite is equal to 4 Å and the kinetic diameter of DMC is equal to 4.7 Å and DEC is 6.3 Å, these molecules have hindered to enter the zeolite pores, while molecules as methanol (3.8 Å), CO_2 (3.3 Å) and water (2.6 Å) can be easily adsorbed inside the zeolite 4A pores. The kinetic diameter is generally a good way to understand why some

molecules could be adsorbed into the molecular sieves as zeolite 4A, however, molecules in the study system have some exceptions, for example, ethanol with higher size than molecular sieve (4.6 Å) is adsorbed while CO_2 (3.3 Å) it is not adsorbed even a long times (data not shown).

In the other side, CO_2, DEC and DMC hindered the pass through the pores because their presence reduces the adsorption capacity of water and alcohols in the zeolite 4A. About the alcohols, it is possible to say that they are competing to occupy adsorption sites. Binary systems of alcohol-water must share the active sites of adsorbent between both compounds and for this reason, decrease the water adsorption capacity. In addition, the time to achieve the equilibrium in the mixtures is faster than with the single compounds.

There are not many reports for components systems adsorption, and the main conclusions in this work showed that CO_2, DMC and DEC are not adsorbed in 4A zeolite but the water adsorption capacity is affected by the number of compounds in negative way, due to a competitive or inhibitory effects of the mixture [59]. The similarities in the polarities and some chemical properties of methanol and water showed the difficulties to separate these two molecules.

The mechanism to describe the behavior of kinetic adsorption for water was IPD. This model express that the diffusion in the pores is the step limit and it also suggests that the adsorbent has a homogenous porous structure [41]. That model affirms that the chemisorption is not a determined step in the adsorption process. Finally, the increment in the temperature decreases the adsorption velocity (k_1) value, because the process is faster than low temperatures.

Alcohols tend to follow IPD kinetic when they are in mixture with water, but the CO_2 presence modifies strongly the kinetic of the system. It is better to describe as Elovich or PSO model systems with CO_2 and methanol. Both mechanisms express a chemisorption process as limit in the adsorption. These results are logic base on some changes as physical evidence in zeolite 4A.

Comparing the adsorption isotherms for multicomponent systems were possible to define that water and alcohols are adsorbed on zeolite 4A at 92°C, 150°C and 200°C. For these systems the quantities of both compounds water and alcohols increased very fast at the beginning because there were enough vacancies in zeolites (diffusion kinetics plays an important role). After a while, the amount of alcohol adsorbed started to decrease and the quantities of water increased. The explanation would be that the adsorption of water is stronger than alcohol, and therefore water molecules begin to snatch the adsorption sites once occupied by alcohol when adsorption equilibrium is starting its determine role. This gives a clue that both the adsorption equilibria and diffusion kinetics influenced the uptakes of water and methanol in zeolite 4A across the time [14].

CHAPTER 2

DIRECT SYNTHESIS OF DIETHYL CARBONATE (DEC) AND DIMETHYL CARBONATE (DMC) USING COPPER-NIQUEL CATALYST ON ACTIVETED CARBON (Cu-Ni/AC) IN THE PRESENCE OF ZEOLITE 4A

2.1. INTRODUCTION

This part shows the generalities for the production of DMC and DEC, different routes, applications and the results obtained with the use of Cu-Ni/AC catalyst in gas and liquid phase through direct synthesis at mild conditions (around 14 Bar and 92 – 150°C) in order to have a reference when the dehydrated agent is added.

2.1.1. Main applications linear carbonates

DEC and DMC are esters used in parallel way with the development of new synthesis more friendly with the environment. DEC and DMC are part of the new green chemicals, after being excluded by the EPA (Environmental Protection Agency) of the definition of VOCs (volatile organic compounds). They exhibit high reactivity due to hydrogen bonds since the electrophilic activation increased by the presence of ions that alter the structure of water or other solvents to form those hydrogen bonds [60]. The importance of linear carbonates production is related to theirs multiple applications. The Figure 38 below estimates global consumption of DMC according to end-use [61].

Other important information about specific properties and global market could be consulted in Appendix 11and

Appendix 12 respectively.

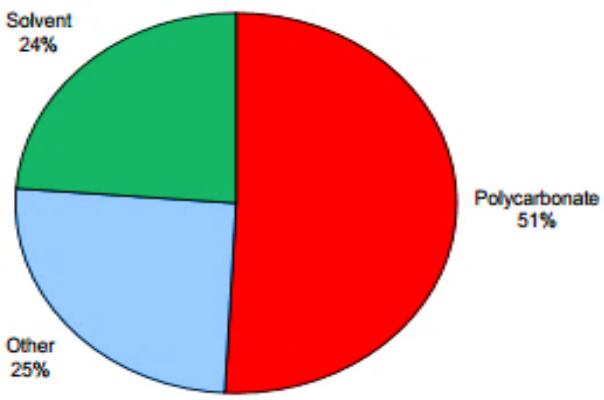

Figure 38 Global DMC consumption by end use

2.1.1.1. Solvent

Linear carbonates can be used as solvents for high quality paints, inks, coatings and adhesives replacing the used of benzene, xylene, ethyl acetate, butyl acetate, acetone, butanone and toluene. It is use as paint remover, solvent for nitro-cotton, cellulose ether, synthetic resin and the traditional resin, solvent for polyamide, polyacrylonitrile, diphenol resin, and solvent for evaporation of cellulose nitrate and in the synthesis of polycarbonate resins [62]. DEC can give uniformity to dyeing process and increase the bleaching quality from the sun. In addition, it can improve the feel in the textiles and the anti-wrinkle quality on the synthetic fibers industry.

2.1.1.2. Reactant

Linear carbonates are considered intermediates in the synthesis of polymers such as polycarbonate, pesticides, antioxidants and high-yield resins [63]. Due to their high reactivity towards molecules like phenols or primary amines, DMC is used as a carbonylation agent for aromatic polycarbonate and isocyanate synthesis [64]. They are an alternative to use phosgene as well as dimethyl sulfate, chloromethane and methylation reactions [65], [66]. It is an ideal substitute for toxic substances such as phosgene, dimethyl sulfate and methyl chloroformate, and methyl halides. Replace the use of toxic compounds by a lower toxicity is currently of great interest. It has reported its use in the production of urethanes, ureas and other esters of aliphatic carboxylic acids such as alkyl carbonates, cyclic carbonates and oxetanes [67]. Linear carbonates works as a solvent and reagent in one system and the waste management is easy and it produces a low environmental impact without danger to people and allows easy control of reactions because their reactions are only slightly exothermic [60].

2.1.1.3. Pharmaceutical products

Its application has been reported as intermediate in the synthesis of various pharmaceuticals [67] such as antibiotics and as particular example, for the synthesis of phenobarbital, which is used as an strong base to prepare diethyl phenylmalonate. [68], [69].

2.1.1.4. Oxygenate fuels

Due to the high oxygen content of linear carbonates (53,3 wt. % DMC), (40,7 wt. % DEC), compared with other additives such as MTBE (18,2 wt. %) and ethanol (34,8 wt. %), [70], [65], [71] linear carbonates are compounds of great interest for fuel industry. A higher oxygen content improves the fuel process (diesel and biodiesel), providing greater thermal efficiency and reducing emissions of particulate matter (carbon monoxide, formaldehyde and unburned hydrocarbons) [72], [73]. It has also been reported that the addition of DMC to fuels increase significantly the octane number compared to other alkylcarbonates (Union Oil Co. patents related to reduce soot emissions).

2.1.1.5. Rechargeable lithium batteries

Being a non-aqueous electrolyte, linear carbonates are obtained each day more application in the field of rechargeable lithium batteries [74]. In lithium batteries, the electrolytes are obtained dissolving lithium salt in organic compounds such as propylene or ethylene carbonate. These traditional solvents have a good dissolution with lithium salts, but their viscosity reduces the electrochemical cycle efficiency. Linear carbonates have a suitable solvating effect towards lithium ions and present a low viscosity. Some studies have shown how DMC addition increasing the electrolyte conductivity and reduce resistance significantly [75] [76] [77]. Given the significant increases in the greener vehicles demand such as hybrid and electric cars, expected a fast increase of linear carbonates since could be used in order to prepare the electrolyte in the capacitor battery and lithium battery.

2.1.2. Methods to produce DEC and DMC in gas phase

Green chemists trays to find a new route in order to produce very important compounds as DMC and DEC. The most important routes are described in this part in order to define the advantages and disadvantages of all these process.

2.1.2.1. Phosgenation

This method has been used mainly with methanol (methanolysis of phosgene), and it has been registered by Bayer (Germany) and Société Nationale des Poudres et Explosif (SNPE, France) Companies.

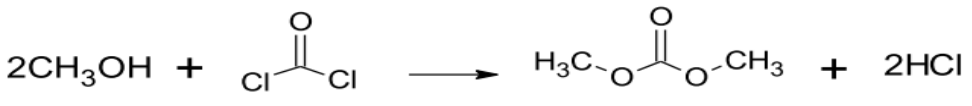

Figure 39 Phosgenation

The reaction (Figure 39) occurs at 0°C in an anhydrous solvent (toluene or dichloromethane) catalyzed by a concentrated solution of sodium hydroxide or in the presence of pyridine

excess. The reaction presents a high yields of 82 % and 85 % based on methanol and phosgene but, the process need neutralize large amounts of pyridine and it is toxicity and corrosiveness (mainly HCl) [78].

The case of DEC is quite similar, ethanol is solubilized at room temperature in dichloromethane with excess pyridine and reacts with phosgene to produce DEC (see Figure 40), which is separated from the reaction mixture by distillation [67]. The yield is around 50% toward DEC but the toxic compounds and, additional step in order to spear it is the disadvantage.

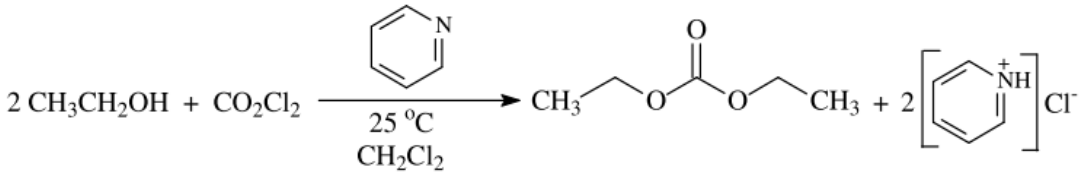

Figure 40 Phosgenation reaction

2.1.2.2. Oxidative carbonylation

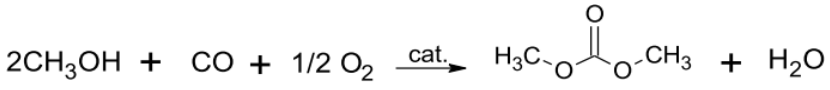

Figure 41 Oxycarbonylation of DEC

The oxidative carbonylation or oxycarbonylation is a process registered by ENIChem (Italy) Company in liquid phase and Dow Chemical Co in vapor phase (Figure 41). The general conditions in gas phase are 120-130 °C and 2 - 3 atm and use of a copper salt, such as copper chloride I (CuCl), as a catalyst. The advantages are the good selectivity and reaction rates but the gas mixture used (CO/O_2) is explosive under certain conditions and the oxygen must be the limiting reagent: The liquid phase conditions are from 100 to 130 °C and from 10 to 30 bar. Liquid phase present low selectivity .[79]. In the case of DEC, the yield is around 30% (Figure 42).

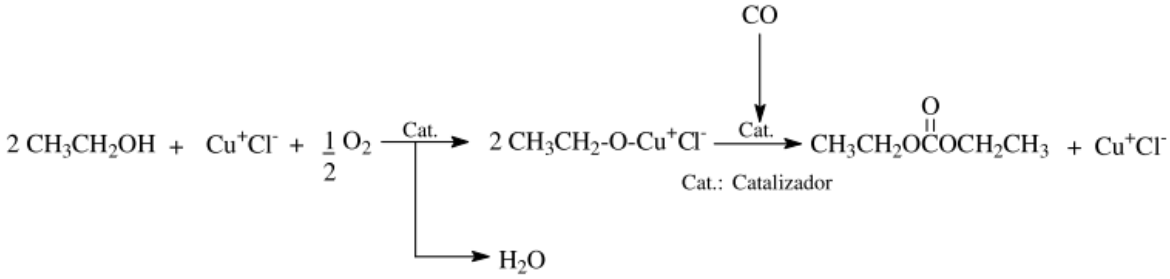

Figure 42 Oxycarbonylation of DMC

2.1.2.3. Methylnitrite Carbonylation

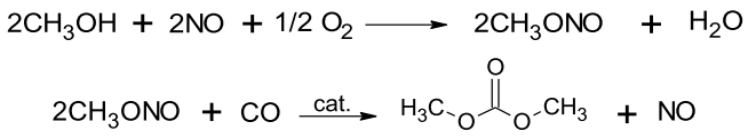

Figure 43 Methylnitrite Carbonylation of DEC

This method is used by UBE Chemical Company (Japan). The reaction occurs in two steps: First Step: Liquid phase at 60 °C, no catalyst is required; Second Step: Second reactor, reaction in vapor phase (Figure 43 for DEC and Figure 44 for DMC). Catalyst: $PdCl_2$ supported over carbon. As advantage, the reaction avoided catalyst deactivation, but, it requires safety hazards and it has explosive limits [80].

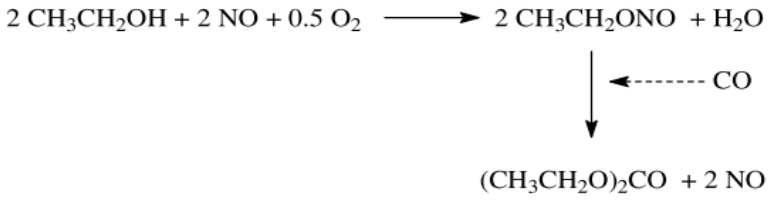

Figure 44 Methylnitrite Carbonylation of DMC

2.1.2.4. Urea alcoholysis

This reaction requires long times in order to form the carbonates and occurs in two steps (DEC and DMC Figure 45 and Figure 46 respectively). The reaction is carried from 150-195 °C for 4.5 hours or at 195-220 °C for 14 hours, depending on the catalyst. The yields of carbonates are typically above 90%; moreover, the ammonia formed during the reaction can be recycled for the synthesis of urea by addition of carbon dioxide [81]. This route is an environmentally friendly and an atom-efficient process because the only by-product (ammonia) can be recycled for the preparation of urea with low cost and low toxicity. However, decomposition of the carbamate leads the production of isocyanic acid or isocyanuric acid, decreasing the selectivity to diethyl carbonate formation.

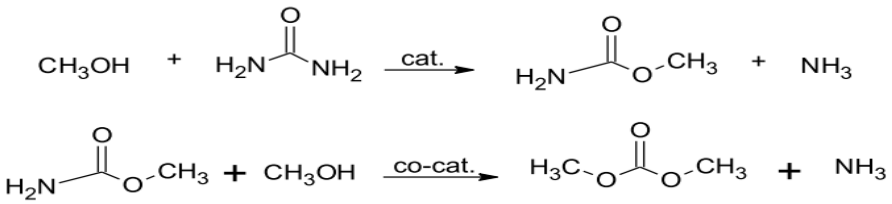

Figure 45 Urea alcoholysis of DEC

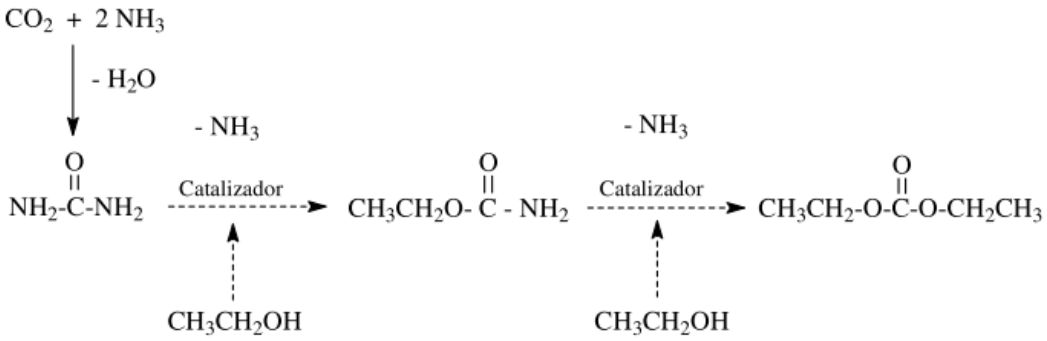

Figure 46 Urea alcoholysis of DMC

2.1.3. Direct synthesis from CO_2 and alcohol

Direct synthesis is defined as the reaction between carbon dioxide and methanol or ethanol to produce dimethyl carbonate (DMC) or diethyl carbonate (DEC) respectively (Reaction 1 and 2). The "phosgene-free" synthesis of organic carbonates (DMC and DEC) is attracting the attention as CO_2 and ethanol/methanol are considered green reagents, nontoxic and biodegradable. Moreover the use of a greenhouse gas as CO_2 is an attractive advantage because of its abundance and it is a non-toxic and economic matter. The reaction responds to the principles of sustainable chemistry and water is the only co-product. The direct synthesis of DMC/DEC is an equilibrium-limited reaction with yields above 2 % [14] and this is the main problem. They have been propose several solutions in order to increase the yield: Use of very high pressures (300 Bar), excess of CO_2 (around 98%) , develop of efficient catalyst and water adsorption [8].

It is well known that the direct synthesis of linear carbonates (DMC and DEC) from CO_2 and alcohol is a highly equilibrium limited reaction at approximately 1-2 % yield. Its equilibrium constant is only 8.5×10^{-6} at 160°C by DMC and 3.5×10^{-6} at 150°C by DEC [82] limiting the yield. When the reaction was carried out at 12MP of CO_2, Hou et al. claimed that methanol conversion as high as 7 % were obtained. For other side the methanol conversion of nearly 50 % after 72 h under 30 MPa was achieved in work of Choi et al. when 3A zeolite was applied as desiccant at room temperature [83]. The Choi study present the use of dibutyltin dimethoxide as catalyst at 300 atm and 180 °C by 24 h and use the external loop with a fixed bed column (at room temperature.

Note that the large excess of applied CO_2 its practical industrial realization since the investment of construction and the cost of routine maintenance of extremely high pressure reaction unit are too big to be sustainable. About the use of external loop, it is important to consider the extra consumption of energy. About the use of water traps has shown to be a good approach to remove the extremely low concentration of water in methanol and ethanol.

Several dehydration systems have been developed to remove water from the reaction media, and these dehydration systems can be divided into two types; non-reactive dehydration systems (gas-phase, membrane separation and inorganic absorbent systems) and reactive dehydration systems (non-catalytic and catalytic dehydration systems). These systems are summarized in Figure 47 until Figure 50 [84]. The reaction can occur in gas and liquid phase. Gas phase allows easy process control, easy catalyst recovery and reduce the capital costs while liquid phase offers lower yield.

Among these dehydration systems, the reactive dehydration system, and in particular, the catalytic dehydration system with nitriles is the most efficient for the synthesis of organic carbonate. Especially, the combination of 2-cyanopyridine with CeO_2 achieved a high DMC yield of 94 % with 96 % selectivity [85]. Although, the selection of catalyst, hydration reaction and dehydration agent is difficult because these factors must work simultaneously under the same reactions.

The used of organic compounds like dicyclohexyl carbodiimide (DCC), orthoesters, acetals and sulfates (Mg, Na) in liquid phase at high pressure and present good yields, but, present hydrolyisis and high cost too [20]. Some organic dehydrating agents like 2,2-dimethoxypropane (DMP) and dicyclohexylcarbodiimide (DCC) have a problem: their high cost in the regeneration process. By contrast, the high availability and easy recovery of inorganic adsorbents like zeolites make them the most promising candidates to remove the water in the direct synthesis of linear carbonates.

Figure 47 express the main catalyst used in homogenous and heterogeneous phase and the conditions. It is possible to see that in Figure 48 there are not reports for Cu-Ni/AC catalytic activity in presence of scavengers yet or its use in liquid phase. For this reason it is important to evaluate the effect of zeolite 4A presence in the yield. The intention was evaluate the behavior of both Cu-Ni/AC catalyst and Zeolite 4A at the same conditions using different assemblies in gas phase: Fluidized, single and mixed bed and the presence of zeolite into the reactor at the same pressure and temperature conditions. Both compounds Cu-Ni/AC catalyst and zeolite 4A offer many advantages: low cost, high regeneration capacity, no deactivation, and any decomposition in presence of water. The zeolites A are available and recyclable and since the Si/Al = 1 ratio present a hydrophilic character with good water adsorption capacity [18]. Figure 48 show too how the use of zeolite type A is still less, however, some studies show how the use of external loops with zeolite 3A is a common method used trough the reaction in gas phase. Decoupling the reaction and the removal of water into different reaction zones increased the DMC yield to 17 % using zeolite 3A at 248 K as drying agent [14]. Other interesting study finds that water-adsorption efficiency of 3A zeolite greatly increases at temperatures far below 273 K suggesting design a new reaction unit with two temperature zones, high-temperature reaction zone and low-temperature water-removal zone [14]. This study includes the use recirculation of the reaction mixture (liquid phase) between the reactor

and the zeolite trap. The yield obtained was near 10 % for DMC at 433 K, 42 bar using ZrO_2 as catalyst and 3A zeolite. The zeolite was 9 times the catalyst.

Figure 49 present the organic dehydrative agents and, it is possible to observe that, Cu-Ni/AC catalyst is not proved yet. Finally, Figure 50, present some system with catalyst reaction.

Consider this reports, here they are presented the results of the formation DMC and DEC through direct synthesis of CO_2 and alcohol in gas and liquid phase at moderate conditions using Cu -Ni / AC as catalyst and zeolite 4A as adsorbent. They were also present some test with butylene oxide (organic dehydrating) in liquid phase. The conditions were 90 ° C and 60 Bar and reaction was made in a Parr reactor during 24 hours. The reaction in gas phase was performed at 150°C and 14 Bar.

Entry	Catalyst	P_{CO_2}/MPa	T/K	t/h	Yield/%	Selc./%
Homogeneous catalyst system						
1	$Bu_2Sn(OBu)_2 + I_2$	2.8	453	20	4.4	—
2	$CH_3OK + CH_3I$	7.3	353	10	0.02	>99
3	Tl(OEt)	0.3	423	70	0.3	—
4	$Ti(OBu)_4$	2.5	453	20	2.8	—
5	$Ni(OAc)_2{\cdot}4H_2O$	7	413	12	2.1	>99
6	$[Nb(OMe)_5]_2$	5	423	28	1.8	—
7	Mg	15	453	12	1.2	>99
Heterogeneous catalyst system						
8	ZrO_2	6	433	16	1.0	>99
9	ZrO_2/SiO_2	20	423	130	0.4	—
10	ZrO_2/C	0.1	353	1	0.47	—
11	H_3PO_4/ZrO_2	6	403	2	0.3	>99
12	$H_3PW_{12}O_{40}/ZrO_2$	(175 mmol)	373	7	4.3	>99
14	CeO_2–ZrO_2	6	383	16	1.7	>99
15	$Ce_{0.5}Zr_{0.5}O_2$	20	373	24	1.4	—
16	$Ce_{0.8}Zr_{0.2}O_2$	5	443	1	0.7	—
17	$Ga_2O_3/Ce_{0.6}Zr_{0.4}O_2$	6	443	3	0.45	>99
18	$H_3PW_{12}O_{40}/Ce_{0.6}Zr_{0.4}O_2$	6	443	3	0.25	>99
19	$Ce_{0.5}Zr_{0.4}Y_{0.1}O_2$	20	373	24	0.8	—
20	CeO_2	6	403	4	0.7	>99
21	CeO_2	5	413	2	0.43	—
22	$H_3PW_{12}O_{10}/Ce_{0.1}Ti_{0.9}O_2$	5	443	12	5	>99
23	Al_2O_3/CeO_2	5	408	5	2.1	>99
24	$Cu_{1.5}PMo_{12}O_{40}$	0.12	323	1	1.7	28
25	SnO_2	20	423	100	1.6	9
26	Sn/SBA-15	18	513	10	0.07	—
27	Sn/SBA-15	18	473	190	0.08	—
28	Sn–SBA–CH_3	20	423	70	0.65	>99
29	Sn–Ph–PMOs-4.0	18	453	30	0.01	—
30	$Co_{1.5}PW_{12}O_{40}$	0.5	353	5	2.4	65
31	Rh/ZSM-5	0.1	393	—	0.2	42
32	Polystylene–Nb	11.4	408	15	1.9	—

Figure 47 Direct synthesis from alcohol and CO_2 without dehydration systems [84].

Entry	Catalyst	Dehydrating agent	Alcohol	P_{CO_2}/MPa	T/K	t/h	Yield/%	Selc./%
Gas phase reaction system								
1	Cu–Ni/VSO	—	MeOH	0.6	453	—	4.5	58
2	Cu–Ni/VO + Photo irradiation (UV)	—	MeOH	1.2	393	—	4.0	85
3	Cu–Ni–V/AC (Active carbon)	—	MeOH	1.2	383	3	7.0	90
4	Cu–Ni/graphite	—	MeOH	1.2	378	—	9.0	88
5	Cu–Ni/graphite oxide	—	MeOH	1.2	378	3	9.1	90
6	Cu–Ni/TEG (Thermally expanded graphite)	—	MeOH	1.2	373	—	4.4	89
7	Cu–Ni/MWCNTs (Multi-walled carbon nanotubes)	—	MeOH	1.2	393	—	3.7	85
8	$CuCl_2$/AC (Active carbon)	—	MeOH	1.2	393	4	(4.8 mmol h^{-1})	90
9	Cu–Ni/GNS (graphene nanosheet)	—	MeOH	1.2	393	3	7.6	83
10	Cu–Ni/diatomite	—	MeOH	1.2	393	GHSV = 600 h^{-1}	4.1	91
11	Cu–Fe/SiO_2	—	MeOH	1.2	393	SV = 360 h^{-1}	4.6	86
12	Cu–Fe–Mo/SiO_2	—	MeOH	0.6	393	SV = 360 h^{-1}	6.1	88
13	$Co_{1.5}PW_{12}O_{40}$	—	MeOH	(60 ml min^{-1}.)	473	MWHSV = 3.25 h^{-1}	6.6	87
Membrane separation system								
14	Cu–KF/MgSiO	Polyimide–silica hybrid membrane	MeOH	0.4	403	SV = 1480 h^{-1}	8.8	96
15	Nb_2O_5/CeO_2	NaA-type tubular ceramic membrane	EtOH	30	408	—	2.3	>99
Inorganic absorbent system								
16	ZrPP–HF	Molecular sieve 3A	MeOH	4	443	12	1.7	5.3
17	$Bu_2Sn(OMe)_2$	Molecular sieve 3A	MeOH	30	453	72	45	—
18	Hydrotalcite	Silica hygel (gas phase reaction)	MeOH	(CH_3OH/CO_2 = 1/25)	403	(0.047 ml min^{-1})	16	>99
19	$Bu_2Sn(OMe)_2$	Molecular sieves	Glycerol	5	450	14	6.9	>99
20	Bu_2SnO	Zeolite 13X	EG	14	393	4	61	>99
21	Bu_2SnO	Zeolite 13X	1,2-PrD	14	393	4	42	>99
22	Bu_2SnO	Zeolite 13X	Glycerol	14	393	4	35	>99

[a] — means no data. EG: Ethylene glycol, 1,2-PrD: 1,2-propanediol.

Figure 48 Non-reactive dehydration systems for organic carbonate synthesis from CO_2 and alcohol [84].

Entry	Catalyst	Dehydrating agent	Alcohol	P_{CO_2}/MPa	T/K	t/h	Yield/ %	Selc./ %
1	K_2CO_3	CH_3I	MeOH	(200 mmol)	353	2	12.3	93
2	K_2CO_3	CH_3I	MeOH	8	343	4	5.2	82
3	—	CH_3I, molecular sieves 4A	MeOH		353	—	(13.4)[b]	—
4	$Bu_2Sn(OBu)_2 + I_2$	Trimethyl phosphate (TMP)	MeOH	2.8	453	20	4.7	—
5	$Ti(OBu)_4$	Trimethyl phosphate (TMP)	MeOH	2.5	423	20	2.9	—
6	$Bu_2Sn(OBu)_2 + I_2$	Dicyclohexyl carbodiimide (DCC)	MeOH	2.8	453	20	6.7	—
7	$Ti(OBu)_4$	Dicyclohexyl carbodiimide (DCC)	MeOH	2.5	423	20	4.0	—
8	CuCl	Dicyclohexyl carbodiimide (DCC)	MeOH	5	338	24	1.7	—
9	CuCl	Dicyclohexyl carbodiimide (DCC)	EtOH	5	338	24	1.3	—
10	Cu_2I_2	Dicyclohexyl carbodiimide (DCC)	Allyl alcohol	5	338	4	12	—
11	$Bu_2Sn(OMe)_2$	2,2-Dimethoxypropane (DMP)	MeOH	200	453	24	9.4	>99
12	$Bu_2Sn(OMe)_2$	2,2-Dimethoxypropane (DMP)	MeOH	20	423	96	1.6	>99
13	$Bu_2SnO + [Ph_2NH_2]OTf$	2,2-Dimethoxypropane (DMP)	MeOH	30	453	24	40	>99
14	$Bu_2SnO + [C_6F_5NH_3]OTf$	2,2-Dimethoxypropane (DMP)	MeOH	30	453	24	40	>99
15	$Ti(O/Pr)_4$ + decyl-18-crown-6	2,2-Dimethoxypropane (DMP)	MeOH	30	453	24	5.6	—
16	CeO_2–ZrO_2	2,2-Dimethoxypropane (DMP)	MeOH	(200 mmol)	383	140	7.2	97
17	$Bu_2Sn(OMe)_2$	4-Methyl-2,2-pentamethylene-1,3-dioxolane	1,2-PrD	15	453	12	3.4	—
18	$Ce_{0.5}Zr_{0.5}O_2$	1,1,1-Trimethoxymethane (TMM)	MeOH	12	373	34	10	—
19	ZrO_2–KCl–MgO	Butylene oxide	MeOH	5	423	8	7.2	53
20	ZrO_2–MgO	Butylene oxide	MeOH	9	423	8	6.2	53
21	CeO_2	Butylene oxide	EtOH	4.5	453	25	1.6	—
22	[Bmim][MeO]/ZrO_2–MgO	([Bmim][MeO])	MeOH	8	393	9	12.7	86
23	$H_3PW_{12}O_{40}/Ce_{0.1}Ti_{0.9}O_2$	EMImCl	MeOH	2.4	413	6	13.0	>99
24	K_2CO_3 (+Microwave irradiation)	CH_3I + [Bmim]Cl	MeOH	0.1	—	0.7	14	—

[a] — means no data. [b] The number in parenthesis is conversion of methanol. 1,2-PrD: 1,2-propanediol.

Figure 49 Non-catalytically reactive dehydration systems for organic carbonate synthesis from CO_2 and alcohol [84].

Table 4 Catalytically reactive dehydration system for organic carbonate synthesis from CO_2 and alcohol[a]

Entry	Catalyst	Dehydrating agent	Alcohol	P_{CO_2}/MPa	T/K	t/h	Yield/%	Selc./%	Ref.
1	CeO_2	Acetonitrile	MeOH	0.5	423	48	8.9	65	38*a*,*b*
2	CeO_2	Acetonitrile	EtOH	0.5	423	16	7.5	94	38*b*
3	CeO_2	Acetonitrile	1-Propanol	0.2	423	24	5.1	96	38*b*
4	$Zn(OAc)_2$	Acetonitrile	EG	10	443	12	11	58	39*a*
5	$Zn(OAc)_2$	Acetonitrile	1,2-PrD	10	443	12	24	62	39*a*
6	$Zn(OAc)_2$	Acetonitrile	1,3-PrD	10	443	12	14	61	39*a*
7	$Zn(OAc)_2$	Acetonitrile	1,2-BuD	10	443	12	17	61	39*a*
8	$Zn(OAc)_2$	Acetonitrile	1,3-BuD	10	443	12	12	62	39*a*
9	$Zn(OAc)_2$	Acetonitrile	1,2-PrD	3	433	2	12	64	39*b*
10	TBD + $(NH_4)_2CO_3$	Acetonitrile	1,2-PrD	10	448	15	22	60	39*c*
11	Cs_2CO_3 + $(NH_4)_2CO_3$	Acetonitrile	1,2-PrD	10	448	15	11	>99	39*d*
12	K_2CO_3	Acetonitrile	1,2-PrD	2	423	12	13	53	39*e*
13	KI/ZnO	Acetonitrile	1,2-PrD	10	433	15	26	61	39*f*
14	$La_2O_3CO_3$–ZnO	Acetonitrile	Glycerol	4	443	12	7	47	39*g*
15	CeO_2	Benzonitrile	MeOH	1	423	86	47	78	38*c*
16	CeO_2	Benzonitrile	EtOH	1	423	24	21	—	38*c*
17	CeO_2	Benzonitrile	1-Propanol	1	423	24	17	—	38*c*
18	CeO_2	Benzonitrile	2-Propanol	1	423	24	13	—	38*c*
19	CeO_2	Benzonitrile	Benzyl alcohol	1	423	24	5	—	38*c*
20	K_2CO_3	Benzonitrile	1,2-PrD	10	448	18	20	45	40
21	K_2CO_3	Benzonitrile	Octane-1,2-diol	10	448	18	10	—	40
22	CeO_2	2-Cyanopyridine	MeOH	5	393	12	94	96	38*d*

[a] — means no data. EG: ethylene glycol, 1,2-PrD: 1,2-propanediol, 1,3-PrD: 1,3-propanediol, 1,2-BuD: 1,2-butanediol, 1,3-BuD: 1,3-butanediol.

Figure 50 Catalytically reactive dehydration systems for organic carbonate synthesis from CO2 and alcohol [84].

2.1.4. Possible mechanisms for DMC and DEC synthesis

Bian *et al.* [86] proposed a possible mechanism for DMC catalytic cycle of three steps from methanol and carbon dioxide (Figure 51). (i) Activation of CH_3OH on M surface to form CH_3O- species; (ii) activation of CO_2 on M surface to form –C=O species, and (iii) reactions between the resulting CH_3O- species and –C=O species leading to DMC and regeneration of M.

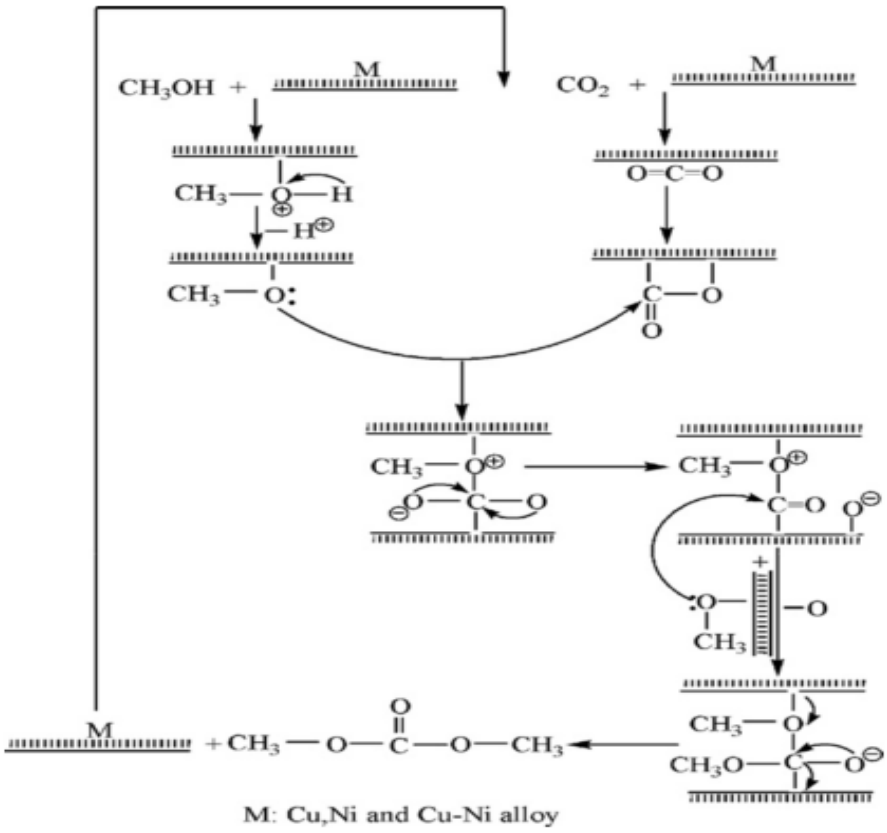

Figure 51 Catalytic mechanism for direct synthesis DMC from CH_3OH and CO_2 over Cu–Ni/graphite nanocomposite catalyst (M: Cu, Ni or Cu–Ni alloy) [86]

A modified mechanism was proposed by Arbeláez *et al.* [12]; the formation of DEC from ethanol and CO_2 using Cu-Ni/AC catalyst (Figure 52) According to this mechanism, ethanol inserts into the catalyst to give CH_3CH_2O groups in two steps: first, activation of CO_2 on M surfaces and second the formation CO_2-M species. The reaction of CH_3CH_2O-M groups and CO_2-M species results in the formation of DMC and regeneration of M sites (Cu, Ni or Cu–Ni alloy). Presumably, CO could be formed in this reaction as a result from the cleavage of C–O bond of the CO_2 species and diethyl ether (side product of this reaction) would come from the activation of species of CH_3CH_2OH [12].

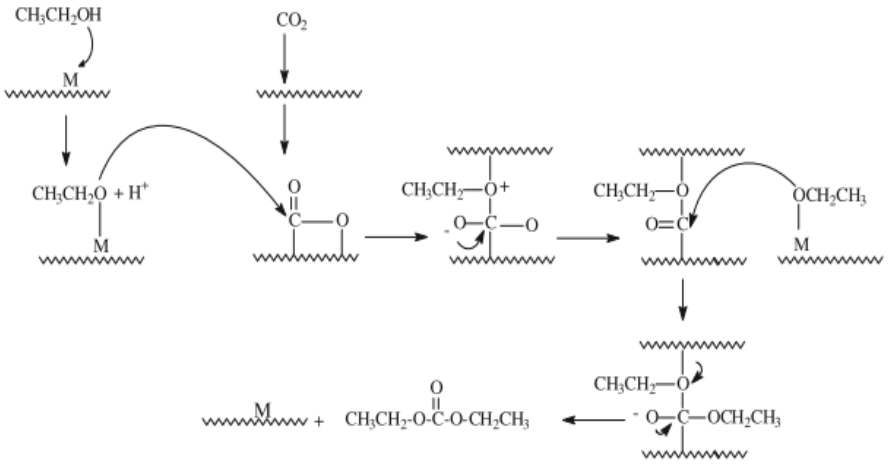

Figure 52 Possible mechanism for direct synthesis of DEC from ethanol and CO_2 ove r Cu–Ni/AC (M: Cu, Ni or Cu–Ni alloy) [12]

2.1.5. Use of CO_2 as raw material

The potential of carbon dioxide (CO_2) as a raw material in the synthesis of chemicals such as carboxylates, carbonates, carbamates has been discussed in order to develop new technologies able to reduce the CO_2 emission and accumulation of CO_2 into the atmosphere [87]. The concentration of CO_2 in the atmosphere has kept steadily increasing in the last 200 years, rising to 380 ppm from ca. 270 ppm in the pre-industrial era. CO_2 is so thermodynamically and kinetically stable that it is sometimes considered as inert. It is cheap and abundant feedstock. However, the central carbon is electrophilic and can be easily attacked by nucleophiles [10].

Currently, 110 Mt CO_2 per year are either converted into chemicals such as urea (70 Mt CO_2 per year), inorganic carbonates and pigments (ca. 30 Mt CO_2 per year) or used as an additive to CO in the synthesis of methanol (6 Mt CO_2 per year). Other chemicals, such as salicylic acid (20 kt CO_2 per year) and propylene carbonate (a few kt per year), have a minor share of the market. In addition, 18 Mt of CO_2 per year are used as a technological fluid [87] four major processes are the synthesis of urea, methanol, cyclic carbonates and salicylic acid [81]. However, only a small amount of CO_2 can be stored or fixed in such method compared to the order of magnitude of carbon emissions. Reorganization of the present infrastructure of chemicals and fundamental research on new CO_2 reactions to synthesize value-added chemicals are needed. In order to achieve zero or negative net carbon emissions, process with efficient catalysts or moderate reaction conditions should be developed [10].

Direct synthesis of DMC and DEC from CO_2 and methanol was favorable not only for reduction of greenhouse gas emissions but also for development of new carbon resource he organometallic compounds as $Bu_2Sn(OMe)$, metal (IV) tetra-alkoxide, magnesium dialkoxide, K_2CO_3, and CH_3I have been employed as catalysts for this one-step process. However, the

activity was low even in the presence of dehydrates and additives due to the limit of reaction itself. Furthermore, the organometals were easily decomposed by water and considered to take place reaction in stoichiometric ratio.

The design of new catalysts and/or the use of efficient dehydrating agent are the key to achieve high yield and selectivity in this reaction. The direct synthesis route could be the most economic process for CO_2 utilization if the handling at the laboratory scale and further at the industrial were achieved.

2.1.6. Alternatives to shift the equilibrium conversion

Figure 53 shows different alternatives to increase the yield by shifting equilibrium applying the Le Chatelier's principle. Where a system at equilibrium is stressed, the reaction will shift to relieve that stress. Chemical reactions can be exposed to stresses for changes in temperature, pressure, the concentration of one or more of the compounds (reactants or products), as well as the presence of a catalyst. Changes in the concentration could be done by elimination of the one of the products, in the case of DMC and DEC synthesis the water removal by a dehydrating agent during the reaction [88].

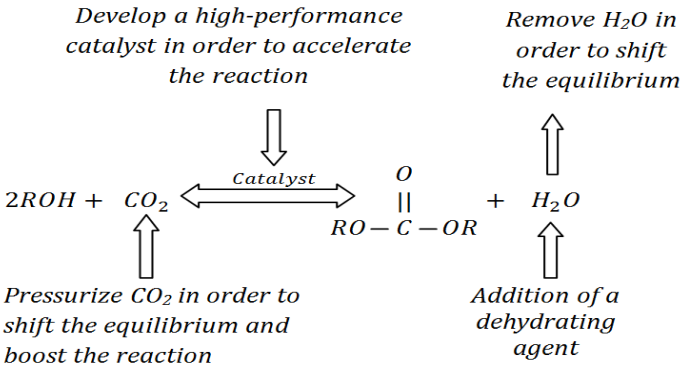

Figure 53 Alternatives to increase equilibrium conversion in direct synthesis linear carbonates from alcohols and CO_2 [8].

Integrating the use of a catalyst with an adsorbent seems to be a viable alternative it takes strength to direct synthesis. In this regard, it has been reported the use of 3A zeolite as adsorbent together the catalyst zirconium oxide (ZrO_2) (248 K, 42 Bar) getting yields close to 17 % by DMC [2]. Choi et. Al. reported yields close to 30% using dibutyltin methoxide as catalyst (453 K, 304 Bar) and an external unit with zeolite 3A at standard conditions [83]. Both strategies require the use of high pressures making them unattractive at industrial level.

From this point of view, both acid and base functions are necessary for linear carbonate synthesis (Reaction 1 and 2) from only methanol and CO_2 [89]. According to authors, the

ZrO_2 catalyst has been reported to have both acidic and basic properties. The basic sites activate CO_2, while acidic sites supply methyl groups from methanol [14],[89].

2.1.7. Copper – nickel catalyst support on activated carbon

The copper nickel catalyst supported in activated carbon (Cu-Ni/AC) is defined as a bimetallic catalyst that it is not present any interaction between the metal and the support phase and present a very good alloying between copper and nickel with better features than monometallic options (Cu/AC and Ni/AC), [12], [90]. The use of Cu-Ni/AC was report for the direct synthesis of DMC (363 K, 10 bar) with yields close to 6% and selectivities around 90% [81]. The implementation of this system is more attractive than other reported systems, by the use of low pressure, inexpensive raw material and regeneration of dehydrated agents and catalyst. Previous work showed that catalytic activity for bimetallic catalyst is better that monometallic since a synergistic effect between copper and nickel producing the formation of Cu-Ni alloy that increase the activity selectivity and stability of the catalyst, and, it has a superior structural, mechanical, chemical, thermal properties [91].

Other important advantage of Cu-Ni/AC catalyst is the no apparent deactivation by the water [90],[92]. Specifically, the DMC values of selectivity were higher than 90% and yield close to 9 % at 100 °C 1.2 MPa and, for the case of DEC, the selectivity was near to 70 % with a yield of 1.54 % under mild temperature and pressure (T<150°C and P<1MPa). Previous work reported that the catalytic activity is proportional to molar ratio Cu:Ni (TOF Cu:Ni-3:1 in 80 times higher than Ni monometallic and 25 times higher than Cu monometallic). The Ni content favors the selectivity while Cu content reduces it.

Table 21 presents the results obtained with the use of this catalyst in gas phase over different conditions en use of different catalyst. It does not have yet results in liquid phase.

Table 21 Direct synthesis of linear carbonates (previous work)

Pressure	Catalyst	Dehydrative agent	Yield and selectivities (%)	Ref.
30 MPa	$TiO(Me)_4$ + polyether	acetal	Until 55 DMC	[13]
30 MPa 180 °C	dibutyltin dimethoxide	Zeolite 3A	Around 46 DMC	[13]
180 °C and 9 MPa	CeO2	butylene oxide	9-fold to DEC (from 0.28 to 2.5 mmol to DEC)	[93]
Autoclave reactor at 248 K and 4.2 MPa	ZrO_2	zeolite 3A	17 DEC	[14]

92 ° C, P <13 bar	Cu-Ni/AC	__	DEC selectivities are obtained above 90% yield to DMC close to 9 %	[12]
30 MPa and 453 K in batch reactor	ZrO_2	zeolite 3A	The process reached a DMC yield of 28%, completely selective to DMC	[14]
300 atm External loop with a fixed bed column (at room temperature)	Dibutyltin dimethoxide	zeolite 3A	The process reached a DMC yield of 33%, completely selective to DMC	[83]

Many of these works were done into gas phase since the easy process control, the easy catalyst recovery and the reduction of capital costs. However the disadvantage was the lower yield compared with the homogeneous reaction. Since catalysts with higher content of Cu, Cu-Ni (3: 1)/AC and Cu-Ni (2:1)/AC and presence of the solid solution showed the highest TOF formation DEC the catalytic activity seems to be directly related with that solid solution. In other side, the difference in the catalytic activity of bimetallic systems can be related to the electronic properties of these materials, specifically the electron density at Fermi level Cu (band d fully) and Ni (band d, partially fully) allows the interaction of Ni and Cu and a variation of their electronic structure in order to improve the catalyst activity. Indeed, substitution by Ni Cu atoms result in filling of the area, affecting catalytic activity by modifying the electronic structure of the catalyst surface [86].

2.1.8. Importance of the catalyst preparation

The catalyst preparation influences the chemical composition, surface area, thermal stability, resistance to poisoning and mechanical properties such as hardness and wear in the catalyst. This means that must be very controled and exactly the techniques used in order to affect the quality and reproducibility of the catalyst. The impregnation step is the most complex process where many factors influencing the distribution of the active phase, among these: nature of the solvent, interaction between precursor and support, time and volume of the impregnation, pH and viscosity of the solution [94].

The preparation of supported catalysts is an extremely laborious process that comprising multiple steps. drying and final heat treatment steps are particularly delicate because they can lead to agglomeration or sintering into the active phase producing low dispersion and loss of catalytic yield [95]. Usually, the incorporation of the active phase on the support is carried out impregnation [96] but this process is not standard. Some authors establish the standard impregnation process in porous solids in order to obtain the desire concentration profiles [97]. However, they are many variations and other changes (vacuum pressure, temperature, and vacuum and impregnation time) that could change the impregnation process. Wet

impregnation preparation allows the pore saturation of the support with solvent and subsequently transferring the solute into the pores by diffusion [98]. There are several variables in order to manage the wet impregnation process: pH (strong or weak interaction), impregnation time (metal distribution) and solution volume (metal charge on the support). The contact time could not be affect the metal distribution if the solute concentration is low and its volume is not enough in excess respect the support pore volume.

The catalyst preparation by wet impregnation allows the saturation of the pore volume in the support with solvent and the subsequently solute transfer into the pores by diffusion. It should identify which is the appropriate solution volume for the preparation of the catalyst because it is possible to generate a volume ratio per gram of support that it is suitable for wet properly all the active carbon.

Bimetallic catalyst copper-nickel (Cu-Ni) supported in active carbon (AC) has been made by incipient wetness impregnation method. They are three main steps in this process: impregnation, drying and activation. Each one steps is decisive in different characteristics of catalyst, but, the impregnation is the most decisive step in active phase distribution since it allows the contact between the support and promoters (dissolved in impregnation solution).

The impregnation conditions, such as pH, time, viscosity and volume of impregnation solution are able to influence the surface of the support. However, the theoretical information available to define the ideal volume of solution impregnation is too narrow, and to know this value is very important because this choose affects the metal charge in the support and the subsequent reproducibly of method. It is known the quantity of impregnation solution is equal to the pore volume of the support, but, in some cases this volume should be enough to wet the support completely. For example, active carbon is highly porous and the volume of impregnation solution may be insufficient to wet all support generating undesirable heterogeneous distribution of the precursor.

For those reasons, it is very important to define a clear methodology to calculate the ideal volume of impregnation solution for preparation method of cupper-nickel catalyst support in active carbon able to wet all mixture. A simple methodology propose to calculate the volume of impregnation solution required for add to specific mass support [94]. The steps are these:

- ✓ Weigh a define quantity of support mass, $W_0\ (g)$
- ✓ Add dropwise solvent (solution impregnation) on the support with stirring. When the pores of the support have been empty with the solvent you see a pulp consistency for the solid. This volume is defined as solution volume $V_0\ (ml)$.
- ✓ Calculate the wetting volume of support, $V_w\ \left(\frac{ml}{g}\right)$.

$$\mathbf{V_w = \frac{V_0}{W_0}} \qquad \textbf{Equation 18}$$

- ✓ Weigh the support mass that wants to impregnate, $W\,(g)$ and determining the volume of impregnating solution need to be used $V\,(ml)$ by the following equation:

$$\mathbf{\frac{V}{W} = \frac{V_0}{W_0} = V_w} \qquad \rightarrow \qquad \mathbf{V = W \times V_w} \qquad \textbf{Equation 19}$$

- ✓ Determining the precursor mass $W_p\,(g)$,

$$\mathbf{W_p = \frac{W \times C_p}{100}} \quad \textbf{Equation 20}$$

Where (Cp) is define as precursor charged $[g\ precursor/100\ g\ support]$

- ✓ Prepare the precursor concentration solution $C\ (\frac{g}{ml})$

$$\mathbf{C = \frac{W_p}{V}} \qquad \textbf{Equation 21}$$

The combination between the wet and incipient wet impregnation methodology is an excellent option to obtain a better procedure in order to prepare the catalyst, more appropriate, more detailed and more reproducibly.

2.2. EXPERIMENTAL PROCEDURE

2.2.1. Materials

2.2.1.1. Catalyst preparation

- ✓ $Cu(NO_3)_2.3H_2O$ (Carlo Erba, USA, 99.5%)
- ✓ $Ni(NO_3)_2.6H_2O$ (Carlo Erba, USA, 99.5%).
- ✓ Activated Carbon Merck, United State (90% particle size < 100 μm)
- ✓ HCl, solution
- ✓ H_2SO_4, Sigma Aldrich, USA
- ✓ Commercial ammonia solution (25%), Merck, USA.
- ✓ Carboxymethylcellulose CMC, Colombia
- ✓ Ethanol, Sigma Aldrich, USA

2.2.1.2. Adsorbents

- ✓ Zeolite 4A, Sigma Aldrich, USA.

- ✓ Butylene oxide (Organic dehydrating), JT Baker, USA.

2.2.1.3. Reaction

- ✓ Anhydrous methanol (99.5 %) JT Baker, USA.
- ✓ Anhydrous ethanol (99.5 %) JT Baker, USA.
- ✓ CO_2 2.8 grade Praxair, Colombia.
- ✓ Diethyl carbonate anhydrous (≥ 99 %) de Sigma-Aldrich, USA.
- ✓ Water Millipore type II, Colombia.

2.2.2. Catalyst preparation

It is going to describe the preparation of bimetallic Cu-Ni catalyst support in activated carbon. There are two catalyst preparations: Cu-Ni/AC (2:1 and 3:1 molar ratio keeping nominal metal oxide loadings), CuO + NiO, at 10 wt. %. The procedure for the different loads was described in the Appendix 13 Description catalyst preparation of Cu-Ni/AC (3:1) catalyst (20% total load). The catalyst preparation includes three important parts: pretreatment, increase of the particle size and impregnation.

2.2.2.1. Pretreatment of activated carbon

The use of activated carbon (AC) as support is able to increase the superficial area. It was necessary to clean the activated carbon of some impurities. The assembly consists of a 2 L volumetric flask, reflux, nest round heating and magnetic stirrer. There was added AC and 2 M HCl solution at the flask (the amount of solution should be enough to covers all activated carbon) Appendix 14 Solutions preparations. The heating mantle temperature was 98 ° C, enough to generate constant bubbling of the mixture. The system was allowed to reflux for 12 hours. The next step consisted in the filtered and washing with deionized water (Millipore type II). The washing starts at acidic pH (around 2 and 3) and it should be at neutral pH (approximately 5.5 to 6 for this kind of water). For drying was used a conventional oven at 110°C for 12 hours. Pass this time the AC was oxidized using 4M H_2SO_4 solution (without excess). The AC was added at 4M H_2SO_4 solution in 1L beaker and stirring for 4 hours. Finally, pretreated AC is filtered, washing and drying again at 110 ° C for 12 hours. Pretreated AC samples were stored in a desiccator before using them as catalyst supports.

2.2.2.2. Increase of the particle size by pelletizing

Cu-Ni bimetallic catalysts supported on activated carbon are active material for obtaining DMC (2:1 ratio) and DEC (3:1 ratio) at gas phase conditions. In order to reduce the drop pressure and use the same particle size, the catalyst will be pelletized to a particle size about 512 μm. It would reduce the total catalyst amount required for packing the same reactor volume, and the formation of hotspots; furthermore, the handling would be easier and adhesion of the fine powders to the inner surface of the reactor walls would be avoided.

For this process, the first step was the calculation of the AC to pelletizing. If you want prepare 50 ml of carboxy methyl cellulose solution (CMC) in ethanol 10 wt. %, the active carbon needed was calculated using the ratio:

$$\frac{\textbf{25 g of AC}}{\textbf{200 mL of the CMC solution 10 wt \% in ethanol}} \quad \textbf{Equation 22}$$

The CMC grams used to prepare the solution depends of the amount of solution to be prepared, according to Equation 22:

$$\textbf{wt.}\,\% = \frac{\textbf{Solute mass}}{\textbf{Solution mass}} * \textbf{100}\% \quad \textbf{Equation 23}$$

The solute mass was calculated with Equation 23

Assuming the density of the solution will not change significantly with the solute, it can be said that the density of the solution is the density of ethanol: $\rho_{etanol} = 0.790\ g/cm^3$.

$$\boldsymbol{\rho_{sln} = \rho_{ethanol} = \frac{\text{Solution mass}}{\text{Solution Volume}}} \quad \textbf{Equation 24}$$

CMC was added at ethanol. This solution remained under soft stirring for 10 minutes to ensure its homogenization. Next, the AC grams were added to the solution and this mixture was left under soft stirring for 24 hours. Passed this time the ethanol had to be removed fully. The mixture was heated to evaporate all ethanol to leave with only the solid compounds. The intention is to form a paste, for this, a minimum amount of distilled water is added to solid (CMC and AC) to form a paste which can be molded.

The paste was pressed (pressure between 1000 - 2000 psi). The goal was to make an extrusion allows obtain AC pellets with uniform size, next by screening and maceration the particle size was 512 μm. The pellets were dry in an oven at 100 °C for 24 hours and calcined in a nitrogen stream flow rate 25 mL/min at 600 °C (0.5 °C/min.) during 3 hours. Finally, for the activation, the pellets pass through 5% H_2/Ar stream at 600°C (0.5ºC/min.) during 2 hours.

2.2.2.3. Impregnation of Ni and Cu

In a volumetric flask, Cu $(NO_3)_2.3\ H_2O$ and Ni $(NO_3)_2.6\ H_2O$ salts were dissolved in 25 wt % commercial ammonia solution. Stirred for approximately 15 minutes, sufficient time to ensure dissolution of crystals. After, pretreated AC is added to mixture of ammonia solution and metals. Stirred vigorously for 2 hours. The mixture was aged for 12 hours to ensure the homogeneous attachment of metals in the AC. Passed this time, the flask containing the mixture of activated carbon and Cu and Ni system was rotaevapored at 350 mmHg. The bath temperature was 90 ° C and rotation speed of 35 rpm. When the catalyst was dry, the material was placed in an oven at 90 ° C. After the drying, the solid was pyrolized at 0.5 ºC /min to 500

° C for 2 h in a flow of N_2 (25 ml/min) and later it is reduced to activate the catalyst at 0.5 ºC /min to 600 ° C for 3 h in a flow of 5% H_2/Ar. The description of this method is present in Appendix 15 Preparation by incipient wet impregnation method for Cu-Ni catalyst support on active carbon..

2.2.2.4. Catalytic test in gas phase

Catalytic tests (see Figure 54) were performed in a continuous stainless steel (SS) tubular fixed-bed reactor (ID 7 mm) packed with 0.5 g of catalyst sample (512 μm). The Cu-Ni/AC catalyst was previously purged with argon during 12 hours. The alcohol vapor was introduced into the reactor by a stream of CO_2/ flowing through a SS bubbler (temperature for ethanol was always 70°C and methanol was 40°C) containing the liquid alcohol. All reactions were carried out for 3 h at 6-14 bar, 92-150°C and total gas flow was about 50 mL/min. The molar ratio alcohol: CO_2 was 1:2 (excess of CO_2) consider the suggestion that excess favor the reaction [99]. The reactor system was installed inside an oven that allowed keep the products at the reactor temperature preventing possible condensation. Input stream (bypass) and products were monitored online by a mass spectrometer QMS Thermostar 200 (Pfeiffer) with a resolution of 0.01 ppm. Catalytic activity was indicated by the methanol and ethanol conversion, DMC and DEC yield and DMC and DEC selectivity. These parameters are calculated according to the following equations:

$$\textbf{Yield}\ (\%) = \textbf{Selectivity} \times \textbf{Conversion} \qquad \textbf{Equation 25}$$

$$\textbf{Conversion OH}\ (\%) = \frac{[\mathbf{OH}]_{\mathbf{in}} - [\mathbf{OH}]_{\mathbf{out}}}{[\mathbf{OH}]_{\mathbf{in}}} \times \mathbf{100} \qquad \textbf{Equation 26}$$

$$\textbf{Selectivity}\ (\%) = \frac{[\mathbf{DMC}]}{[\mathbf{DMC}] + [\mathbf{by-products}]} \times \mathbf{100} \qquad \textbf{Equation 27}$$

The yield was calculated with equation 25, based on equations 26 and 27.

Previous study showed that there is not formation of diethyl ether by decomposition of ethanol at 13 bar and 110°C but diethyl carbonate or dehydration. The formation of diethyl ether could be occurred by dehydration of ethanol at temperature more than 150°C [12] and DEC decomposition when it passed through Cu-Ni/AC catalyst reduce the selectivity [100].

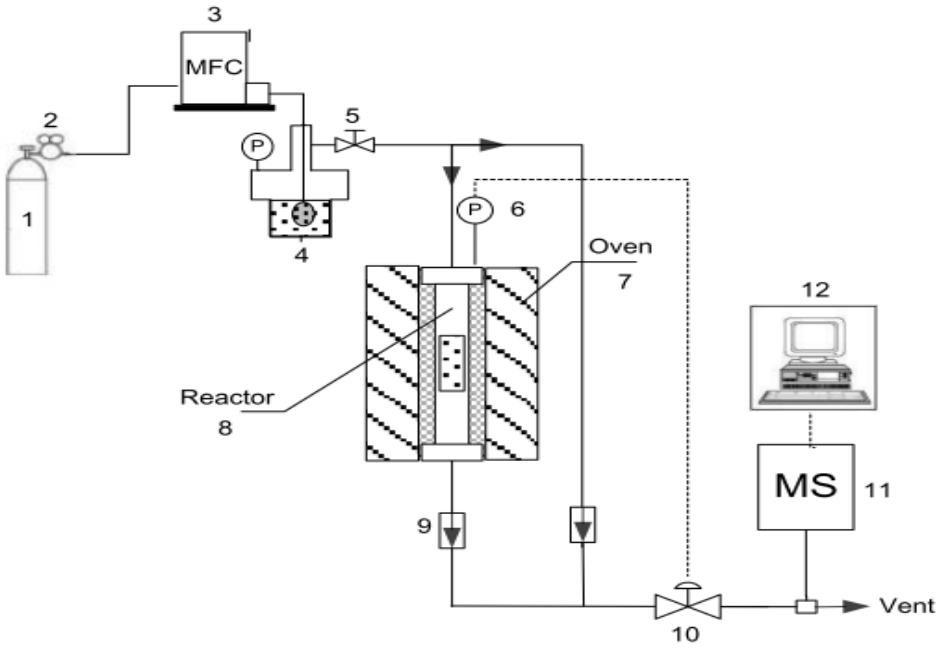

Figure 54 Reaction system setup for gas phase synthesis of DMC from methanol and CO_2. (1) CO_2/He gas mixture, (2) pressure reducer, (3) mass flow control (MFC), (4) bubbler containing methanol, (5) valve, (6) pressure gauge, (7) Oven (Temperature Control), (8) tubular fixed-bed reactor (7 mm I.D), (9) check valve, (10) Control Valve, (11) MS Spectrometer (ThermoStar QMS 200, Pfeiffer), (12) Data Processor [81].

For the case of the direct synthesis of linear carbonates in gas phase with simultaneous water removal (assembly catalyst – adsorbent), the conditions were quite similar to catalyst test. The catalyst and the zeolite 4 A, were placed in four different configurations as is shown in Figure 55. In order to guarantee the reproducibility of these tests, each test was repeated 3 times.

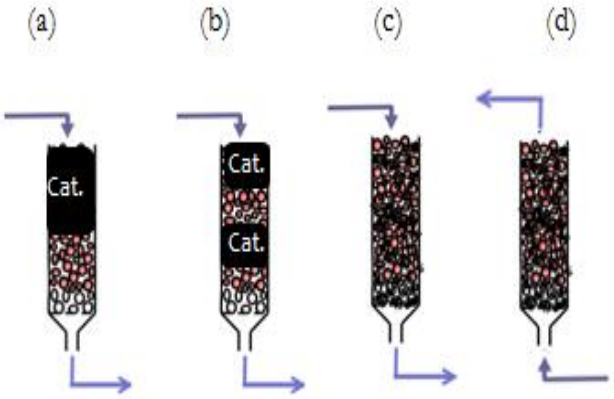

Figure 55 Catalyst – zeolite 4A assemblies evaluated (a) fixed bed: catalyst/adsorbent; (b) fixed bed: catalyst/adsorbent/catalyst/adsorbent; (c) Single bed; (d) Fluidized bed.

2.2.3. Catalytic test in liquid phase

There are not resulst reported about the use of Cu-Ni/AC catalyst in liquid phase reaction until the moment. The liquid phase reaction were carried out in a stainless steel autoclave (Parr reactor, 100 mL capacity) equipped with a stirrer and electric heating mantle Standard procedure was to add 100 or 200 mg of Cu-Ni/AC, 55 mL of ethanol and methanol with CO_2 pressurized to 60 psi in order to obtain DEC and DMC respectively. Within the reactor they were deposited 100 or 200 mg of Cu- Ni/AC and it was pressurized to 60 psi CO_2 (4 bar) at 90 ° C for 24 hours with at constant stirring (See Figure 56)

In order to prove the behavior in presence of organic dehydrating, the test was made with 100 and 200 mg of Cu-Ni/AC, 55 mL of ethanol with CO_2 pressurized to 60 psi and, the organic dehydrating agent: butylene oxide 0.13 mL and 0.26 mL as suggest Ewelina et. al. [9] at 90 ° C for 24 hours with at constant stirring.

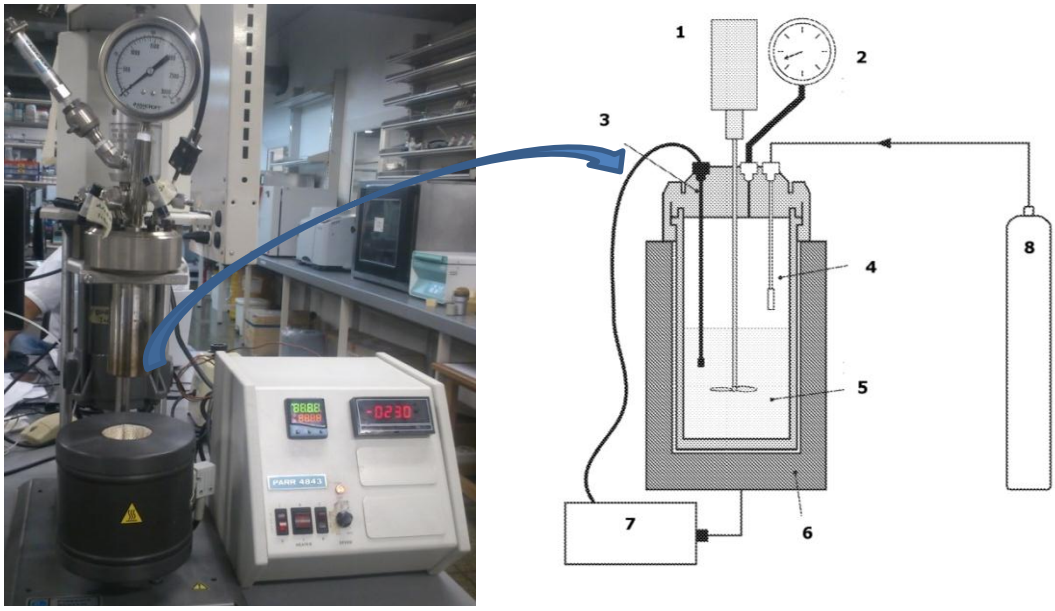

Figure 56 Parr reactor (1) Stirring system, (2) Pressure Gauge, (3) Temperature Gauge, (4) gas inlet, (5) reactor, (6) jacket heating, (7) Temperature controller, and (8) CO_2 Cylinder

After reaction time, Parr reactor was cooled and subsequently depressurized to atmospheric pressure. Liquid samples were stored and subsequently analyzed with gas chromatograph (Agilent Technologies 7890A) using capillary columns DB-1 equipped with detectors FID and TCD. Each compound was identified as an area under the curve at a specific time and detection different for each compound. The

Appendix 16. Calibration curves liquid phase (concentration vs. area under the curve) and Appendix 17 Chromatograph injection method show more information about the calibration curves used in liquid phase system and the chromatograph injection method respectively.

2.2.4. Catalyst characterization

The catalysts were characterized by:

- **ASS**

Chemical composition copper and nickel loadings were determined by atomic absorption spectroscopy (AAS) on a Philips PU9200. This technique analyze energy absorption in the transition from an atom from its ground state to an excited state, within a wavelength characteristic for each element [90], ASS allows to know the metal loading in the catalyst.

- **BET**

BET (Brunauer, Emmet y Teller) method determines the superficial area (m^2/g). It is based on the nitrogen adsorption/desorption isotherms (monolayer adsorption). The type of isotherm obtained depends of the solid porosity and the adsorption and liquefaction heat [101]. In this work the isotherm of the catalysts was determined by N_2 physisorption of liquid nitrogen at 77 K using a Micromeritics 2375 BET instrument. Prior to the experiments, samples were degassed for 2 h at 250 °C and 0.15 mbar to ensure a clean and dry surface.

- **SEM**

The morphology was determined by a Scanning Electron Microscope (SEM) with a JEOL JSM-6490 microscope using an accelerating voltage of 20kV. The samples were covered by a thin layer of Au (i.e., 15 to 20 nm) by metal sputtering, providing electrical and thermal conductivity to the otherwise nonconductive samples. The SEM images allow knowing the size, shape and other characteristics of particle aggregates.

- **EDS**

Elemental analysis was performed by Energy Dispersive X-ray Spectroscopy (EDS) instrument coupled to the SEM equipment. This technique allows collect the X -rays information and perform various analyzes and images of distribution of elements over the surface. In this work the EDS results were useful in order to identify the alloy in the catalyst.

- **TEM**

Transmission Electron Microscopy (TEM) allows to know the particle morphology, size and size distribution of metal particles dispersed on the activated carbon support The system was operated with an accelerating voltage of 200 kV and emission current of 124 μA in a FEI Tecnai G2-F20 unit with an accelerating voltage of 400 kV. Using ethanol as dispersing agent and Au grid. Several TEM micrographs were recorded and analyzed for particle size distribution before and after reaction.

- **TPR**

Temperature Programmed Reduction (TPR) was performed in a Micromeritics Autochem II 2920 apparatus. Samples (50 mg) were pretreated at 5°C /min to 250 °C for 1 h in flowing helium (70 mL/min), and then cooled to 40 °C. Thereafter, the samples were heated to 800 °C using 5% H_2/Ar (70 mL/min) at 8 °C /min. The signals of H_2 consumption were continuously monitored by a thermal conductivity detector (TCD). TPR analyses is use to determine the catalytic species under the catalyst surface.

- **XRD**

The crystallinity was determined by X-ray diffraction (XRD) at room temperature on a Phillips PW 1740 using Ni-filtered and Cu Kα radiation. The scanning range was $5° \leq 2\theta \leq 70°$ at 2° / min. The diffractograms were compared to JCPDS (Joint Committee of Powder Diffraction Standards) data. The XRD analyses allow determining the catalytic species under the catalyst surface. When an electron beam irradiated over solid the diffraction pattern changes depends of its crystallographic planes.

- **TGA**

Thermogravimetric analyses (TGA) were performed on Q500 TGA V20.8 (TA Instruments) where the sample was heated up to 600 ºC at 10 ºC/min in flowing air (100 mL/min) It provides a qualitative and quantitative measurement of the composition and structure of the catalyst phases from weight changes.

2.3. RESULTS AND DISCUSSION

2.3.1. Catalytic activity in gas phase

2.3.1.1. Effect of the reaction temperature in the carbonates yield

Figure 57 shows the results of variation of temperature and pressure in the catalytic activity for DMC. At 150°C and 14 Bar was obtained the maximum yield using methanol/CO_2 molar ratio (1:2). In the case of DEC (Figure 58) the best yield was obtained at the same temperature and

pressure but lower than DMC yield (1.23 % and 2.26%). The data at lower pressure are not present because the yields were near zero.

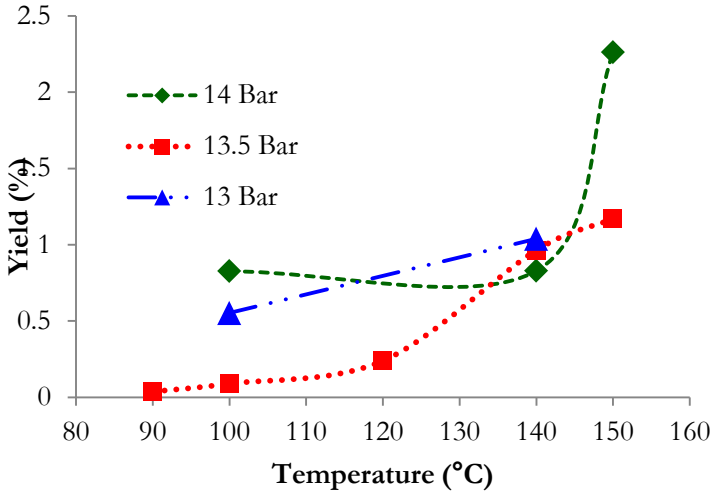

Figure 57 Effect of the temperature and pressure variation in the DMC yield using Cu-Ni/AC

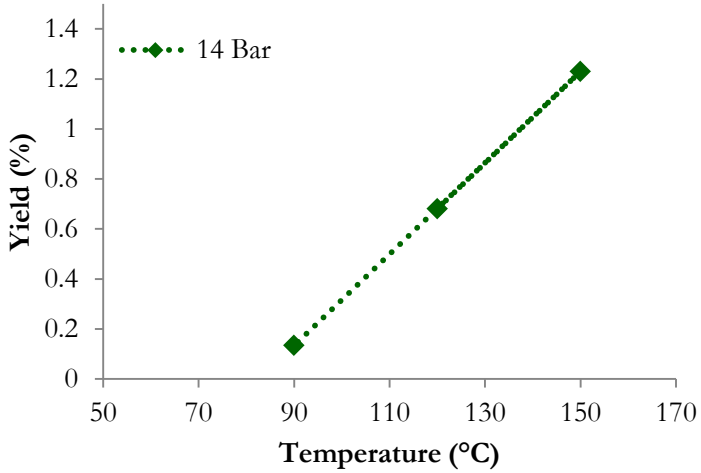

Figure 58 Effect of the temperature in the DEC yield using Cu-Ni/AC

2.3.1.2. Catalytic activity in gas phase for assembly catalyst – adsorbent

Table 22 presents the yield results for DMC for the integration catalyst –adsorbent (Cu-Ni/AC – Zeolite 4A) using the configurations presented in Figure 55.

Table 22 Yield to DMC with the assembly system catalyst – zeolite 4A

System	Cu-Ni/CA (g)	Zeolite 4A (g)	DMC (%)	DEC (%)

Only Catalyst	0.05	-	2.26	1.21
One fixed bed	0.05	0.1	2.28	1.18
Two fixed bed	0.025 per bed	0.025 per bed	2.60	-
Single bed	0.05	0.05	3.02	-
Fluidized bed	0.05	0.05	1.93	-

Reaction conditions: Temperature: 150°C; Pressure: 14 bar; 60 mL/min Time: 2 hours

These preliminary results show a slightly reduction in the yield of DMC and DEC when the system evaluated is one fixed bed. However, when it was increased the number of beds (two fixed bed) the DMC yield performance increases. In the table is possible to observe that there were not include results for DEC yield in the two fixed bed, single or fluidized bed because, the results of the tests were meaningless, and, during the experimental work, it was not possible to obtain a good data. In the case of DMC yield, the better results were obtained with two fixed bed and single bed configurations. Fluidized bed presents the worst results.

Concerning to the by-products dimethylether (DME) or diethylether (DEE), the production was always below the detection limit of the mass spectrometry. These results did not confirm any dehydration of the alcohols during the reaction. This is not surprising considering the fact that DME is only easily formed on the strong acid sites [14]. Cu-Ni catalyst support in activated carbon does not either acidic or basic Lewis sites, it is feasible to use these results as a first approximation to the analysis to Cu-Ni metallic sites [5]. Therefore, the selectivity to DMC and DEC is essentially 100%. It is important consider the short time required to achieve the equilibrium achieved at constant concentration value. The results, contradicted the traditional results: lower reaction temperatures led in order to obtained higher DMC and DEC yields at equilibrium.

2.3.2. Catalytic activity in liquid phase for DEC and DMC

2.3.2.1. Results in presence of catalyst (100 and 200 g)

Table 23 and Table 24 present the results obtained during variations with presence of catalyst for the synthesis of DEC and DMC.

Table 23 Conversion, Selectivity and yield in DEC synthesis

Reaction	**Conversion (%)**		**Selectivity (%)**	**Yield (%)**
Detector	**TCD**	**FID**	**TCD/FID**	**TCD/FID**
Cu-Ni/AC (100g)	0.7126	0.4376	0	0

Cu-Ni/AC (200g)	0	0	0	0

Reaction conditions: 90°C, 60 Psi of CO_2, 55 mL of ethanol, stirring during 24 hours.

Table 24 Conversion, Selectivity and yield in DMC synthesis

Reaction	**Conversion (%)**		**Selectivity (%)**	**Yield (%)**
Detector	**TCD**	**FID**	**TCD/FID**	**TCD/FID**
Cu-Ni/AC (100g)	1.28	1.24	0	0
Cu-Ni/AC (200g)	0	0	0	0

Reaction conditions: 90°C, 60 Psi of CO_2, 55 mL of methanol, stirring during 24 hours.

Any satisfactory result was obtained in the DEC and DMC synthesis in a liquid phase reactor. Consider the characterization of liquid used Cu-Ni/AC catalysts; it is possible to think that the catalyst suffered some deactivation or damage since the stirring and liquid used.

2.3.2.2. Catalytic activity in liquid phase for assembly catalyst – adsorbent

Table 25 and Table 26 list the conversion, selectivity and yield obtained for DMC and DEC after 24 hours at constant pressure and temperature. The only variation was the grams of catalyst and adsorbent (100 mg and 200 mg).

Table 25 Conversion, selectivity and yield results in liquid phase DMC

Reaction	**Conversion (%)**		**Selectivity (%)**	**Yield (%)**
Type detector	**TCD**	**FID**	**TCD/FID**	**TCD/FID**
Cu-Ni/AC - Zeolite 4A (100 mg)	0.3782	0.2363	0	0
Cu-Ni/AC - Zeolite 4A (200 mg)	0.8594	0.8287	0	0
Cu-Ni/AC (100 mg) - Butylene oxide (0.13 mL)	0	0	0	0
Cu-Ni/AC (200 mg) - Butylene oxide (0.13 mL)	0	0	0	0

Reaction conditions: 90°C, 60 Psi of CO_2, 55 mL of methanol, 24 hours.

Table 26 Conversion, selectivity and yield results in liquid phase DEC

Reaction	**Conversion (%)**		**Selectivity (%)**	**Yield (%)**
Type detector	**TCD**	**FID**	**TCD/FID**	**TCD/FI**

				D
Cu-Ni/AC - Zeolite 4A (100 mg)	0	0	0	0
Cu-Ni/AC - Zeolite 4A (200 mg)	0.8289	0.4998	0	0
Cu-Ni/AC (100 mg) - Butylene oxide (0.13 mL)	0	0	0	0
Cu-Ni/AC (200 mg) - Butylene oxide (0.13 mL)	0	0	0	0

Reaction conditions: 90°C, 60 psi of CO_2, 55 mL of ethanol, 24 hours.

Selectivity and yield were equal to zero since the imperceptible formation of DMC and DEC was observed (probably formation is less than the detection limit of the equipment). With zeolite 4A presence, there is an apparent conversion of 0.8594 and 0.8289 for DMC and DEC, what are not higher than the result obtained with zeolite only.

The reactions in presence of Butylene oxide presented an additional characteristic: alcohol with green color when removing the reaction after 24 hours. This means the deactivation by lost of active phase since the nickel sulfate present a green color and, copper sulfate blue color. All these results allow to conclude that the catalyst is not recommended to use in gas and liquid phase.

2.3.3. Catalyst reuse test

Figure 59 shows the reuse of Cu-Ni/AC (2:1) catalyst using during five tests in order to determine if there was a significant lost of activity before it is used in the reaction over the most extreme conditions: 150°C and 14 Bar. The results show that the catalyst can be reused without appreciable lost of their catalytic activity due to reagents (carbon dioxide and ethanol). Each test was performed during two hours.

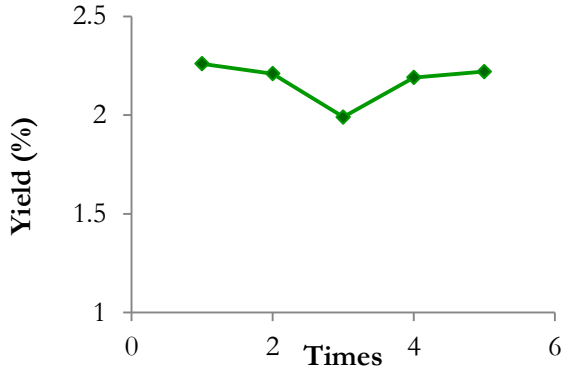

Figure 59 Reuse of Cu-Ni (2.1)/AC catalyst in DMC gas phase reaction. Conditions: 150°C, 14 Bar.

2.4. Catalyst characterization

2.4.1. Physicochemical properties of catalyst

Loading of Cu and Ni in the catalyst was determined by atomic absorption (ASS) and results are shown in Table 27

Table 27 ASS for Cu-Ni/AC catalysts

Cu and Ni loading (%)	2:1	3:1
Wt. % Cu	10.03	7.19
Wt. % Ni	4.89	2.20
Molar ratio Cu:Ni	1.89:1	3.02:1

Previous work defined that molar ratio Cu:Ni 2:1 and 3:1 are the ideal loading in order to obtain the best yields [81], [100]. This result, show that the real load is quite similar at theoretical value. However, the metal loading for Cu-Ni 2:1 is less than the nominal load (20 % w/w CuO + NiO), probably as a result of leaching losses of precursors, Cu $(NO_3)_2 \bullet 3H_2O$ and Ni $(NO_3)_2 \bullet 6H_2O$ during catalyst preparation by wet impregnation.

Table 28 BET surface area of Cu-Ni/AC catalysts before and after use

	Support	Fresh	Used	
	AC	**Cu - Ni/AC**	**Gas phase**	**Liquid phase**
Surface Area (m^2/g)	764	458	548	272
Total pore volume (m^3/g)	0.44	0.2170	0.2694	0.1289

The BET was reported in Table 28 and shows the AC pore volume was lower than fresh catalyst, and, the used catalyst present a significant different between gas and liquid phase. Liquid phase is less than gas and this means that the catalyst in the liquid phase has less catalytic activity [81]- In the other hand; the reduction of the pore volume expresses a clusters formation. Previous work also shows that an increase in the Copper content decreases the catalysts dispersion, probably by the clusters formation. Respect surface area, this reduce like consequence of metal incorporation and high calcination and reduction temperatures (600 ° C) in the catalyst preparation. It is observed that the catalyst used in liquid phase presents a significant reduction in the surface area; this suggests a possible catalytic deactivation.

2.4.1.1. XRD

Figure 60 shows diffractograms in the range 2θ = 42° - 70°, what are the most representative diffraction signals. According with the JCPDS classification, the characteristic copper signals are 2θ = 43.3° (111) and 50.4° (200) JCPDS 4-0836 with centered cubic structure on the face (FCC: face center cubic) and for nickel are 2θ = 44.5° (111), 51.8° (200) JCPDS 4-0850. It is possible to see that the bimetallic catalyst Cu-Ni/AC always has its characteristic signal slightly displaced. It suggests the formation of a solid solution in these catalysts with diffraction lines 2θ = 43,7° and 50,9°, JCPDS 07- 1406 [16]. Cu:Ni/AC (2:1) catalyst used in gas and liquid

phase present several signals among 2θ = 10° – 40°. A peak that corresponds to oxides diffraction of CuO at 2θ = 35.5° (110) JCPDS 80-1916, is observed. In the case of Cu-Ni/AC (3:1) used it is possible to see a very define pattern with high intensity. It is possible that the increase of Cu content help the incorporation of Cu into Ni structure.

Some studies show that Cu-Ni/AC (bimetallic catalyst) helps the formation of solid solution and increase the net parameter as concentration; notwithstanding, the formation of a Cu-Ni alloy in the composition range studied was not possible to confirm. Finally, these catalysts present less dispersion suggesting that the higher Cu content favors the formation of clusters, this means that they would present greater chemical stability, what is associated with the presence of metal-metal bonds in its structure.

The XRD patters show similar behaviors for gas and liquid phase used with Cu:Ni (2:1) (Figure 60 b and f), with a possible oxide presence in liquid phase. About Cu:Ni (3:1) (Figure 60 c and e) was observed an increment in the signal, that means increase of crystallinity.

The mixture catalyst/zeolite in gas phase (Figure 61, c) presents interference between the traditional signals for zeolite and signal for Cu-Ni/AC catalyst (possible contamination in the catalyst sample). About the mixture catalyst/zeolite in liquid phase (Figure 61, e) the patter has greater intensity than in the fresh sample. That can be associated with the zeolite 4A presence, what can reduce the possible catalyst deactivation by water presence; however, it was not enough in order to promote the reaction.

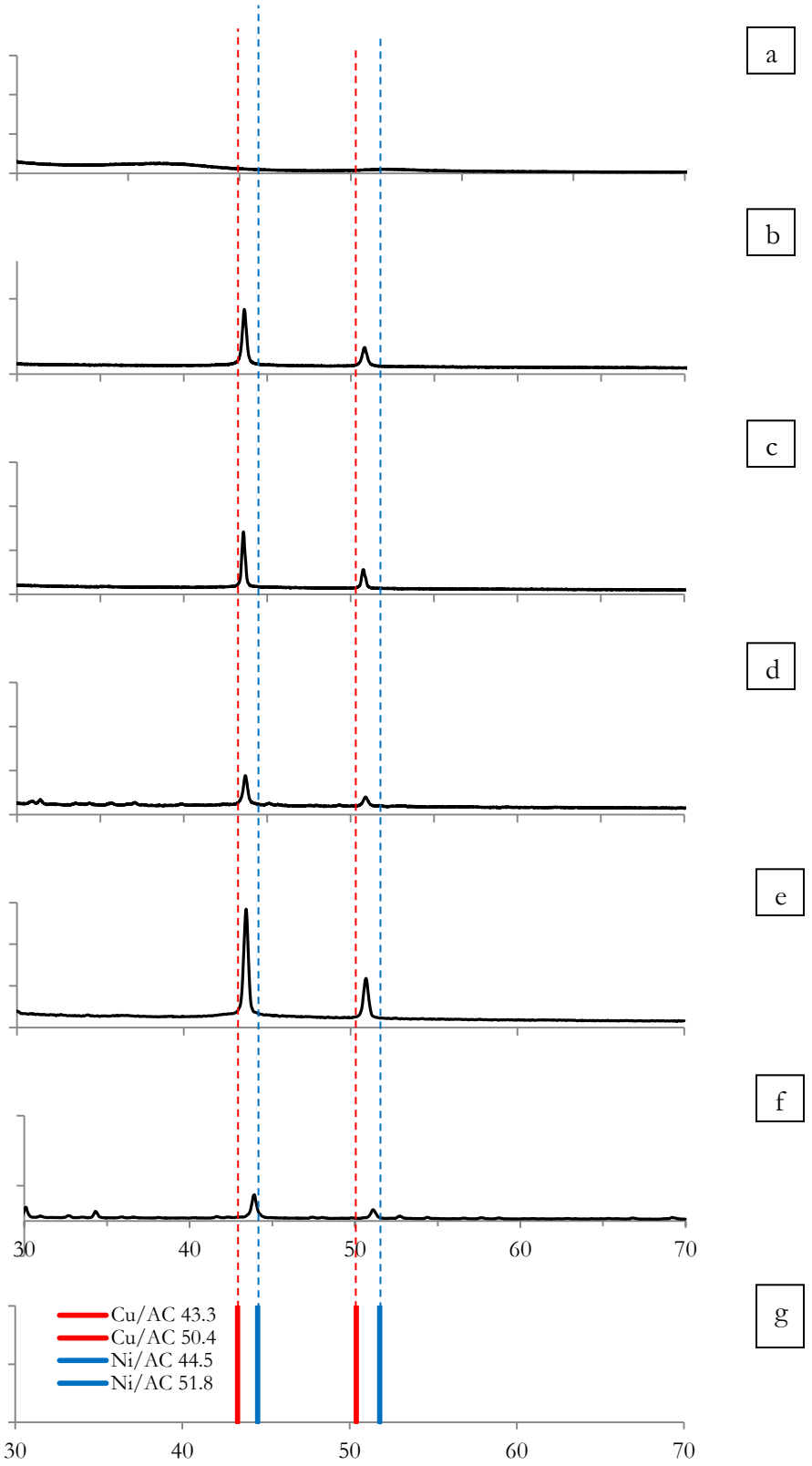

Figure 60 XRD patterns of (a) CA; (b) Cu:Ni (2:1); (c) Cu:Ni (3:1); (d) Cu:Ni (2:1) used in gas phase; (e) Cu:Ni (3:1) used in gas phase; (f) Cu:Ni (2:1) used in liquid phase; (g) Patter cu/AC Ni/AC

Figure 61 XRD patterns of (a) fresh catalyst; (b) Used gas phase; (c) Used mixture catalyst/zeolite gas phase; (d) Used liquid phase; (e) Used mixture catalyst/zeolite liquid phase; (f) Patter cu/AC Ni/AC

2.4.2. TGA

TGA profiles of Cu-Ni/AC (2:1) and (3.1) are shown in Figure 62. Both samples showed an initial weight loss around 10% between 20 ° C and 90°C what could be attributed to the removal of physically adsorbed water and this means that activated carbon can adsorb water at room temperature. For this reason, the catalyst always must be pretreated in-situ with an inert gas at temperatures up to 300 °C before running the reaction. It is interesting to observe that Cu-Ni/AC (3:1) present mayor stability from the main weight starts at 430 ° C up to 500 °C, and is associated with carbon combustion in the presence of oxygen while Cu-Ni/AC (2:1) presets the main loss until 330° C to 500 °C. This combustion informs of the stability of the support up to 500 °C in the case of pyrolysis and activation treatments. The drastic drop in weight corresponds with the incorporation of metals and it accelerates carbon combustion.

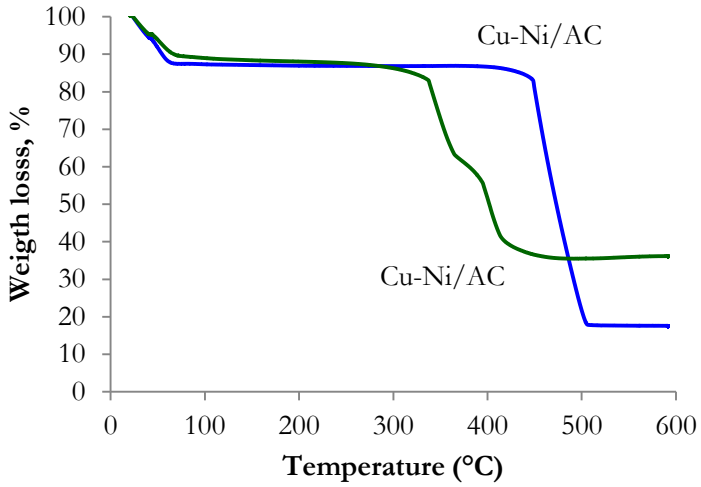

Figure 62 TGA profiles of Cu-Ni/AC catalysts

2.4.3. SEM

SEM micrographs for AC support and Cu-Ni/AC catalysts at 1000X, 5000X and 1000X are shown in Figure 63. The first images can be seen that the carbon grains are highly porous and with smooth edges and there is not definite the pattern for AC particles but some elongated and cylindrical shapes can be noted. Figure 63**¡Error! No se encuentra el origen de la eferencia.** (b) shows micrographs of both fresh Cu-Ni/AC and the active metal particles are evenly dispersed on the surface of AC and it showed a cylindrical shape. It is possible to absorb clusters of metal particles on the surface of the support and a several size (Figure 64 present the distribution of fresh Cu:Ni/AC catalyst). When the catalyst is used in gas phase (c) and liquid phase (d) and (e) change the clusters size because the used catalyst exhibited some agglomerations on the porous channels of AC support after reaction.

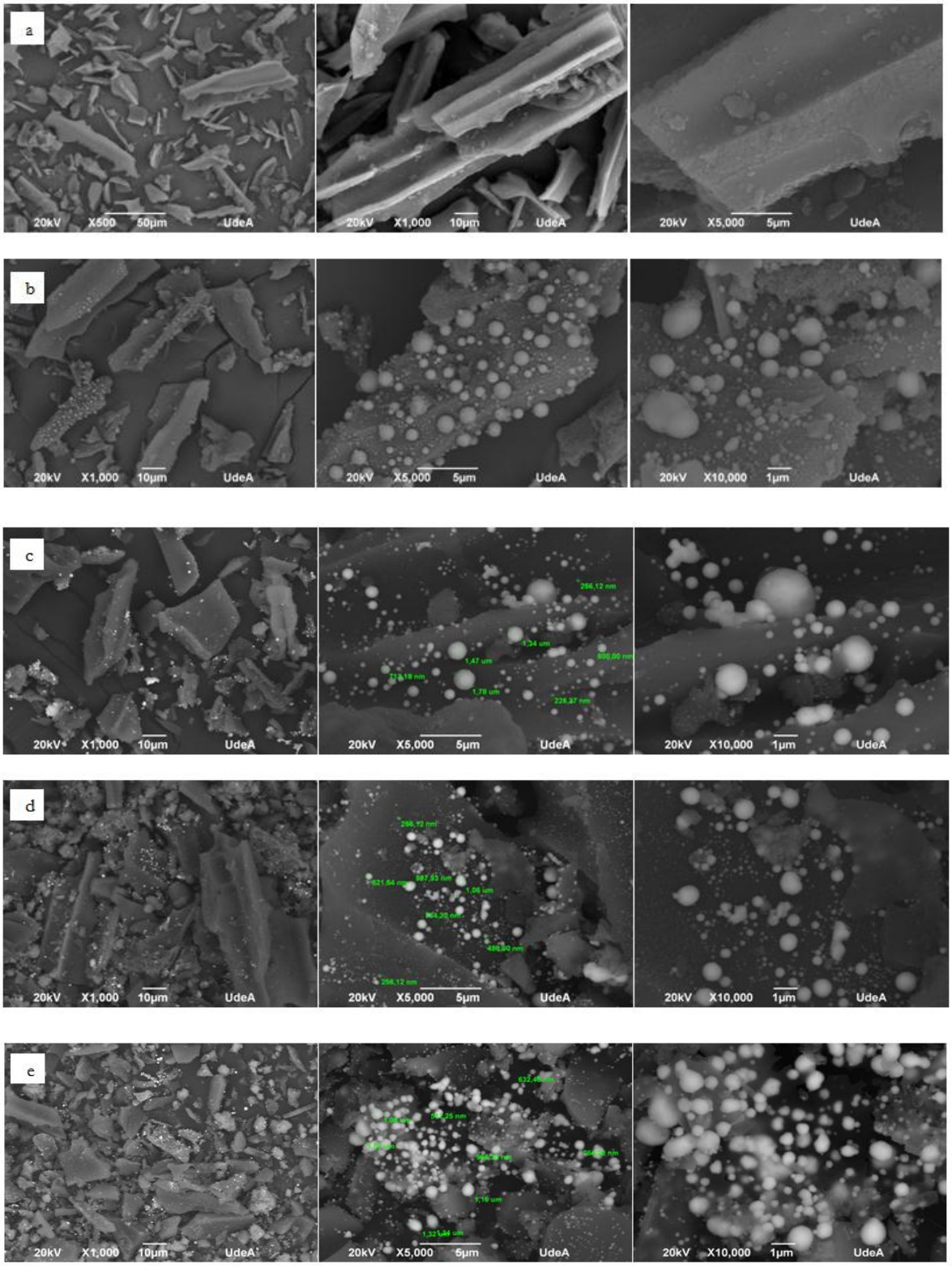

Figure 63 SEM images of (a) AC; (b) Fresh Cu-Ni/AC; (c) Used Cu-Ni/AC gas phase;(d) Cu-Ni/AC (2:1) used in liquid; (e) Cu-Ni/AC (2:1) used in liquid phase.

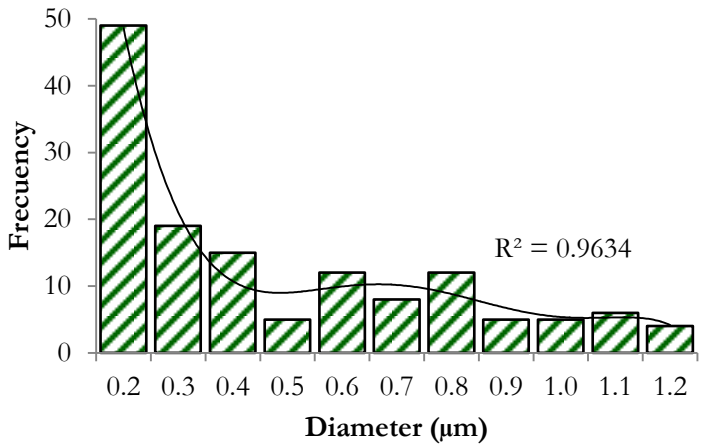

Figure 64 Particle size distribution for fresh Cu:Ni/AC catalyst

For assemblies fixed bed: Cu-Ni (2:1)/AC - zeolite 4A in gas phase for DMC formation and mixture catalyst/zeolite 4A in liquid phase for DEC and DMC reaction, there were present the SEM results (Figure 65) showed a difference in the catalyst when the catalyst was used in gas and liquid phase: the size of the metal dispersion. Figure 66 show how the particle size distribution changed in liquid phase, it means that the liquid phase reduces the size or perhaps there was a catalyst deactivation for the excess of alcohol and continues stirring.

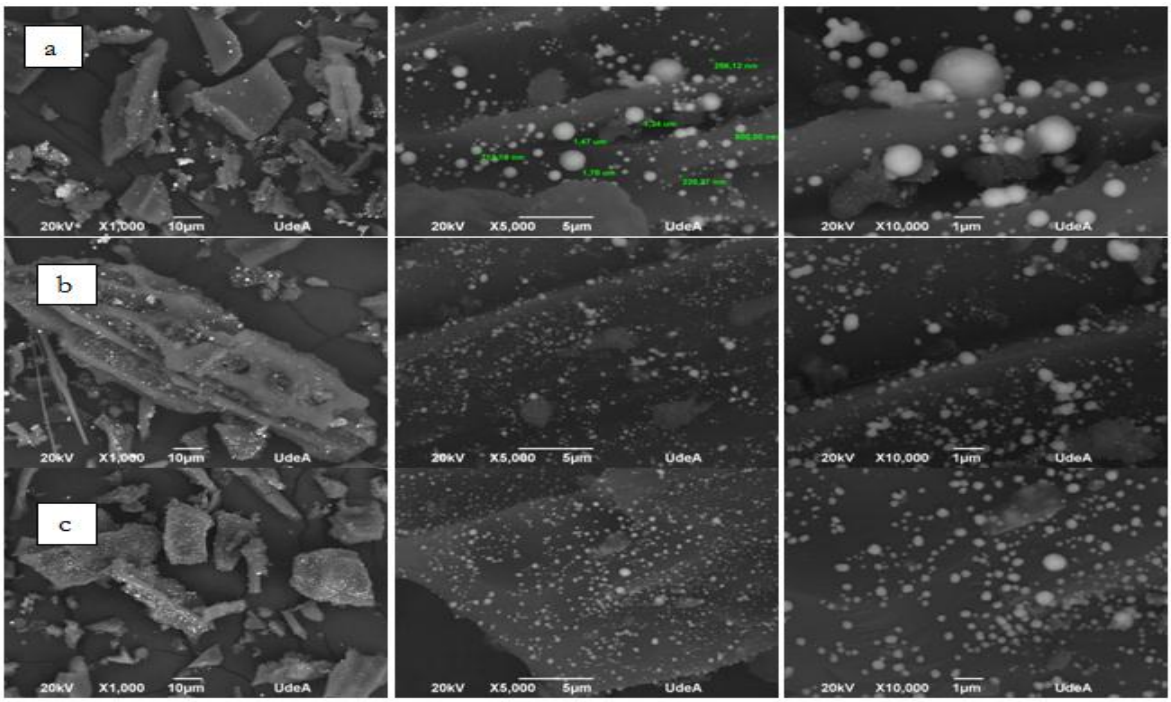

Figure 65 Cu-Ni/AC catalyst /Zeolite 4A used mixture. (a) Gas phase: Cu-Ni (2:1)/AC – Zeolite 4A; (b) Liquid phase: Cu-Ni (2:1)/AC – Zeolite 4A; (c) Liquid phase: Cu-Ni (3:1)/AC – Zeolite 4A

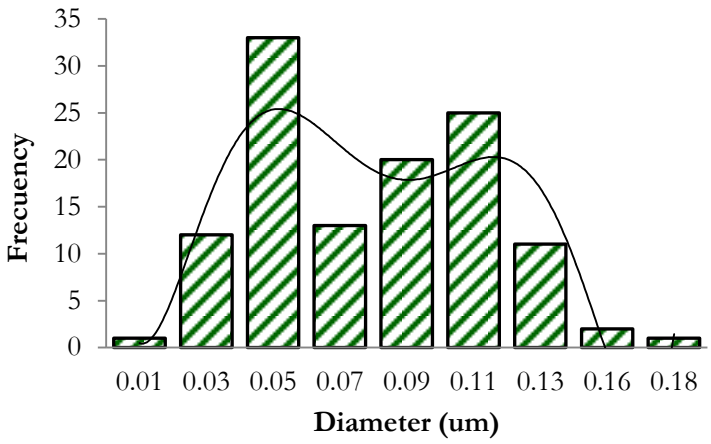

Figure 66 Particle size distribution mixture: Cu-Ni/AC catalyst – Zeolite 4A. Used. Liquid phase. Molar ratio: 3:1.

2.4.4. EDS analysis

Figure 67 and Figure 68 shows the mapping of composition for the fresh catalyst Cu-Ni/AC molar ratio 2:1 and 3:1 respectively. The presence of carbon, nickel, copper, silicon and aluminum is observed. Is really interesting analyze nickel and copper particles occupy the same places confirm the alloy between Cu-Ni. In the other hand, the intensity of cupper is higher than nickel since the molar ratio Cu:Ni (2:1) and (3:1).

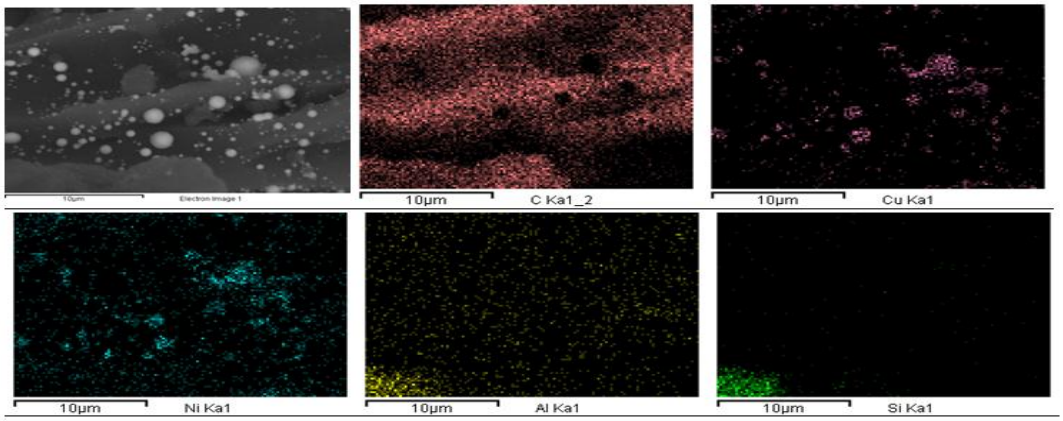

Figure 67 EDS pattern for Cu-Ni (2:1)/AC

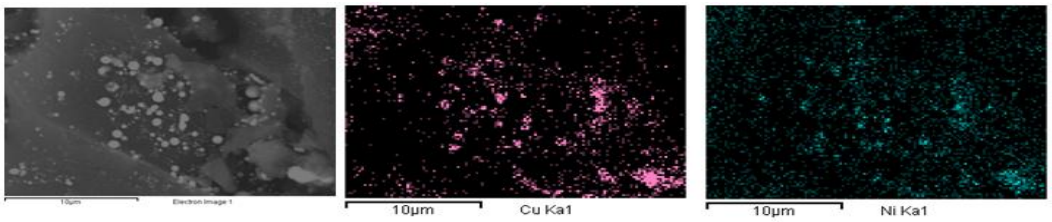

Figure 68 EDS pattern for Cu-Ni (2:1)/AC

2.4.5. TEM

Transmission Electron Microscopy (TEM) images of Cu–Ni (2:1)/AC and Cu–Ni (3:1)/AC catalyst (fresh and used in liquid and gas phase) were present in Figure 69. The TEM images shows the same morphology of metal particles (spherical and a few elliptical shape). In general, some metal particles agglomerates are observed. The mean diameter obtained for Cu-Ni alloy is close to 0.2 μm (distribution obtained by TEM in Figure 66).

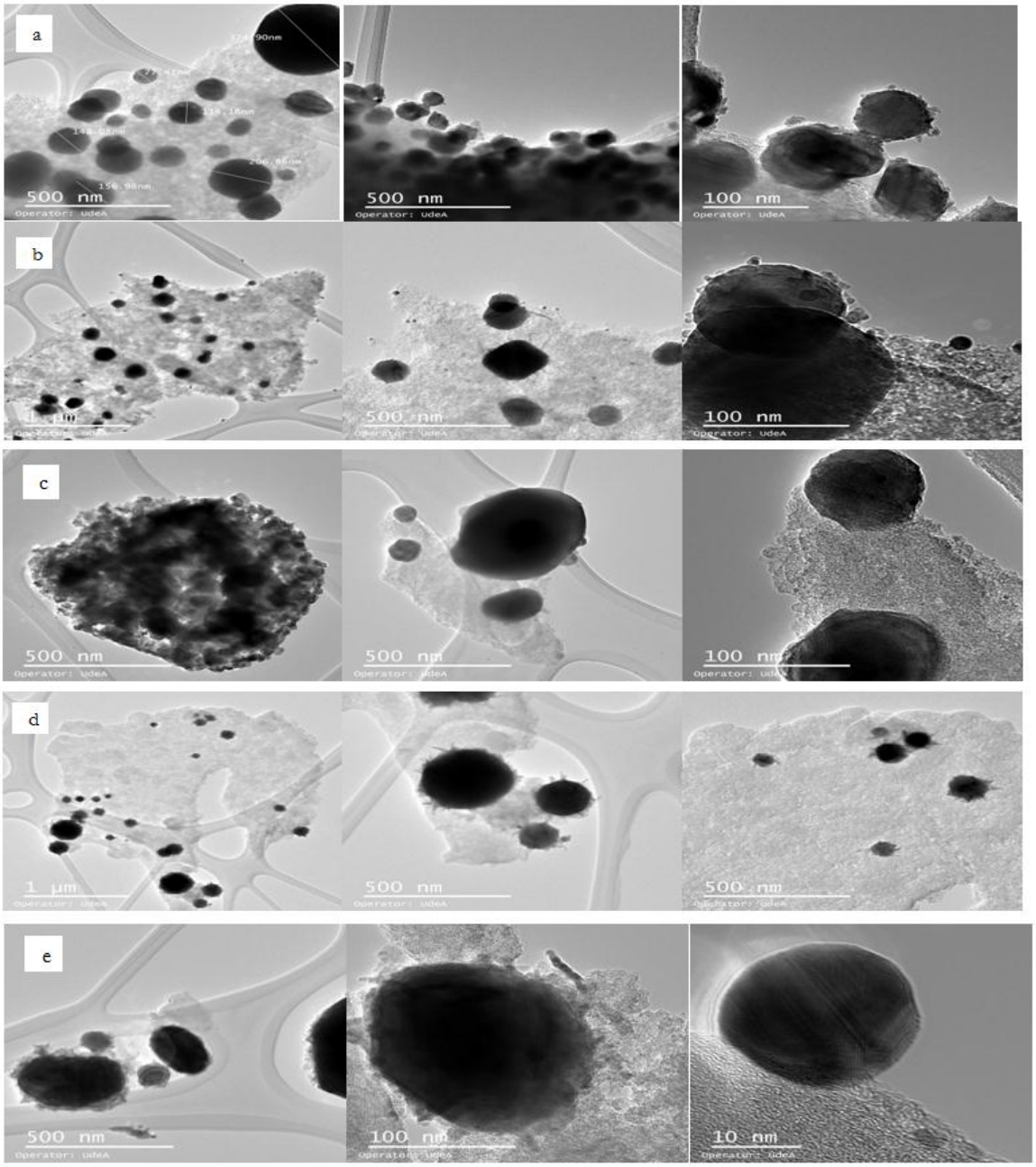

Figure 69 TEM images for (a) Cu-Ni/AC (2:1); (b) Cu-Ni/AC (3:1); (c) Cu-Ni/AC (2:1) used gas phase; (d) Cu-Ni/AC (2:1) used liquid phase; (e) Cu-Ni/AC (3:1) used liquid phase.

2.4.6. TPR analysis

The Temperature Program Reduction (TPR) profile of fresh Cu-Ni (2:1)/AC catalyst (Figure 70) showed two peaks with the main reduction peak at 267°C and a weak peak at 192 °C. The behavior of the samples used in gas and liquid phase for DMC reaction showed the presence of one peak at 202°C each time more weak. This suggests that the use of the catalyst at liquid phase deactivate the catalyst or leach the metal from the catalyst.

Over 500 °C, there was a broad peak at high temperature with a maximum at 660 °C in Cu-Ni/AC catalyst and 560°C in gas phase used catalyst. These peaks were associated with the partial gasification of carbon support due to a possible formation of CH_4 from the reaction of C and H_2.

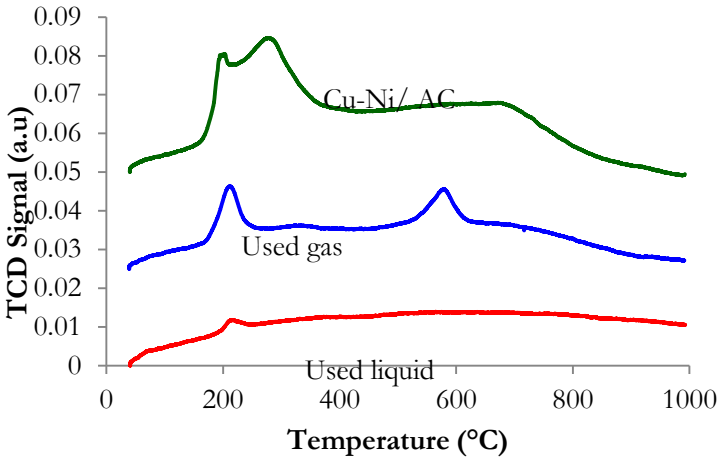

Figure 70 TPR analysis of Cu-Ni (2:1)/AC fresh and used

2.5. PARTIAL CONCLUSIONS

Dimethyl carbonate and diethyl carbonate (DMC and DEC, respectively) are nontoxic and biodegradable compounds with a wide industrial application. The current production of those carbonates involves the use phosgene and dimethylsulphate (DMS) or diethylsulphate (DES) as reactants (very toxic compounds). The environmental requirements nowadays force to find new routes, cleaner than traditional process. Chemical industry must develop cleaner processes through innovative design and environmentally benign chemical reactions (Green chemistry).

Catalysts characterization of the Cu-Ni/AC revealed higher surface area and formation of Cu-Ni alloy because the co-existence of metal sites of Cu and Ni and the metal particles were dispersed on the surface of carbon. This alloy likely occurs via mingling of copper and nickel at atomic scale, resulting in one crystalline phase [81]. The alloy Cu-Ni generates active sites that are more stable and reactive for catalyzing the direct synthesis of linear carbonates from CO_2.

The catalytic activity could be attributed to the synergistic effect of metals Cu, Ni and Cu-Ni alloy which may play a significant role on methanol and/or CO_2 activation.

The direct synthesis of DMC in gas-phase conditions was presented in this work as a clean alternative to conventional production methods. Although its application is strongly influenced by the chemical equilibrium, advances on heterogeneous catalysts are ongoing. Based on the results obtained of both theoretical (study of chemical equilibrium and gas phase behavior) and experimental (using Cu-Ni bimetallic catalyst) perspectives, we can conclude the following.

In gas phase, the catalytic activity of Cu-Ni/AC catalyst, in terms of yield of DMC was comparable with literature report. The best yield trough DMC was 2.26 % at 150°C and 14 Bar with molar ratio CO_2/Methanol 2:1. It has not detected a decomposition of alcohol even at this temperature. The liquid phase results did not show any activity under the conditions of this work, because there was not conversion and there were any product or consumption of the reagents.

Finally, all previous studies in the Cu-Ni bimetallic catalysts have been conducted in powder form; therefore, as a breakthrough in the application of the direct synthesis at a larger scale, the catalyst was successfully pelletized. Preparation conditions that guarantee obtaining a pellet with high surface area using CMC as a binder, such as dilution percent of binder in the ethanolic solution, the carbon-binder mixture proportion, and pyrolysis treatment, were selected carefully. The bimetallic Cu-Ni catalyst supported on AC retained its activity when pelletized under favorable conditions. This is the result of the strong similarity of physicochemical properties of pellets and powders. In fact, the formation of alloy species, co-existence of metal sites of Cu and Ni, and the presence of well-dispersed metal particles were also observed in the pellets.

The best reaction conditions to obtain DEC were 150°C and 14 Bar, the catalyst present a relative deactivation (0.2 %) during 5 hours proves it. The integration of Cu-Ni/CA and zeolite 4A increase the yield of DMC from 2.26 % to 2.28 and 2.60 % with fixed bed configurations. The results for single bed are better (3.02%) and the lower (1.934%) with fluidized bed. About the liquid phase, the results show under pressure and temperature conditions an unfavorable behavior, no products were detected. Testing at higher pressures could bring greater clarity of the behavior of the system.

GENERAL CONCLUSIONS

The direct synthesis of linear carbonates, from carbon dioxide (CO_2) and alcohols (methanol and ethanol) is a safe and clean route since the only by-product is water. However, the very low equilibrium conversion (5.6% in gas phase) limits the process. In order to avoid the restriction, some authors reported the use of high pressures (from 30 to 300 bar), active catalyst and dehydrating agents (molecular sieves and organic compounds), but any way it is enough to increase the yield in the process beyond the equilibrium conversion, doing it impractical and expensive.

The performance of the catalysts based on the bimetallic Cu–Ni/activated carbon (Cu-Ni/AC) on the direct synthesis of linear carbonates in gas phase at moderate pressure and temperature (13 bar, 90 °C) showed in the case of DEC synthesis a selectivity of 72 % with an ethanol conversion near to 2.7% and in the synthesis of DMC a 85 % in selectivity with a 1.8 % conversion of methanol. The analysis of the combination of the use a dehydrative agent, such as zeolite 4A, with the Cu-Ni/AC catalyst is an unexplored option that it was evaluated in this work.

This work presents experimental results for the reaction at gas phase (92°C until 14 Bar) and liquid phase (92°C and 4 Bar) added dehydrating agents (mainly zeolite 4A) and used Cu-Ni/AC catalyst. The thermodynamic limitation leads to achievable a DMC and DEC yield using Cu-Ni/AC catalyst around 1-2% if the produced water is not removed of the system. To get water eliminated dehydrating agents were used in order to shift the reaction towards a higher DMC and DEC yield. Therefore, a novel combination of a fixed bed reactor was combined with zeolite 4A at the same conditions. The results showed that the equilibrium conversion is strongly influenced by the pressure and temperature of the system: conversion increase when increasing the pressure and temperature, however, the water adsorption capacity of zeolite was always worse when temperature increase and it is not affected by pressure.

The effect of the alcohols (methanol or ethanol), CO_2, and linear carbonates (DMC or DEC) in the adsorption of water capacity of the zeolite 4A was first evaluated using the mass spectrometry as a quantification technique. According with adsorption isotherms and kinetics studies of the adsorption for mono and multicomponent systems, there was an effect of the temperature and the pressure in the behavior of zeolite 4A. The adsorption temperature affects the adsorption capacity at 0.84 atm, when the temperature was increased from 20 to 150 °C the water adsorption decreased from 233 until 10 mg_{H20}/g_{4A} . When the pressure was increased any change was observed. It is also possible to say that the presence of alcohols and CO_2 produce a competitive and inhibitory effect in the water adsorption respectively. The hydrogen bonds with CO_2 formation and particle size of alcohols are responsible. The Langmuir model could be interpreted all isotherm adsorption data; this means the adsorption of water, ethanol

and methanol over zeolite 4A and their mixtures are all in one layer when inner pores of zeolites can be filled with a constant amount of molecules.

Comparing the effect of the pressure (P and the temperature (T) in the water adsorption capacity, it is possible to say that the increment of both ones affects the adsorption in negative way. At reactions conditions there are two contrary effects between catalyst and zeolite 4A (the first improvement with the increase of T and P but spoils the adsorbent). At 92°C and 0.83 atm Zeolite 4A presents an excellent regeneration capacity.

The study allows to affirm that adsorption capacity of the zeolite 4A is affect with more factors than pore diameter and size of molecules. The diameter is generally a good way to understand why some molecules could be adsorbed into the molecular sieves but, not always it is the only reason. Ethanol with higher size than molecular sieve (4.6 Å) is adsorbed while CO_2 (3.3 Å) is not adsorbed even a long times. The work allows finding different information about kinetic and isotherm of adsorption for multicompound system. It is possible to say that, the presence of alcohols produce a competitive effect in the water adsorption and, the presence of CO2 inhibits the water adsorption, maybe by hydrogen bonds formation.

Cu-Ni/AC catalyst was characterized before reaction by several techniques such as atomic absorption spectroscopy (AAS), single point Brunauer, Emmet and Teller method (BET), X-ray diffraction (XRD), Temperature Programmed Reduction (TPR), Thermogravimetric analysis (TGA), Scanning Electron Microscope (SEM), Transmission Electron Microscopy (TEM) and Energy Dispersive X-ray Spectroscopy (EDS). The catalysts were tested in the presence of dehydrating agent in gas and liquid phase, but low improvements were observed. In gas phase, the catalytic activity of Cu-Ni/AC catalyst, in terms of yield of DMC was comparable with literature report. The best yield trough DMC was 2.26 % at 150 °C and 14 Bar with molar ratio CO_2/Methanol 2:1. The integration of Cu-Ni/CA and zeolite 4A increases the yield of DMC from 2.26 % to 2.28 and 2.60 % with fixed bed configurations. The results for single bed are better (3.02%) and the lower (1.934%) with fluidized bed. About the liquid phase, the results show under pressure and temperature conditions an unfavorable behavior, no products were detected. Testing at higher pressures could bring greater clarity of the behavior of the system.

RECOMMENDATIONS

For the liquid phase reactions, it is necessary to prove the reaction with Cu-Ni/AC and zeolite 4A at higher pressure (around 50 Bar) in order to rule out the catalyst.

To consider the interesting behavior of multicomponent system: methanol, CO_2, water, DMC it is recommended an exhaustive work to deep more in a possible chemisorption, changes in the kinetic and reduction of the adsorption capacity.

REFERENCES

[1] T. Sakakura, Y. Saito, M. Okano, J.-C. Choi, and T. Sako, "Selective Conversion of Carbon Dioxide to Dimethyl Carbonate by Molecular Catalysis," *J. Org. Chem.*, vol. 63, no. 20, pp. 7095–7096, Oct. 1998.

[2] H. Van Bekkum and H. W. Kouwenhoven, "Progress in the use of zeolites in organic synthesis," in *Introduction to Zeolite Science and Practice*, 3rd Revise., vol. 168, J. Cejka, H. Van Bekkam, A. Carma, and F. Schiit, Eds. Elsevier, 2007, pp. 947–998.

[3] G. Rokicki, J. Pawlicki, and W. Kuran, "A New Route to Carbonate Monomers for Synthesis of Polycarbonates," *Polym. J.*, vol. 14, no. 11, pp. 839–845, Nov. 1982.

[4] E. Leino, P. Mäki-Arvela, V. Eta, N. Kumar, F. Demoisson, A. Samikannu, A.-R. Leino, A. Shchukarev, D. Y. Murzin, and J.-P. Mikkola, "The influence of various synthesis methods on the catalytic activity of cerium oxide in one-pot synthesis of diethyl carbonate starting from CO2, ethanol and butylene oxide," *Catal. Today*, vol. 210, pp. 47–54, Jul. 2013.

[5] D. N. Briggs, K. H. Lawrence, and A. T. Bell, "An investigation of carbon-supported CuCl2/PdCl2 catalysts for diethyl carbonate synthesis," *Appl. Catal. A Gen.*, vol. 366, no. 1, pp. 71–83, Sep. 2009.

[6] A. Dibenedetto and A. Angelini, "CO2 Chemistry," *Adv. Inorg. Chem.*, vol. 66, pp. 25–81, 2014.

[7] T. Sakakura, J. Choi, and H. Yasuda, "Transformation of carbon dioxide.," *Chem. Rev.*, vol. 107, no. 6, pp. 2365–87, Jun. 2007.

[8] T. Sakakura and K. Kohno, "The synthesis of organic carbonates from carbon dioxide.," *Chem. Commun. (Camb).*, no. 11, pp. 1312–30, Mar. 2009.

[9] E. Leino, P. Mäki-Arvela, K. Eränen, M. Tenho, D. Y. Murzin, T. Salmi, and J.-P. Mikkola, "Enhanced yields of diethyl carbonate via one-pot synthesis from ethanol, carbon dioxide and butylene oxide over cerium (IV) oxide," *Chem. Eng. J.*, vol. 176–177, pp. 124–133, Dec. 2011.

[10] L. Li, N. Zhao, W. Wei, and Y. Sun, "A review of research progress on CO2 capture, storage, and utilization in Chinese Academy of Sciences," *Fuel*, vol. 108, pp. 112–130, Jun. 2013.

[11] H. Chen, S. Wang, M. Xiao, D. Han, Y. Lu, and Y. Meng, "Direct Synthesis of Dimethyl Carbonate from CO2 and CH3OH Using 0.4 nm Molecular Sieve Supported Cu-Ni Bimetal Catalyst," *Chinese J. Chem. Eng.*, vol. 20, no. 5, pp. 906–913, Oct. 2012.

[12] O. Arbeláez, A. Orrego, F. Bustamante, and A. L. Villa, "Direct Synthesis of Diethyl Carbonate from CO2 and CH3CH2OH Over Cu–Ni/AC Catalyst," *Top. Catal.*, vol. 55, no. 7–10, pp. 668–672, Jun. 2012.

[13] X. L. Wu, Y. Z. Meng, M. Xiao, and Y. X. Lu, "Direct synthesis of dimethyl carbonate (DMC) using Cu-Ni/VSO as catalyst," *J. Mol. Catal. A Chem.*, vol. 249, no. 1–2, pp. 93–97, Apr. 2006.

[14] H. Dou, "Catalyzed Synthesis of Dimethyl Carbonate," PhD Thesis, Department of Chemistry, Technical University of Munich, Munich, 2010.

[15] A. Rivera, P. Bejarano, and G. Rodríguez, "Modelado de curvas de ruptura en la adsorción de agua sobre sílica gel y zeolita 4A," *Rev. Fac. Ing. Univ. Antioquia*, vol. 71, pp. 179–190, 2014.

[16] F. Bustamante, A. F. Orrego, S. Villegas, and A. L. Villa, "Modeling of Chemical Equilibrium and Gas Phase Behavior for the Direct Synthesis of Dimethyl Carbonate from CO 2 and Methanol," *Ind. Eng. Chem. Res.*, vol. 51, no. 26, pp. 8945–8956, Jul. 2012.

[17] T. Leppäjärvi, I. Malinen, J. Kangas, and J. Tanskanen, "Utilization of Pisat temperature-dependency in modelling adsorption on zeolites," *Chem. Eng. Sci.*, vol. 69, no. 1, pp. 503–513, Feb. 2012.

[18] D. Breck, *Zeolite molecular sieves: structure, chemistry, and use Wiley-Interscience Publication*, 99, illust. Toronto, Canada, 1974, p. 771.

[19] Y. Li, H. Yi, X. Tang, F. Li, and Q. Yuan, "Adsorption separation of CO2/CH4 gas mixture on the commercial zeolites at atmospheric pressure," *Chem. Eng. J.*, vol. 229, pp. 50–56, Aug. 2013.

[20] A. Gorbach, M. Stegmaier, and G. Eigenberger, "Measurement and Modeling of Water Vapor Adsorption on Zeolite 4A—Equilibria and Kinetics," *Adsorption*, vol. 10, no. 1, pp. 29–46, Jan. 2004.

[21] G. Aguilar and S. Toledo, "Adsorción de vapores de agua en zeolita natural mexicana," *Superf. y Vacío*, vol. 1, pp. 142–147, 1989.

[22] F. B. Cortés, F. Chejne, F. Carrasco-Marín, C. Moreno-Castilla, and a. F. Pérez-Cadenas, "Water adsorption on zeolite 13X: comparison of the two methods based on mass spectrometry and thermogravimetry," *Adsorption*, vol. 16, no. 3, pp. 141–146, Feb. 2010.

[23] P. . Walker, L. G. Austin, and S. P. Nandi, "Activated Diffusion of Gases in Molecular - Sieve Materials," *chem. Phys. Carbon*, vol. 2, pp. 251–371, 1966.

[24] Sigma-Aldrich, "Molecular Sieves - Technical Information Bulletin," 2016. [Online]. Available: http://www.sigmaaldrich.com/chemistry/chemical-synthesis/learning-center/technical-bulletins/al-1430/molecular-sieves.html.

[25] Sigma-Aldrich, "Product Information: Molecular Sieves." [Online]. Available: http://www.sigmaaldrich.com/content/dam/sigma-aldrich/docs/Sigma/Product_Information_Sheet/96096pis.pdf.

[26] R. Lin, A. Ladshaw, Y. Nan, J. Liu, S. Yiacoumi, C. Tsouris, D. W. DePaoli, and L. L. Tavlarides, "Isotherms for Water Adsorption on Molecular Sieve 3A: Influence of Cation Composition," *Ind. Eng. Chem. Res.*, vol. 54, no. 42, pp. 10442–10448, Oct. 2015.

[27] J. Keller and R. Staudt, *Gas Adsorption Equilibria*. Boston: Kluwer Academic Publishers, 2005.

[28] F. Cortés, "Adsorción de agua en materiales compuestos y en zeolita," PhD Thesis, Escuela de Procesos y Energía, Universidad Nacional, Facultad de Minas, Medellín, 2009.

[29] A. L. Myers, "Chapter 21, Thermodynamics of adsorption," in *Chemical Thermodynamics for Industry*, T. M. Letcher, Ed. Cambridge: Royal Society of Chemistry, 2007, pp. 244–253.

[30] M. Pera-Titus, C. Fité, V. Sebastián, E. Lorente, J. Llorens, and F. Cunill, "Modeling Pervaporation of Ethanol/Water Mixtures within 'Real' Zeolite NaA Membranes," *Ind. Eng. Chem. Res.*, vol. 47, no. 9, pp. 3213–3224, May 2008.

[31] R. Vallinayagam, S. Vedharaj, W. M. Yang, P. S. Lee, K. J. E. Chua, and S. K. Chou, "Pine oil–biodiesel blends: A double biofuel strategy to completely eliminate the use of diesel in a diesel engine," *Appl. Energy*, vol. 130, pp. 466–473, Oct. 2014.

[32] S. Villegas, "Modelación y simulación de la síntesis directa de dimetil carbonato a partir de metanol Y CO2 con remoción in situ de agua mediante una membrana selectiva." PhD. Thesis, Departamento de Ingeniería, Universidad de Antioquia, Medellín, p. 199, 2011.

[33] W. J. Weber and J. A. Borchardt, "Chapter 5. Adsorption.," in *Physicochemical processes for water quality control.*, New York N.Y: Wiley-Interscience, 1972.

[34] F. Alberto and A. Villa, "Estudio de la adsorción de una mezcla binaria de colorantes de interés industrial sobre cascarilla de arroz." MsC. Thesis, Facultad de Ciencias, Universidad Nacional, Medellín, p. 134, 2015.

[35] H. Chen and D. S. Sholl, "Examining the accuracy of ideal adsorbed solution theory without curve-fitting using transition matrix Monte Carlo simulations.," *Langmuir*, vol. 23, no. 11, pp. 6431–7, May 2007.

[36] K. S. Walton and D. S. Sholl, "Predicting multicomponent adsorption: 50 years of the ideal adsorbed solution theory," *AIChE J.*, vol. 61, no. 9, pp. 2757–2762, Sep. 2015.

[37] A. L. Myers and J. M. Prausnitz, "Thermodynamics of mixed-gas adsorption," *AIChE J.*, vol. 11, no. 1, pp. 121–127, Jan. 1965.

[38] P. Bai, M. Tsapatsis, and J. I. Siepmann, "Multicomponent adsorption of alcohols onto silicalite-1 from aqueous solution: isotherms, structural analysis, and assessment of ideal adsorbed solution theory.," *Langmuir*, vol. 28, no. 44, pp. 15566–76, Nov. 2012.

[39] A. Hidalgo, "Biosorcion de plomo y cadmio mediante el aprovechamiento de residuos de madera (aserrin de pino) y extractos de algas marinas (alginato de calcio)." Tesis de grado, Facultad de Biología, Universidad de Michoacana de San Nicolas de Hidalgo, Michoacán, 2010.

[40] H. Nourmoradi, M. Khiadani, and M. Nikaeen, "Multi-Component Adsorption of Benzene, Toluene, Ethylbenzene, and Xylene from Aqueous Solutions by Montmorillonite Modified with Tetradecyl Trimethyl Ammonium Bromide," *J. Chem.*, vol. 2013, pp. 1–10, 2013.

[41] M. L. Pinzón-Bedoya and L. E. V. Villamizar, "Modelamiento de la Cinética de Bioadsorción de Cr (III) usando Cáscara de Naranja," *Dyna*, vol. 76, no. 160, pp. 97–106, 2009.

[42] C. Mahamadi and E. Mawere, "Kinetic Modeling of Methylene Blue and Crystal Violet Dyes Adsorption on Alginate-Fixed Water Hyacinth in Single and Binary Systems," *Am. J. Anal. Chem.*, vol. 04, no. 10, pp. 17–24, 2013.

[43] K. Zhang, R. P. Lively, J. D. Noel, M. E. Dose, B. a McCool, R. R. Chance, and W. J. Koros, "Adsorption of water and ethanol in MFI-type zeolites.," *Langmuir*, vol. 28, no. 23, pp. 8664–73, Jun. 2012.

[44] Y. P. Ryazantsev and V. P. Kurnoskina, "High-temperature adsorption of water vapor on Type A zeolite," *Chem. Technol. Fuels Oils*, vol. 12, no. 1, pp. 24–26, Jan. 1976.

[45] L. Hauchhum and P. Mahanta, "Carbon dioxide adsorption on zeolites and activated carbon by pressure swing adsorption in a fixed bed," *Int. J. Energy Environ. Eng.*, vol. 5, no. 4, pp. 349–356, Aug. 2014.

[46] P. Zhang, M. Fan, and P. Jiang, "A novel method to reduce the influence of by-product water on the catalytic performance of PdCl2/Cu-HMS catalysts for the synthesis of diethyl carbonate," *RSC Adv.*, vol. 2, no. 11, p. 4593, 2012.

[47] M. Chaplin, "The CO2-Water Cluster," *Water Structure and Science*, 2016. [Online]. Available: http://www1.lsbu.ac.uk/water/co2.html.

[48] I. Tunón, E. Ortí, C. Gómez, J. Pascual-Ahuir, and I. Monzó, "Tema 7 . Superficies sólidas : adsorción y catálisis heterogénea," in *Química Física Avanzada*, Universida., Apuntes de Química Física Avanzada Departamento de Química Física Univèrsitat de València, 2009, p. 28.

[49] Víctor Rosas, "Adsorción," *Universidad Autónoma de Nuevo León*, 1999. [Online]. Available: http://lqi.tripod.com/FQAv/isoterms.htm.

[50] R. V Siriwardane, M. Shen, E. P. Fisher, and J. A. Poston, "Adsorption of CO 2 on Molecular Sieves and Activated Carbon," *Energy & Fuels*, vol. 15, no. 2, pp. 279–284, Mar. 2001.

[51] L. J. Burcham and I. E. Wachs, "The origin of the support effect in supported metal oxide catalysts: in situ infrared and kinetic studies during methanol oxidation," *Catal. Today*, vol. 49, no. 4, pp. 467–484, Mar. 1999.

[52] P. Salvador and W. Kladnig, "Estudio fisicoquímico de la interacción de zeolitas H-Y y Na-Y con metanol," *Rev. Port. Química*, vol. 19, no. 1–4, pp. 149–154, 1977.

[53] M. L. H. Figueroa and B. L. Rodríguez, "Cinética e isotermas de adsorción de Pb (II) en suelo de Monterrey," *Ingenierias*, vol. XI, no. 41, pp. 24–31, 2008.

[54] M. M. J. Treacy and J. . Higgins, *Collection of Simulated XRD Powder Patterns for Zeolites*. Amsterdam, London, New York, Oxford, Paris, Tokyo, 2001, p. 586.

[55] G. Picasso and I. Salazar, "Síntesis de catalizadores nanoestructurados basados en óxido de Mn para la eliminación de n-hexano," *Rev. Soc. Quím. Perú*, vol. 77, no. 1, pp. 11–26, 2011.

[56] Y. Yaneth, A. Pertuz, L. Alfredo, O. Aguiar, and U. N. Uribe, "Modifications of the textural and structural properties of zeolite usy and its mixture with kaolin clay and chlorhydrol as consequence of the hydrothermal treatment," *Rev.Colomb.Quim.*, vol. 35, no. 1, pp. 7–17, 2006.

[57] C. Valderrama, "Síntesis y Caracterización de Membranas hidrofílicas sobre soportes porosos para la obtención de aditivos oxigenantes para gasolina." MsC. Thesis, Facultad de Ingenería, Universidad de Antioquía, Medellín, 2013.

[58] Y. Suzuki, T. Miyanaga, H. Hoshino, N. Matsumoto, and T. Ainai, "In-Situ XAFS Study of Ag Clusters in Zeolite 4A," *Phys. Scr.*, vol. T115, pp. 765–768, 2005.

[59] E. Hernández, V. Alcántara, L. M. González, and A. L. Villa, "Adsorption of water in the multi-component system used in the synthesis of linear carbonates." 2do Simposio Iberoamericano de Adsorción, Universidad de los Andes, Cartagena, pp. 27–28, 2015.

[60] Meq, "Las reacciones del dimetil carbonato," *la Rev. química útil*, vol. 19, pp. 18– 21, 2011.

[61] Chemsystems, "Dymethyl Carbonate.," 2012. [Online]. Available: http://www.chemsystems.com/reports/search/docs/abstracts/2012S12_abs_R1.pdf.

[62] Hans-Josef Buysch, "Carbonic Esters," in *Ullmann's Encyclopedia of Industrial Chemistry: Electronic Release*, Six Editio., Weinheim, Germany: Wiley-VCH Verlag GmbH & Co. KGaA, 2000.

[63] P. Tundo and M. Selva, "The Chemistry of Dimethyl Carbonate," *Acc. Chem. Res.*, vol. 35, no. 9, pp. 706–716, Sep. 2002.

[64] Y. Ono, "Dimethyl carbonate for environmentally benign reactions," *Catal. Today*, vol. 35, no. 1–2, pp. 15–25, Mar. 1997.

[65] Y. Ono, "Catalysis in the production and reactions of dimethyl carbonate, an environmentally benign building block," *Appl. Catal. A Gen.*, vol. 155, no. 2, pp. 133–166, Jul. 1997.

[66] D. Delledonne, F. Rivetti, and U. Romano, "Developments in the production and application of dimethylcarbonate," *Appl. Catal. A Gen.*, vol. 221, no. 1–2, pp. 241–251, Nov. 2001.

[67] A. G. Shaikh and S. Sivaram, "Organic Carbonates †," *Chem. Rev.*, vol. 96, no. 3, pp. 951–976, Jan. 1996.

[68] G. Wypych, "A Properties Database. ChemTec Publishing.," *Knovel Solvents*, 2003. [Online]. Available: http://app.knovel.com/hotlink/toc/id:kpKSAPD005/knovel-solvents-properties.

[69] J. P. Parrish, R. N. Salvatore, and K. W. Jung, "Perspectives on Alkyl Carbonates in Organic Synthesis," *Tetrahedron*, vol. 56, no. 42, pp. 8207–8237, Oct. 2000.

[70] I. C. Arango and A. L. Villa, "Equilibrio multifásico de mezclas binarias y ternarias de carbonato de dietilo (DEC), agua y etanol," *Rev. ion*, vol. 25, no. 1, pp. 43–49, 2012.

[71] F. Ancillotti and V. Fattore, "Oxygenate fuels: Market expansion and catalytic aspect of synthesis," *Fuel Process. Technol.*, vol. 57, no. 3, pp. 163–194, Oct. 1998.

[72] A. Sinha and M. . Thomson, "The chemical structures of opposed flow diffusion flames of C3 oxygenated hydrocarbons (isopropanol, dimethoxy methane, and dimethyl carbonate) and their mixtures," *Combust. Flame*, vol. 136, no. 4, pp. 548–556, Mar. 2004.

[73] M. A. Pacheco and C. L. Marshall, "Review of Dimethyl Carbonate (DMC) Manufacture and Its Characteristics as a Fuel Additive," *Energy & Fuels*, vol. 11, no. 1, pp. 2–29, Jan. 1997.

[74] B. Scrosati, "Recent advances in lithium ion battery materials," *Electrochim. Acta*, vol. 45, no. 15–16, pp. 2461–2466, May 2000.

[75] "Ube Industries acuerda establecer una joint venture para Dimetil Carbonato en China.," *Ube Industries Ltd.*, 2012. [Online]. Available: http://www.ube-ind.co.jp/spanish/news/2012/20120409_01.htm.

[76] M. Berhil, N. Lebrun, A. Tranchant, and R. Messina, "Reactivity and cycling behaviour of lithium in propylene carbonate-ethylene carbonate-dimethyl carbonate mixtures," *J. Power Sources*, vol. 55, no. 2, pp. 205–210, Jun. 1995.

[77] R. Naejus, R. Coudert, P. Willmann, and D. Lemordant, "Ion solvation in carbonate-based lithium battery electrolyte solutions," *Electrochim. Acta*, vol. 43, no. 3–4, pp. 275–284, Jan. 1998.

[78] H. Lin, B. Yang, J. Sun, X. Wang, and D. Wang, "Kinetics studies for the synthesis of dimethyl carbonate from urea and methanol," *Chem. Eng. J.*, vol. 103, no. 1–3, pp. 21–27, Oct. 2004.

[79] U. Romano, R. Tesel, M. M. Mauri, and P. Rebora, "Synthesis of Dimethyl Carbonate from Methanol, Carbon Monoxide, and Oxygen Catalyzed by Copper Compounds," *Ind. Eng. Chem. Prod. Res. Dev.*, vol. 19, no. 3, pp. 396–403, Sep. 1980.

[80] T. Matsuzaki, T. Shimamura, S. Fujitsu, and Y. Toriyahara, "Method of producing carbonic acid diester," US Patent 5292916 A, March 8, 1994.

[81] A. F. Orrego, "Direct Synthesis of Dimethyl Carbonate from CO2 and Methanol in gas-phase." PhD. Thesis, Departamento de Ingeniería, Universidad de Antioquia, Medellín, p. 162, 2014.

[82] Y. Wang, D. Jia, Z. Zhu, and Y. Sun, "Synthesis of Diethyl Carbonate from Carbon Dioxide, Propylene Oxide and Ethanol over KNO3-CeO2 and KBr-KNO3-CeO2 Catalysts," *Catalysts*, vol. 6, no. 4, p. 52, Mar. 2016.

[83] J.-C. Choi, L.-N. He, H. Yasuda, and T. Sakakura, "Selective and high yield synthesis of dimethyl carbonate directly from carbon dioxide and methanol," *Green Chem.*, vol. 4, no. 3, pp. 230–234, Jun. 2002.

[84] M. Honda, M. Tamura, Y. Nakagawa, and K. Tomishige, "Catalytic CO 2 conversion to organic carbonates with alcohols in combination with dehydration system," *Catal. Sci. Technol.*, vol. 4, no. 9, p. 2830, May 2014.

[85] M. Honda, M. Tamura, Y. Nakagawa, S. Sonehara, K. Suzuki, K.-I. Fujimoto, and K. Tomishige, "Ceria-catalyzed conversion of carbon dioxide into dimethyl carbonate with 2-cyanopyridine.," *ChemSusChem*, vol. 6, no. 8, pp. 1341–4, Aug. 2013.

[86] J. Bian, M. Xiao, S. Wang, X. Wang, Y. Lu, and Y. Meng, "Highly effective synthesis of dimethyl carbonate from methanol and carbon dioxide using a novel copper–nickel/graphite bimetallic nanocomposite catalyst," *Chem. Eng. J.*, vol. 147, no. 2–3, pp. 287–296, Apr. 2009.

[87] M. Aresta and A. Dibenedetto, "Utilisation of CO2 as a chemical feedstock: opportunities and challenges.," *Dalton Trans.*, no. 28, pp. 2975–92, Jul. 2007.

[88] J. L. Rosenberg, L. M. Epstein, and P. J. Krieger, "Thermodynamics and Chemical Equilibrium," in *Schaum's Easy Outlines of College Chemistry*, 2nd Revise., Schaum Outline Series, Ed. New York, 2008, p. 160.

[89] K. Tomishige, T. Sakaihori, Y. Ikeda, and K. Fujimoto, "A novel method of direct synthesis of dimethyl carbonate from methanol and carbon dioxide catalyzed by zirconia," *Catal. Letters*, vol. 58, no. 4, pp. 225–229, 1999.

[90] O. Arbeláez, T. R. Reina, S. Ivanova, F. Bustamante, A. L. Villa, M. a. Centeno, and J. a. Odriozola, "Mono and bimetallic Cu-Ni structured catalysts for the water gas shift reaction," *Appl. Catal. A Gen.*, vol. 497, pp. 1–9, May 2015.

[91] G. Merza, B. László, A. Oszkó, G. Pótári, K. Baán, and A. Erdőhelyi, "The direct synthesis of dimethyl carbonate by the oxicarbonylation of methanol over Cu supported on carbon nanotube," *J. Mol. Catal. A Chem.*, vol. 393, pp. 117–124, Nov. 2014.

[92] J. Bian, X. W. Wei, Y. R. Jin, L. Wang, D. C. Luan, and Z. P. Guan, "Direct synthesis of dimethyl carbonate over activated carbon supported Cu-based catalysts," *Chem. Eng. J.*, vol. 165, no. 2, pp. 686–692, Dec. 2010.

[93] E. Leino, P. Mäki-Arvela, V. Eta, D. Y. Murzin, T. Salmi, and J.-P. Mikkola, "Conventional synthesis methods of short-chain dialkylcarbonates and novel production technology via direct route from alcohol and waste CO2," *Appl. Catal. A Gen.*, vol. 383, no. 1–2, pp. 1–13, Jul. 2010.

[94] C. A. Ferretti, "Valoración catalítica de Glicerol: Síntesis de Monoglicéridos." PhD. Thesis, Facultad de Ingenieria Química, Universidad Nacional del Litoral, Argentina, p. 73, 2010.

[95] C. Perego and P. Villa, "Catalyst preparation methods," *Catal. Today*, vol. 34, pp. 281–305, 1997.

[96] X. Xu and J. A. Moulijn, "Structured Catalysts and Reactors," in *Transformation of a Structured Carrier into Structured Catalyst*, vol. 20052222, A. Cybulski and J. Moulijn, Eds. CRC Press, 2005, pp. 751–778.

[97] M. Komiyama, "Design and Preparation of Impregnated Catalysts," *Catal. Rev.*, vol. 27, no. 2, pp. 341–372, Dec. 2006.

[98] M. Mestanza, "Estudio de materiales adsorbentes para el tratamiento de aguas contaminadas con colorantes," 2012.

[99] J. Bian, M. Xiao, S. Wang, Y. Lu, and Y. Meng, "Direct synthesis of DMC from CH3OH and CO2 over V-doped Cu-Ni/AC catalysts," *Catal. Commun.*, vol. 10, no. 8, pp. 1142–1145, Mar. 2009.

[100] O. Arbeláez, "Síntesis Directa de Dietil Carbonato a Partir de Dióxido de Carbono y Etanol utilizando un Reactor Catalítico de Membrana." PhD. Thesis, Departamento de Ingeniería, Universidad de Antioquia, Medellín, pp. 1–168, 2015.

[101] G. Leofanti, M. Padovan, G. Tozzola, and B. Venturelli, "Surface area and pore texture of catalysts," *Catal. Today*, vol. 41, no. 1–3, pp. 207–219, May 1998.

[102] Sigma-Aldrich, "Molecular Sieves. Product Information." [Online]. Available: http://www.sigmaaldrich.com/content/dam/sigma-aldrich/docs/Sigma/Product_Information_Sheet/96096pis.pdf.

[103] Sigma-Aldrich, "Technical Information Bulleting." [Online]. Available: http://www.sigmaaldrich.com/chemistry/chemical-synthesis/learning-center/technical-bulletins/al-1430/molecular-sieves.html .

[104] C. Yaws, K. Narasimhan, Prasad, and C. Gabbula, *Yaws' Handbook of Antoine Coefficients for Vapor Pressure*, 2nd Electr. 2005.

[105] "Dietilo carbonato. Material Safety Data Sheet (MSDS) 802898," *Merck Millipore*. [Online]. Available: http://www.merckmillipore.com/CO/es/product/Dietilo-carbonato,MDA_CHEM-802898?ReferrerURL=https://www.google.com.co/.

[106] S. co. C. & L. Equipment., "Diethyl Carbonate." [Online]. Available: http://www.sciencelab.com.

[107] M. Millipore, "Dimetilo carbonato. Material Safety Data Sheet (MSDS) 803525," *Merck Millipore*. [Online]. Available: https://www.merckmillipore.com/CO/es/product/Dimetilo-carbonato,MDA_CHEM-8035251000?ReferrerURL=https://www.google.com.co/&CatalogCategoryID=.

[108] Sciencelab.com Chemicals & Laboratory Equipment, "Dimethyl Carbonate," *Sciencelab.com Chemicals*, 1997. [Online]. Available: http://www.sciencelab.com/page/S/PVAR/SLD2551.

[109] Globaledge, "Colombia: Trade Statistics," *Global Edge*, 2014. [Online]. Available: http://globaledge.msu.edu/countries/colombia/tradestats.

[110] Trademape, "Trade Map - Trade Competitiveness Map. Colombia," 2015. [Online]. Available: http://www.trademap.org/countrymap/Country_SelProductCountry_TS_Graph.aspx.

[111] "Trade Map. Colombia," *ITC*, 2015. [Online]. Available: http://www.trademap.org/index.aspx?nvpm=1|170|||TOTAL|||2|1|1|1|2|1|2|1|.

[112] Aladi, "Estadísticas Colombia," 2016. [Online]. Available: http://consultawebv2.aladi.org/sicoexV2/jsf/arancel_vigente_item_arancelario_resultado.seam?retorno=tree&cid=95549.

APPENDIXES

Appendix 1 Zeolites references [102] [103]

Zeolite	Pore diameter (Å)	Moisture (%)	Cody	Lot	Name
13X	10	<2	Micromeritics	-	-
3A	3	<2	233676	MKBQ3216V	beads, 4-8 mesh (Sigma-Aldrich) Linear Formula $K_nNa_{12-n}[(AlO_2)_{12}(SiO_2)_{12}] \cdot xH_2O$
4A	4	<2	688363	MKBB3183	powder, activated, −325 mesh particle size (Sigma-Aldrich) Linear Formula $Na_{12}[(AlO_2)_{12}(SiO_2)_{12}] \cdot xH_2O$
5A	5	<2	233676	MKB69011V	powder, undried (Sigma-Aldrich) Linear Formula $Ca_{/n}Na_{12-2n}[(AlO_2)_{12}(SiO_2)_{12}] \cdot xH_2O$

Appendix 2 Conversion of concentration units (% Vol.) at µmol/gs

To convert units (% Vol.) at µmol/gs the following calculation was performed:

Assuming calculating base 1% for ideal gas.

$$1\% = \frac{1\text{mg}}{\text{L}} = \frac{1\text{mmol}}{\text{L}} = \frac{1\mu\text{mol}}{\text{mL}} \text{ (for ideal gas)}$$

The flow is 60 ml/min (1ml/s)

$$\frac{1\mu\text{mol}}{\text{mL}} \times \frac{1\text{ml}}{\text{s}} = \frac{1\mu\text{mol}}{\text{s}}$$

Dividing for the average weight of dry zeolite 4A (0.0784 g).

$$\frac{1\mu\text{mol}}{0.0784\ \text{gs}} = 12.75 \frac{\mu\text{mol}}{\text{gs}}$$

Appendix 3 Conversion % to µmol/gs

Assuming calculate base 1%

$$1\% = \frac{1\text{mg}}{\text{L}} = \frac{1\text{mmol}}{\text{L}} = \frac{1\mu\text{mol}}{\text{mL}} \text{ (For ideal gas)}$$

As it has flow of 60ml/min (1ml/s)

$$\frac{1\mu\text{mol}}{\text{mL}} \times \frac{1\text{ml}}{\text{s}} = \frac{1\mu\text{mol}}{\text{s}}$$

Dividing by average weight of 0.08 g catalyst:

$$\frac{1\mu\text{mol}}{0.08\text{ gs}} = 12.5\frac{\mu\text{mol}}{\text{gs}}$$

Appendix 4. Antoine Constants [104]

Using equation:

$$P = 10^{\left(A - \frac{B}{(T+C)}\right)}$$

The Antoine coefficients for organic e inorganic compounds are:

Compound	CAS Registry	Molecular formula	A	B	C	Tmin. (°C)	Tmax. (°C)
carbon dioxide	124-38-9	CO_2	7.58828	861.82	271.883	-56.57	31.04
methyl alcohol	67-56-1	CH_4O	8.09126	1582.91	239.096	-97.68	239.43
ethyl alcohol	64-17-5	C_2H_6O	8.13484	1662.48	238.131	-114.1	243.1
water	7732-18-5	H_2O	8.05573	1723.64	233.076	0.01	373.98
diethyl carbonate	105-58-8	$C_5H_{10}O_3$	7.61056	1741.06	241.309	-42	302.85
Dimethyl carbonate	616-38-6	$C_3H_6O_3$	6.4337	1413	-44.25	21.9	-
Diethyl ether	60-29-7	$C_2H_{10}O$	6.9722	1099.4	237.2	19.5	6.9722
Dimethyl ether	115-10-6	C_2H_6O	7.10736	946.89	248.645	-102	127

Appendix 5 Mass characteristics pattern used in mass spectrometer

The mass specified for the quantification of each of the components were chosen like shows in the next table. With this quantization matrix was measured the concentration for each experiment made in various mixtures. The equipment provides data over time based on the signal intensities detected by the computer.

Mass characteristic	4	13	14	15	16	17	18	22*	24	25	28	29	30	31	32	33	44	45	46	47*	59*	60	61	73*	74*	91*
Helium	●																									
Water						●	●																			
Ethanol									●	●		●	●	●			●									
Methanol							●				●	●	●	●	●	●										
DEC								●				●	●	●			●							●		●
DMC				●	●							●	●	●		●		●	●		●	●	●			
Carbon dioxide								●									●									
Diethyl ether								●				●		●										●	●	
Dimethyl ether		●	●	●		●	●	●				●		●		●	●		●	●						

Appendix 6 Calibration factor (the compounds percent).

Compound	%	Compound	%
Water	2.7798	**DEC**	1.2824
Ethanol	6.7648	**DMC**	7.3194
Methanol	15.019	**DEE**	62.6799
CO_2	39.9798	**DME**	38.82

Pressure: 0.83 Bar, Temperature: 20°C. The concentration of CO_2 was taken using a current of Helium and CO2 equal at 50 ml/min. Measure the real flow and calculate the fraction

Appendix 7 Isotherms two compounds

The ethanol adsorption in presence of CO_2 and DEC produces a contrary tendency with CO_2 because the increase of temperature increase the adsorption but, if it compare the adsorption capacity for single ethanol (at 92°C = 184 mg/g, at 150°C= 132 mg/g and at 200°C = 69 mg/g) it is possible to think that DEC does not affect in strong way the adsorption. About methanol isotherm, the presence of CO_2 and DMC reduce the methanol adsorption capacity to 250 mg/g with CO_2 and 295 mg/g with DMC (single methanol adsorption is 400 mg/g at 92°C). Again, this adsorption does not follow the common tendency because the increase of temperature does not reduce the adsorption capacity.

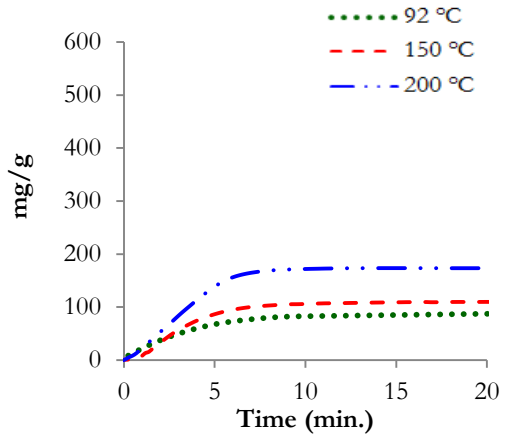

Ethanol adsorption isotherm in ethanol – CO_2 mixture

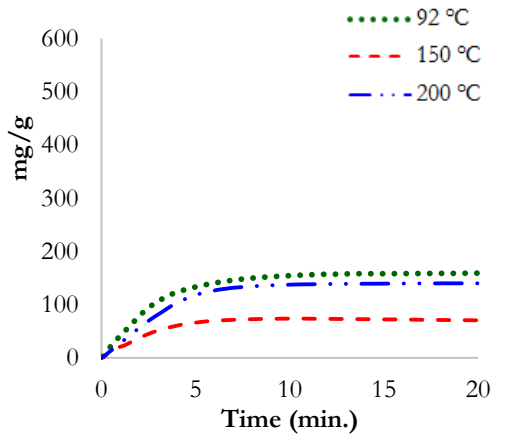

Ethanol adsorption isotherm in ethanol – DEC mixture

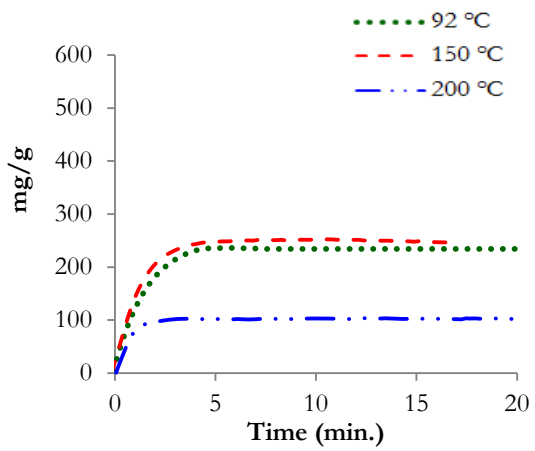

Methanol adsorption isotherm in methanol – CO_2 mixture

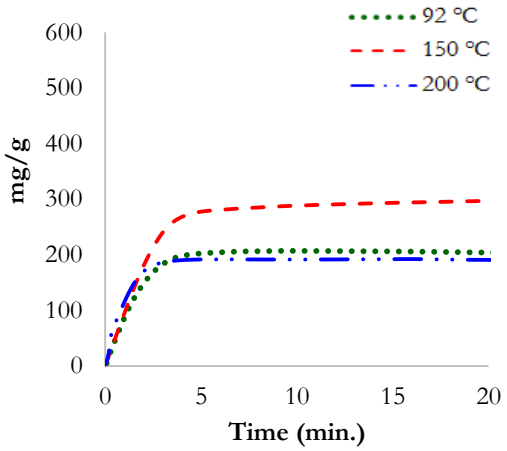

Methanol adsorption isotherm in methanol – DMC mixture

Appendix 8 Three components adsorption isotherms

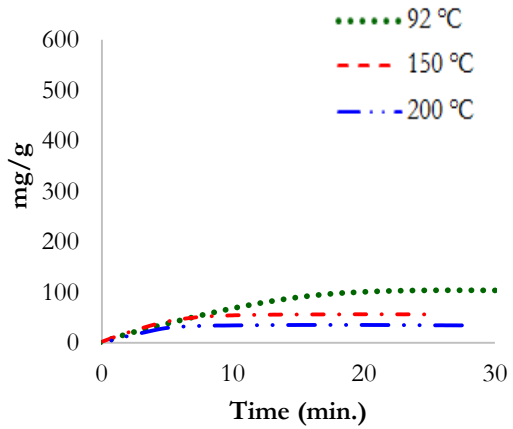

Water adsorption isotherm in water - ethanol – CO_2 mixture

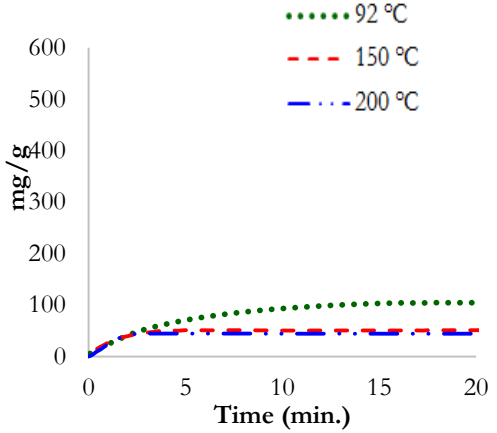

Ethanol adsorption isotherm in water - ethanol – CO_2 mixture

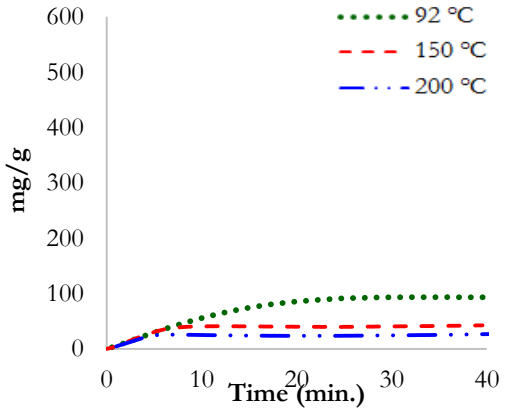

Water adsorption isotherm in water - methanol – CO_2 mixture

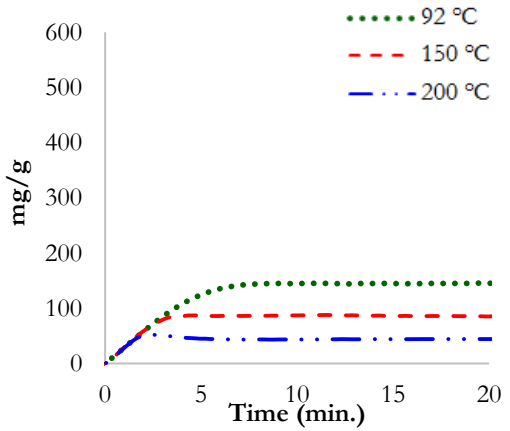

Methanol adsorption isotherm in water - methanol – CO_2 mixture

Appendix 9 Four components adsorption isotherms

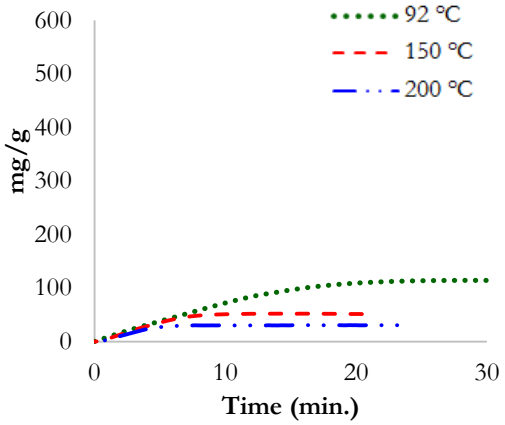

Water adsorption isotherm in water - ethanol – DEC - CO_2 mixture

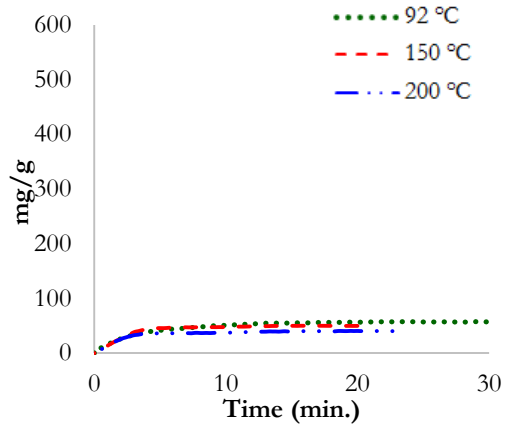

Ethanol adsorption isotherm in water - ethanol – DEC - CO_2 mixture

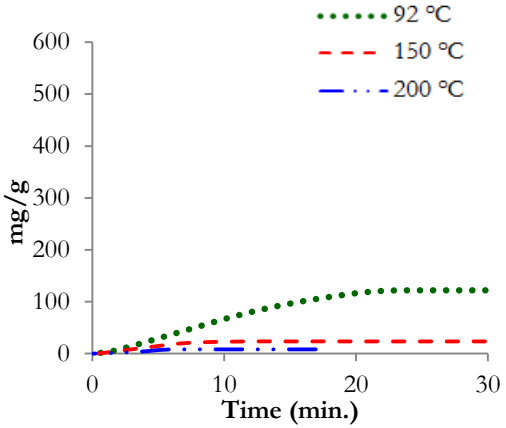

Water adsorption isotherm in water - methanol – DMC - CO_2 mixture

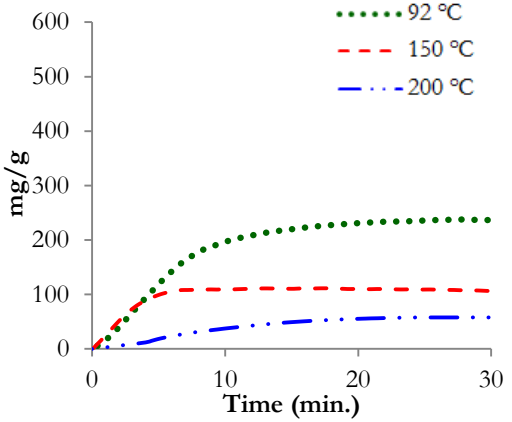

Methanol adsorption isotherm in water - methanol – DMC - CO_2 mixture

Appendix 10 Kinetics

Kinetic parameters for ethanol in the mixture: water - ethanol - CO_2

T (°C)	PFO			PSO			IPD		Elovich		
	$\mathbf{qe}\ \left(\frac{\mathbf{mg}}{\mathbf{g}}\right)$	$\mathbf{k_1}\ (\mathbf{min^{-1}})$	$\mathbf{R^2}$	$\mathbf{qe}\ \left(\frac{\mathbf{mg}}{\mathbf{g}}\right)$	$\mathbf{k_1}\ \left(\frac{\mathbf{g}}{\mathbf{mg}\cdot\mathbf{min}}\right)$	$\mathbf{R^2}$	$\mathbf{k_{dif}}\ \left(\frac{\mathbf{mg}}{\mathbf{g}\cdot\mathbf{min^{0.5}}}\right)$	$\mathbf{R^2}$	$\boldsymbol{\beta}\ \left(\frac{\mathbf{g}}{\mathbf{mg}}\right)$	$\boldsymbol{\alpha}\ \left(\frac{\mathbf{mg}}{\mathbf{g}\cdot\mathbf{min}}\right)$	$\mathbf{R^2}$
92	**116.63**	**0.2351**	**0.9850**	135.14	1.62E-03	0.9998	25.03	0.9609	0.0321	59.86	0.9974
150	**48.91**	**0.6575**	**0.9862**	65.79	1.13E-02	0.9955	18.54	0.9264	0.0479	68.43	0.9720
200	**91.10**	**1.4600**	**0.9887**	99.90	3.15E-03	0.8312	17.47	0.9440	0.0466	29.51	0.9799
Average			**0.9866**			0.9422		0.9438			0.9831

Kinetic parameters for methanol in the mixture: water- methanol - CO_2

T (°C)	PFO			PSO			IPD		Elovich		
	$\mathbf{qe}\ \left(\frac{\mathbf{mg}}{\mathbf{g}}\right)$	$\mathbf{k_1}\ (\mathbf{min^{-1}})$	$\mathbf{R^2}$	$\mathbf{qe}\ \left(\frac{\mathbf{mg}}{\mathbf{g}}\right)$	$\mathbf{k_1}\ \left(\frac{\mathbf{g}}{\mathbf{mg}\cdot\mathbf{min}}\right)$	$\mathbf{R^2}$	$\mathbf{k_{dif}}\ \left(\frac{\mathbf{mg}}{\mathbf{g}\cdot\mathbf{min^{0.5}}}\right)$	$\mathbf{R^2}$	$\boldsymbol{\beta}\ \left(\frac{\mathbf{g}}{\mathbf{mg}}\right)$	$\boldsymbol{\alpha}\ \left(\frac{\mathbf{mg}}{\mathbf{g}\cdot\mathbf{min}}\right)$	$\mathbf{R^2}$
92	225.20	0.4281	0.9934	304.04	4.14E-04	0.9129	64.69	0.9638	**0.0158**	**84.63**	**0.9883**
150	135.50	1.7930	0.9758	247.83	5.09E-04	0.4838	50.22	0.9766	**0.0361**	**82.61**	**0.9876**
200	201.95	0.9799	0.9880	179.31	1.34E-03	0.9004	51.62	0.9427	**0.0241**	**85.97**	**0.9738**
Average			0.9857			0.7657		0.9610			**0.9832**

Kinetic parameters for ethanol in the mixture: water- ethanol - DEC - CO_2

T (°C)	PFO			PSO			IPD		Elovich		
	$\mathbf{qe}\ \left(\frac{\mathbf{mg}}{\mathbf{g}}\right)$	$\mathbf{k_1}\ (\mathbf{min^{-1}})$	$\mathbf{R^2}$	$\mathbf{qe}\ \left(\frac{\mathbf{mg}}{\mathbf{g}}\right)$	$\mathbf{k_1}\ \left(\frac{\mathbf{g}}{\mathbf{mg \cdot min}}\right)$	$\mathbf{R^2}$	$\mathbf{k_{dif}}\ \left(\frac{\mathbf{mg}}{\mathbf{g \cdot min^{0.5}}}\right)$	$\mathbf{R^2}$	$\boldsymbol{\beta}\ \left(\frac{\mathbf{g}}{\mathbf{mg}}\right)$	$\boldsymbol{\alpha}\ \left(\frac{\mathbf{mg}}{\mathbf{g \cdot min}}\right)$	$\mathbf{R^2}$
92	**44.35**	**0.1823**	**0.9939**	66.80	4.74E-03	0.9995	12.45	0.9398	0.0677	45.12	0.9943
150	**74.37**	**0.6200**	**0.9871**	94.79	2.10E-03	0.9057	25.03	0.9486	0.0459	37.99	0.9778
200	**52.14**	**0.7180**	**0.9955**	120.71	1.03E-03	0.7854	25.78	0.9922	0.0598	37.43	0.9957
Average			**0.9922**			0.8969		0.9602			0.9893

Kinetic parameters for methanol in the mixture: water- methanol - DMC - CO_2

T (°C)	PFO			PSO			IPD		Elovich		
	$\mathbf{qe}\ \left(\frac{\mathbf{mg}}{\mathbf{g}}\right)$	$\mathbf{k_1}\ (\mathbf{min^{-1}})$	$\mathbf{R^2}$	$\mathbf{qe}\ \left(\frac{\mathbf{mg}}{\mathbf{g}}\right)$	$\mathbf{k_1}\ \left(\frac{\mathbf{g}}{\mathbf{mg \cdot min}}\right)$	$\mathbf{R^2}$	$\mathbf{k_{dif}}\ \left(\frac{\mathbf{mg}}{\mathbf{g \cdot min^{0.5}}}\right)$	$\mathbf{R^2}$	$\boldsymbol{\beta}\ \left(\frac{\mathbf{g}}{\mathbf{mg}}\right)$	$\boldsymbol{\alpha}\ \left(\frac{\mathbf{mg}}{\mathbf{g \cdot min}}\right)$	$\mathbf{R^2}$
92	335.63	0.4632	0.9508	2998.41	1.83E-06	0.0315	64.43	0.9866	**0.0154**	**51.64**	**0.9736**
150	228.83	0.5684	0.9822	289.02	3.50E-04	0.7777	55.41	0.9611	**0.0198**	**73.33**	**0.9858**
Average			0.9665			0.4046		0.9739			**0.9797**

Appendix 11 Chemical and physical properties of DEC and DMC

Chemical profile of DEC [105]

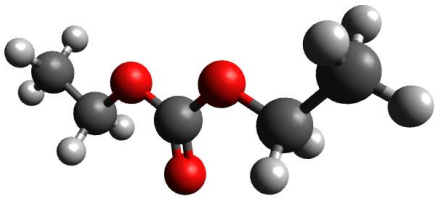

DEC Chemical Structure

- ✓ Synonyms: ethyl carbonate, carbonic acid, diethyl ester
- ✓ Chemical Category: ester
- ✓ Molecular formula: $C_5H_{10}O_3$
- ✓ Nº CAS: 105-58-8
- ✓ Nº UN: 2366

Physical and thermodynamic properties of DEC [68] [105]:

Aggregation state	Liquid
Appearance	Colorless
Density	**T °C** **g/cm³** 20 0.98
Molar mass	118.13 g/mol
Melting point	-43 °C
Boiling point	126 °C
Viscosity	**T(°C)** **(mPa·s)** 25 0.75
Vapor pressure	**T(°C)** **(kPa)** 20 1.1
Specific Gravity (Water = 1)	0.98
Vapor Density (Air = 1)	4.07
Water solubility	20°C , It is insoluble
Flammable Limits	1.4 - 11 (%Vol.)
Flash point	25 °C
Heat of combustion	23.42 MJ/kg
Enthalpy of vaporization	39.1 kJ/mol
Critical temperature	Not applicable

Toxicity of DEC [106]

Safety diamond DEC

- ✓ Skin contact: causes irritation.
- ✓ Eye contact: causes irritation.
- ✓ Inhalation: causes irritation to the respiratory tract.
- ✓ Ingestion: may cause digestive tract irritation with nausea, vomiting, and diarrhea.
- ✓ Carcinogenic effects: not applicable.
- ✓ Mutagenic effects: Not applicable.

✓ Repeated or prolonged exposure is not worse for the health

Chemical profile of DMC [68] [107].

✓ Synonyms: methyl carbonate, carbonic acid dimethyl ester
✓ Chemical Category: Ester
✓ Molecular formula: $C_3H_6O_3$
✓ Nº CAS: 616-38-6
✓ Nº UN: 1161

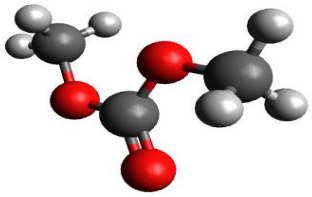

DMC chemical structure

Physical and thermodynamic properties od DMC [68] [107].

Aggregation state	Liquid
Appearance	Colorless
Density	**T °C** **g/cm³** 17 1.069
Molar mass	90.08 g/mol
Melting point	2-4 °C
Boiling point	90 °C
Viscosity	**T(°C)** **(mPa·s)** 25 0.585
Vapor pressure	**T(°C)** **(kPa)** 25 7.38
Specific Gravity (Water = 1)	1.069
Vapor Density (Air = 1)	3.1
Water solubility	**T (°C)** **g/l** 20 139
Flammable Limits	4.22 - 12.87 %(V)
Flash point	17 °C
Heat of combustion	23.42 MJ/kg
Enthalpy of vaporization	36.4 kJ/mol
Critical temperature	278.2°C

Toxicity

✓ Skin contact: causes irritation. It could be adsorbing.
✓ Eye contact: causes irritation.
✓ Inhalation: causes irritation to the respiratory tract. It can cause drowsiness, unconsciousness and depression of the central nervous system. Vapors may cause dizziness or suffocation.

Safety diamond DMC

✓ Ingestion: may cause digestive tract irritation.
✓ Carcinogenic effects: not applicable.

- ✓ Mutagenic effects: Not applicable.
- ✓ The substance may be toxic to the central nervous system
- ✓ Repeated or prolonged exposure to the substance can cause disorders in target organs. [108].

Appendix 12 Data of import and export market

The classification codes for DMC and DEC corresponding to the import and export statistics in Colombia. The next table shows the data import and export description and classification by harmonized system.

Harmonized System code (HS)		Description
2920.90.00	Organic Chemicals	Esters of other inorganic acids of non- metals (excluding esters of hydrogen halides) and their salts; their halogenated, sulfonated , nitrated or nitrosated

Colombian market for DEC and DMC is very small. The next table shows values for the organic chemicals export and import and their position respect the global market during 2015 [109]. It is clear that our country does not have a great influence in the global economy with this kind of products.

Colombia statistics for organic chemicals

Export ($)	Export (%)	Export Rank*	% of Global Exports	Import ($)	Import (%)	Import Rank*	% of Global Imports
$165,840,116	0.30%	49	0.04%	$2,380,401,781	3.72%	29	0.54%

*(To 129 Countries)

The next figure presents the historic export values for organic chemicals (HS 2920.90.00) in free zones and at the world [110], [111]. It is possible to see a significantly reduction for organic chemicals export in free zones and the world.

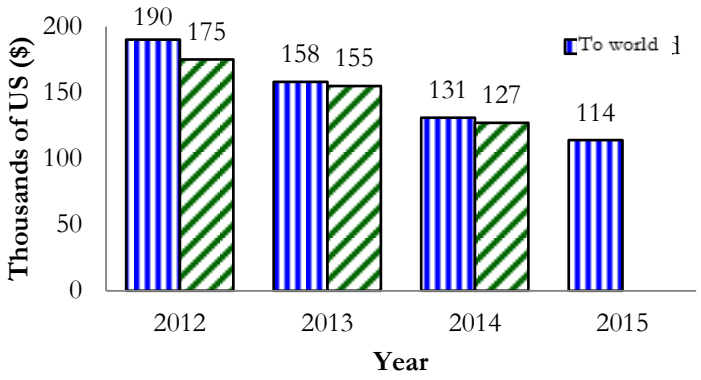

Colombia exports (2012 – 2015)

The import of these products increases. You show how China provides the main quantities, and countries like India and Italia begins to take importance [112].

Main countries that export chemical products consume by Colombia

Country	2012	2013	2014	2015
China	5086	4463	3230	6465
Germany	665	579	578	664
Taiwan	480	537	537	455
Italia	0	38	0	111
USA	202	144	146	93
India	0	0	1	90
South Korea	100	0	8	17
Spain	109	62	13	11

These data confirm the importance of efficient and sustainable production methods research by linear carbonates such as DEC and DMC in order to improve the economical develop of this country and satisfy the growing demand.

Appendix 13 Description catalyst preparation of Cu-Ni/AC (3:1) catalyst (20% total load)

If it has 10g of AC, that correspond to 80% of catalyst, 2 g corresponding 20% resting of nickel and copper oxide ration.

$$\mathbf{CuO + NiO = 2.1g}\quad \textbf{Equation 28}$$

$$1\text{mol Cu} = 3\text{mol Ni}$$

By stoichiometry

$$1\text{mol CuO} = 3\text{mol NiO}$$

Expressing this relationship in a mass way

$$1\text{mol CuO} \times \text{PM}_{\text{CuO}} = 3\text{mol NiO} \times \text{PM}_{\text{NiO}}$$

$$79.5454\text{gCuO} = 3(74.6928\text{gNiO})$$

$$1\text{m CuO} = 2.817\ \text{m NiO} \quad \textbf{Equation 29}$$

Equation 28 into 27

$$2.817\ \text{m NiO} + \text{m NiO} = 2.1\text{g}$$

$$\text{NiO} = 0.5502\ \text{g} \quad \text{and} \quad \text{CuO} = 1.5498\ \text{g}$$

The equivalent mole amount

$$\text{NiO} = 7.3662 * 10^{-3}\text{mol} \quad \text{and} \quad \text{CuO} = 0.01948\ \text{mol}$$

$$7.3662 * 10^{-3}\ \text{mol NiO} \times \frac{1\ \text{mol Ni(NO}_3)_2\text{6H}_2\text{O}}{1\ \text{mol NiO}} \times \frac{290.7954\ \text{g Ni(NO}_3)_2\text{6H}_2\text{O}}{1\ \text{mol Ni(NO}_3)_2\text{6H}_2\text{O}}$$
$$= 2.1421\ \text{g Ni(NO}_3)_2\text{6H}_2\text{O}$$

$$0.01948\ \text{mol NiO} \times \frac{1\ \text{mol Cu(NO}_3)_2\text{3H}_2\text{O}}{1\ \text{mol CuO}} \times \frac{241.6023\ \text{g Cu(NO}_3)_2\text{3H}_2\text{O}}{1\ \text{mol g Cu(NO}_3)_2\text{3H}_2\text{O}} = 4.7064\ \text{g Cu(NO}_3)_2\text{3H}_2\text{O}$$

Real weight: $2.1611\ \text{g Ni(NO}_3)_2\text{6H}_2\text{O}$ and $4.7292\ \text{g Cu(NO}_3)_2\text{3H}_2\text{O}$

56 mL of ammonia solution for impregnation commercial activated carbon was used

The preparation of 10g of Cu-Ni (2:1) catalyst 20% total load was similar: Real weight: $3.5186\ \text{g Ni(NO}_3)_2\text{6H}_2\text{O}$ and $5.1470\text{g Cu(NO}_3)_2\text{3H}_2\text{O}$ and 73 mL of ammonia solution for impregnation commercial activated carbon was used

Appendix 14 Solutions preparations

- To produce 1 L of 2 M HCl solution

$$\frac{2\ \text{mol HCl}}{1\ \text{L}} \times \frac{36.46\ \text{g HCl}}{1\ \text{mol HCl}} \times \frac{100\ \text{g s/n HCl}}{38\ \text{g HCl}} \times 1\text{L} \times \frac{\text{ml HCl}}{1.189\ \text{g HCl}} = 161.391\ \text{ml s/n HCl}$$

- To produce 500 mL of 4 M H_2SO_4solution

$$\frac{4\ \text{mol HCl}}{1\ \text{L}} \times \frac{98.08\ \text{g}\ H_2SO_4}{1\ \text{mol}\ H_2SO_4} \times \frac{100\ \text{g s/n}\ H_2SO_4}{95\ \text{g}\ H_2SO_4} \times 0.5\text{L} \times \frac{\text{ml}\ H_2SO_4}{1.84\ \text{g}\ H_2SO_4} = 112.22\ \text{ml s/n H2SO4}$$

Appendix 15 Preparation by incipient wet impregnation method for Cu-Ni catalyst support on active carbon.

Description for preparation of 20g Cu-Ni Catalyst 3:1 (molar ratio) 20% total load. It was used $\mathbf{q_i = q_i^{sat} \frac{K_i p_i}{1+K_i p_i}}$ (Equation 1 until $\mathbf{C = \frac{W_p}{V}}$ Equation 21:

$Cu(NO_3)_2.3H_2O = 8.9610\ \text{g}$ $Ni(NO_3)_2.6H_2O = 4.0798\ \text{g}$ AC = 16 g

- ✓ Pretreatment active carbon
- ✓ Experimental is calculate the V_w

$$W_0 = 1.9996\ \text{g}\ \ V_0 = 10\text{ml}$$

$$V_w = \frac{V_0}{W_0} = \frac{6\ \text{ml}}{1.9996\ \text{g}} = 3\ \text{ml/g}$$

- ✓ It have W= 16 g of CA

$$V = W \times V_w = 16\ \text{g} \times 3\frac{\text{ml}}{\text{g}}$$

$$V = 48\ \text{ml}$$

- ✓ For calculate the precursor charged, Cp, we have 13.1 g total of precursor per each 16 g of active carbon

$$\frac{13.1\ \text{g precursor}}{16\ \text{g support}} = 0.8188\ \frac{\text{g precursor}}{\text{g support}}$$

$$Cp = 81.88\ \frac{\text{g precursor}}{100\ \text{g support}}$$

$$W_p = \frac{16 \times 81.88}{100} = 13.1\ \text{g}$$

- ✓ Precursor concentration solution C

$$C = \frac{W_p}{V} = \frac{13.1\ \text{g}}{48\ \text{ml}} = 0.2729\ \text{g/ml}$$

- ✓ Add dropwise the volume V
- ✓ Aging for twelve hours and rotary evaporator (less than 100°C)
- ✓ Dry at 90 °C in an oven, Calcined at 500 °C for 2 hours in a stream of N_2 and activate at 600 °C for 2 h in a stream of 5% H_2/Ar

Appendix 16. Calibration curves liquid phase (concentration vs. area under the curve)

Detector	TCD	FID
Water	y = 4E+08x	-
Ethanol	y = 3E+08x	y = 6E+09x
DEC	y = 3E+08x	y = 6E+09x
Methanol	y = 3E+08x	y = 4E+09x
DMC	y = 3E+08x	y = 3E+09x

Appendix 17 Chromatograph injection method

INSTRUMENT CONTROL PARAMETERS: 7890A-5975C

D:\MSDCHEM\1\METHODS\ISIS.M
Tue Jun 30 09:19:41 2015

Control Information
------- -----------

Sample Inlet : GC
Injection Source : GC ALS
Mass Spectrometer : Disabled

Headspace Parameters

Headspace Device: Agilent G1888 Headspace Sampler()
Communications Mode: 10.1.1.103
Serial Number: IT01012026
Vial Size (mL): 20
Handshake Mode: Proceed if GC Not Ready
Oven Stabilization Time (min): 1.00
Pressure Units: psi
Carrier Connection: None
Vial EPC: None
Loop Size (µL): 0

Multiple Headspace Extraction mode: Off
GC Cycle Time (min): 10.00
Inject Time (min): 1.00
Loop Equilibration Time (min): 0.05
Loop Fill Time(min): 0.20
Loop Temperature: 90
Oven Temperature: 70
Shake: Off
Transfer Line Temperature: 100
Vial Equilibration Time (min): 5.00
Vial Pressurization Time (min): 0.20
Vial Pressure (psi): 0.00

Carrier Gas Pressure (psi): 0.00

No Sample Prep method has been assigned to this method.

Oven
Equilibration Time 1 min
Max Temperature 230 degrees C
Slow Fan Disabled
Oven Program On
60 °C for 1 min
#1 then 20 °C/min to 70 °C for 1 min
#2 then 30 °C/min to 120 °C for 2 min
Run Time 6.1667 min
Cryo Off

Back Injector
Syringe Size 10 µL
Injection Volume 1 µL
Injection Repetitions 1
Injection Delay 0 sec
Solvent A Washes (PreInj) 2
Solvent A Washes (PostInj) 2
Solvent A Volume 8 µL
Solvent B Washes (PreInj) 2
Solvent B Washes (PostInj) 2
Solvent B Volume 8 µL
Sample Washes 0
Sample Wash Volume 8 µL
Sample Pumps 3
Dwell Time (PreInj) 0 min
Dwell Time (PostInj) 0 min
Solvent Wash Draw Speed 300 µL/min
Solvent Wash Dispense Speed 6000 µL/min
Sample Wash Draw Speed 300 µL/min
Sample Wash Dispense Speed 6000 µL/min
Injection Dispense Speed 6000 µL/min
Viscosity Delay 0 sec
Sample Depth Disabled

Sample Overlap
Sample overlap is not enabled

Front SS Inlet He
Excluded from Affecting GC's Readiness State
Mode Splitless
Heater On 250 °C
Pressure On 5.3728 psi
Total Flow On 51.323 mL/min
Septum Purge Flow On 1 mL/min
Gas Saver On 15 mL/min After 2 min
Purge Flow to Split Vent 50 mL/min at 2 min

Back SS Inlet He
Mode Split
Heater On 225 °C

Pressure On 5.6188 psi
Total Flow On 77 mL/min
Septum Purge Flow On 1 mL/min
Gas Saver On 15 mL/min After 2 min
Split Ratio 75 :1
Split Flow 75 mL/min

Thermal Aux 2 (MSD Transfer Line)
Heater On
Temperature Program On
280 °C for 0 min
Run Time 6.1667 min

Column #1
J&W 112-2532: 1195.40749
Cyclodex-B
230 °C: 30 m x 250 µm x 0.25 µm
In: Front SS Inlet He
Out: Aux EPC 1

(Initial) 60 °C
Pressure 5.706 psi
Flow 0.32316 mL/min
Average Velocity 9.9662 cm/sec
Holdup Time 5.017 min
Flow Program On
0.32316 mL/min for 0 min
Run Time 6.1667 min

Column #2
J&W 123-1032: 006
DB-1
325 °C: 30 m x 320 µm x 0.25 µm
In: Front SS Inlet He
Out: Aux EPC 1

(Initial) 60 °C
Pressure 5.3728 psi
Flow 0.8 mL/min
Average Velocity 15.196 cm/sec
Holdup Time 3.2904 min
Flow Program Off
0.8 mL/min for 0 min
Run Time 6.1667 min

Column #3
J&W 123-7033DB-WAX
240 °C: 30 m x 320 µm x 0.5 µm
In: Back SS Inlet He
Out: Back Detector TCD

(Initial) 60 °C
Pressure 5.6188 psi
Flow 1 mL/min
Average Velocity 19.395 cm/sec

Holdup Time 2.5779 min
Flow Program On
1 mL/min for 0 min
Run Time 6.1667 min

Column #4
Agilent 160-2615: 0004
Retention Gap
350 °C: 5 m x 180 µm x 0 µm
In: Aux EPC 1 He
Out: Vacuum

(Initial) 60 °C
Pressure 0.99999 psi
Flow 0.76175 mL/min
Average Velocity 78.295 cm/sec
Holdup Time 0.10644 min
Pressure Program On
0.99999 psi for 0 min
Run Time 6.1667 min

Column #5
Agilent 160-2615-2: 005
Retention Gap
350 °C: 2 m x 180 µm x 0 µm
In: Aux EPC 1 He
Out: Front Detector FID

(Initial) 60 °C
Pressure 0.99999 psi
Flow 0.23493 mL/min
Average Velocity 16.621 cm/sec
Holdup Time 0.20055 min
Pressure Program On
0.99999 psi for 0 min
Run Time 6.1667 min

Front Detector FID
Heater On 270 °C
H2 Flow On 45 mL/min
Air Flow On 450 mL/min
Makeup Flow On 5 mL/min
Const Col + Makeup Off
Flame On
Electrometer On

Back Detector TCD
Heater On 250 °C
Reference Flow On 20 mL/min
Makeup Flow On 10 mL/min
Const Col + Makeup Off
Negative Polarity Off
Filament On

Valve 1

Gas Sampling Valve
GSV Loop Volume 0.25 mL
Load Time 0.5 min
Inject Time 0.5 min

Valve 2
Switching Valve Off

Aux EPC 1 He: Supplies Column 4
Excluded from Affecting GC's Readiness State

Aux EPC 2 He
Excluded from Affecting GC's Readiness State
Pressure Program On
2.0376 psi for 0 min
Run Time 6.1667 min

Aux EPC 3 He
Excluded from Affecting GC's Readiness State
Pressure Program On
3 psi for 0 min
Run Time 6.1667 min

Aux EPC 4 He
Excluded from Affecting GC's Readiness State
Pressure Program Off
16 psi for 0 min
Run Time 6.1667 min

Aux EPC 5 He
Excluded from Affecting GC's Readiness State
Pressure Program Off
0 psi for 0 min
Run Time 6.1667 min

Aux EPC 6 He
Excluded from Affecting GC's Readiness State
Pressure Program Off
0 psi for 0 min
Run Time 6.1667 min

Valve Box
Heater On 200 °C

Signals
Signal #1: Back Signal Save On
20 Hz
Zero @ 0 min

Signal #2: Front Signal Save On
5 Hz
Zero @ 0 min

Signal #3: Test Plot Save Off
50 Hz

Signal #4: Test Plot Save Off
50 Hz

TUNE PARAMETERS for SN: US81819751

Trace Ion Detection is OFF.

EMISSION : 34.610
ENERGY : 69.922
REPELLER : 24.929
IONFOCUS : 90.157
ENTRANCE_LE : 28.500
EMVOLTS : 1388.235
Actual EMV : 1388.23
GAIN FACTOR : 0.18
AMUGAIN : 2346.000
AMUOFFSET : 122.750
FILAMENT : 1.000
DCPOLARITY : 0.000
ENTLENSOFFS : 18.573
MASSGAIN : -335.000
MASSOFFSET : -37.000

END OF TUNE PARAMETERS

END OF INSTRUMENT CONTROL PARAMETERS